ESSAYS ON SOCIAL NETWORKS AND COOPERATION: THE CASE OF NATURAL RESOURCES

Jorge Marco Renau

Essays on Social Networks and Cooperation: The Case of Natural Resources

Jorge Marco Renau

Supervisor: Prof. Renan U. Goetz

Department of Economics
University of Girona

This dissertation is submitted for the degree of
Doctor of Economics

University of Girona May 2018

Dedicated to

my parents

Jorge Marco and Verónica Renau

my "sparky" love

Natalia Castro

in memory of my first mentor

Luís Recatalá

Declaration

I hereby declare that except where specific reference is made to the work of others, the contents of this dissertation are original and have not been submitted in whole or in part for consideration for any other degree or qualification in this, or any other university. This dissertation is my own work and contains nothing which is the outcome of work done in collaboration with Renan U. Goetz, except as specified in the text.

Jorge Marco Renau
May 2018

Acknowledgements

Firstly, I would like to express my sincere gratitude to my supervisor Prof. Renan U. Goetz for this continuous support of my Ph.D. thesis and related research, for his patience, motivation, and expert knowledge. His guidance helped me throughout the research and writing of this thesis. I cannot imagine having a better supervisor and mentor for this thesis.

My sincere thanks also goes to Prof. Tomás Barraquer, Prof. Matthew Jackson, and Dr. Alessandro Tavoni, who provided me with the opportunity to join their team as a Ph.D. visitor, and who gave me unlimited access to the research facilities.

On the other hand, I gratefully acknowledge the financial support from the Ministerio de Economía y Competitividad under the grants ECO2013-45861R and ECO2016-75927R, and from the Govern de Catalunya under the grants XREPP and 2014 SGR1360. Moreover, I would also like to thank the Department of Economics for helping me financially and allowing me to do some stages abroad as well as attend congresses related to my research.

I have many people to thank for listening to and, at times, having to tolerate me over the last few years. I cannot begin to express my gratitude and appreciation for their friendship. Ana Serrano, Javier Valbuena, Amílcar Pérez and Marc Castells, have been unwavering in their personal and professional support during the time I spent at the University of Girona. Thank you very much for many memorable evenings.

Finally, a very special thank you to my parents who offered their encouragement through phone calls, despite my own limited devotion to this kind of communication.

And you, Natalia, a sweet coincidence in The Upside Down.

Summary

The tragedy of the commons is a concept used in environmental economics to highlight the conflict between individual and collective rationality. The tragedy occurs when a natural resource is easily available to all users and every user tries to reap the greatest short-term benefit from the resource. In situations of this kind, demand greatly outweighs replenishment and eventually the natural resource will be unavailable for the users. From the 1990s onwards, scholars have found many examples that suggest that agents are capable of overcoming the tragedy of the commons and sustaining the natural resource. Examples include resource property rights and community management through collective action. This thesis focuses on collective action and the determinants of cooperation. At the community level, many factors impacting cooperation (i.e., trust, communication, social pressure) are very dependent on the underlying structure of social interactions, often formalized by a social network. The aim of this thesis is to assess social networks and their explicit role in the emergence and maintenance of cooperation in resource use. This is done by coupling resource stock dynamics with social dynamics concerning compliance to a cooperative norm prescribing the socially optimal use of the natural resource. Among the single aspects analyzed in the literature, cohesiveness and the share of norm-complying agents (compliers) stand out. The definition for cohesiveness is most frequently based on links between agents. However, in the case of cooperativeness or the exercise of social pressure, not only are the links between agents important, but so too are the agents' chosen strategies. If two compliers are linked, one can expect they will experience greater social pressure than if every complier were linked to a defector but not linked between them. For this reason, we propose a new connectivity measure that is based on links and the strategy chosen. We have called it "local cohessiveness of compliers" as it considers the links between the compliers in the neighborhood of an agent. As such it is a "small-world or micro" characteristic of the social network and is different from more "large-world or macro" characteristics such as the degree, size or density. Although the share of compliers is often seen as the most important driving force for cooperativeness, it is independent of the network size and density. As such, its indicative

power to foresee a possible propagation of compliers within social networks is likely to be limited. The asymmetry and irregularity of real social networks suggests that merely focusing on a single aspect of the network does not offer a reliable instrument to accurately analyze the range of cooperativeness. For these reasons, we analyze the underlying forces of cooperation by evaluating to what extent macro and micro characteristics of the structure of social interaction support social norms. In our models, macro and micro characteristics of social interaction lead to social pressure that depends on the share of compliers, the local cohesiveness of compliers and the state of the natural resource. The consideration of monetary or non-monetary punishment leads to a second important question. In particular, it allows analyzing the question to what extent pro-social behavior can be induced by informal enforcement (social pressure) or by legal enforcement (taxes or subsidies). Our analysis shed new light on this question by determining the conditions where only legal enforcement is able to induce cooperativeness and the conditions where informal and legal enforcement are both able to support cooperativeness. Likewise, it offers a concept to measure their substitutability. How to best design network-orientated policies to promote cooperation within the community remains an interesting topic for future research. Apart from addressing policies-related questions this research contributes to the understanding of drivers of cooperation in relation with social networks in several ways: (i) we link dynamic economic decision problems with different classes of social networks to study their effect on the decision problem, (ii) our study offers a metric for the cohesiveness of compliers – as opposed to social ties – and determines its influence on cooperativeness between the agents, and (iii) our models offer an equilibrium concept and determine the possible equilibria as a function of different classes of social networks, the evolution of a stock variable and dynamic strategy choices by the agents.

Resumen

La tragedia de los comunes es un concepto utilizado en economía ambiental para destacar el conflicto entre racionalidad individual y colectiva. La tragedia ocurre cuando un recurso natural está ampliamente disponible para todos los usuarios y cada usuario trata de obtener a corto plazo su mayor beneficio del recurso. En este tipo de situaciones, la demanda supera ampliamente el reabastecimiento y, con el tiempo, los recursos naturales dejan de estar disponibles para los usuarios. Desde la década de 1990 en adelante, los académicos han encontrado numerosos ejemplos que sugieren que los agentes son capaces de superar la tragedia de los comunes y mantener el recurso natural. Los ejemplos incluyen derechos de propiedad de los recursos y gestión comunitaria a través de la acción colectiva. Esta tesis se centra en la acción colectiva y los determinantes de la cooperación. A nivel comunitario, muchos factores que repercuten en la cooperación (por ejemplo; la confianza, la comunicación o la presión social) dependen en gran medida de la estructura subyacente de las interacciones sociales, a menudo formalizadas por la red social. El objetivo de esta tesis es evaluar las redes sociales y su papel explícito en el establecimiento y mantenimiento de la cooperación en el uso de los recursos. Esto se hace mediante el estudio conjunto de la dinámica del stock del recurso natural con la dinámica social en relación con el cumplimiento de una norma cooperativa que prescribe el uso socialmente óptimo del recurso natural. Entre los factores analizados en la literatura, destacan la cohesión y la participación de los agentes que cumplen con la norma (cumplidores). La definición de cohesión se basa en los vínculos entre los agentes. Sin embargo, en el caso de la cooperación o la presión social, no solo son importantes los vínculos entre los agentes, sino también las estrategias elegidas por estos. Si se relacionan dos cumplidores, se puede esperar que estos ejerzan una mayor presión social que si, por ejemplo, cada cumplidor estuviese vinculado a un desertor pero no vinculado entre ellos. Por esta razón, proponemos una nueva medida de conectividad que se basa en los vínculos y la estrategia elegida. A esta medida la llamamos “cohesión local de cumplidores” ya que considera los vínculos entre los cumplidores en la vecindad de un agente. Como tal, es una característica de “mundo pequeño o micro” de la red social y es diferente de

otras características de “mundo grande o macro” como el grado, tamaño o densidad. Aunque la participación de los cumplidores se considera a menudo como la fuerza motriz más importante para la cooperación, es independiente del tamaño y la densidad de la red. Así, es probable que su poder indicativo para prever una posible propagación de cumplidores dentro de la comunidad sea limitado. La asimetría e irregularidad de las redes sociales reales sugiere que enfocarse en un solo aspecto de la red no ofrece un instrumento fiable para analizar con precisión el rango de cooperación. Por eso, analizamos las fuerzas subyacentes de la cooperación al evaluar hasta qué punto las características macro y micro de la estructura de la interacción social respaldan las normas sociales. En nuestros modelos, las características macro y micro de la interacción social conducen a una presión social que depende de la participación de los cumplidores, la cohesión local de los cumplidores y el estado del recurso natural. La consideración de castigo monetario o no monetario conduce a una segunda pregunta importante. En particular, permite analizar la pregunta de en qué medida la conducta pro-social puede ser inducida por el refuerzo informal (presión social) o por el refuerzo legal (impuestos o subsidios). Nuestro análisis arroja nueva luz sobre esta cuestión al determinar las condiciones en las que solo el refuerzo legal puede inducir la cooperación y las condiciones en las que los refuerzos informal y legal pueden apoyar la cooperación. Asimismo, ofrece un concepto para medir su sustitución. La mejor forma de diseñar políticas orientadas a la red social para promover la cooperación dentro de la comunidad sigue siendo un tema interesante para futuras investigaciones. Además de abordar cuestiones relacionadas con políticas económicas, esta investigación contribuye a la comprensión de los factores que inducen a la cooperación en relación con las redes sociales de varias maneras: (i) vinculamos problemas dinámicos de decisión económica con diferentes clases de redes sociales para estudiar su efecto sobre el problema de decisión, (ii) nuestro estudio ofrece una métrica para la cohesión de los cumplidores, en oposición a los vínculos sociales, y determina su influencia en la cooperación entre los agentes, y (iii) nuestros modelos ofrecen un concepto de equilibrio y determinan los posibles equilibrios como función de las diferentes clases de redes sociales, la evolución del recurso natural y las estrategias tomadas por parte de los agentes en cada instante.

Resum

La tragèdia dels bens comuns és un concepte utilitzat en economia ambiental que destaca el conflicte entre racionalitat individual i col · lectiva. La tragèdia es produeix quan un recurs natural està àmpliament disponible per a tots els usuaris i cada usuari tracta d'obtenir a curt termini el seu major benefici del recurs. En aquest tipus de situacions, la demanda supera àmpliament l'abastiment i, amb el temps, els recursos naturals deixen d'estar disponibles per als usuaris. Des de la dècada de 1990 endavant, els acadèmics han trobat nombrosos exemples que suggereixen que els agents són capaços de superar la tragèdia dels bens comuns i mantenir el recurs natural. Els exemples inclouen drets de propietat dels recursos i gestió comunitària a través de l'acció col · lectiva. Aquesta tesi es centra en l'acció col · lectiva i els determinants de la cooperació. A nivell comunitari, molts factors que repercuteixen en la cooperació (per exemple, la confiança, la comunicació o la pressió social) depenen en gran mesura de l'estructura subjacent de les interaccions socials, moltes vegades formalitzades per la xarxa social. L'objectiu d'aquesta tesi és avaluar les xarxes socials i el seu paper explícit en l'establiment i manteniment de la cooperació en l'ús dels recursos. Això es fa mitjançant l'estudi conjunt de la dinàmica del stock del recurs natural amb la dinàmica social en relació amb el compliment d'una norma cooperativa que prescriu la utilització socialment òptima del recurs natural. Entre els factors analitzats en la literatura, destaquen la cohesió i la participació dels agents que compleixen amb la norma (complidors). La definició de cohesió es basa en els vincles entre els agents. No obstant, en el cas de la cooperació o la pressió social, no només són importants els vincles entre els agents, sinó també les estratègies escollides per aquests. Si es relacionen dos complidors, es pot esperar que aquests implementen una major pressió social que si, per exemple, cada complidor estigués vinculat a un desertor però no vinculat entre ells. Per aquesta raó, proposem una nova mètrica de cohesió que es basa en els vincles i la estratègia triada. A aquesta mesura l'anomenem "cohesió local dels complidors" ja que considera els vincles entre els complidors en l'entorn d'un agent. Com a tal, és una característica de "món petit o micro" de la xarxa social i és diferent d'altres característiques de "món gran o macro" com el grau, tamany o

densitat. Tot i que la participació dels complidors es considera sovint com la força motriu més important per a la cooperació, és independent del tamany i de la densitat de la xarxa. Així, és probable que el seu poder indicatiu per preveure una possible propagació de complidors dins de la comunitat sigui limitat. La asimetria i irregularitat de les xarxes socials reals suggereix que enfocar-se en un únic aspecte de la xarxa no ofereix un instrument rellevant per analitzar amb precisió el rang de cooperació. Per això, analitzem les forces subjacents de la cooperació al avaluar fins a quin punt les característiques macro i micro de la estructura de la interacció social avalen les normes socials. En els nostres models, les característiques macro i micro de la interacció social condueixen a una pressió social que depèn de la participació dels complidors, la cohesió local dels complidors i l'estat del recurs natural. La consideració de càstig monetari o no monetari condueix a una segona pregunta important. En particular, permet analitzar la pregunta de en quina mesura la conducta pro-social pot ser induïda pel reforçament informal (pressió social) o pel reforçament formal (impostos o subsidis). El nostre anàlisi llança nova llum sobre aquesta qüestió al determinar les condicions en què només el reforçament legal pot induir la cooperació i les condicions en què els reforçaments informals i legals poden recolzar la cooperació. Així mateix, ofereix un concepte per mesurar la seva substitució. La millor forma de dissenyar polítiques orientades a la xarxa social per promoure la cooperació dins de la comunitat segueix sent un tema interessant per a futures investigacions. A més d'abordar qüestions relacionades amb polítiques econòmiques, aquesta investigació contribueix a la comprensió dels factors que indueixen a la cooperació en relació amb les xarxes socials de diverses maneres: (i) vinculem problemes dinàmics d'economia de decisions amb diferents classes de xarxes socials per estudiar el seu efecte sobre el problema de la decisió, (ii) el nostre estudi ofereix una mètrica per a la cohesió dels complidors, en oposició als vincles socials, i determina la seva influència en la cooperació entre els agents, i (iii) els nostres models ofereixen un concepte l'equilibri i determinen els possibles equilibris com a funció de les diferents classes de xarxes socials, l'evolució del recurs natural i les estratègies preses per part dels agents s cada instant.

Contents

List of Figures

List of Tables

Chapter 1

Introduction

1.1 Motivation

In economics, natural resources are considered common-pool resources. Common-pool resources are characterized by high exclusion costs related to establishing and maintaining private rights and rivalry; which, in turn, means exploitation by one party reduces the availability of the resource for others. These two characteristics create management vulnerabilities when the benefits of exploitation are privatized and some of the costs are socialized. The dilemma here is that if each economic agent takes as much as they can, inevitably the resource will be depleted. The prediction that a community of agents exploiting a natural resource leads to its inevitable overuse, the so-called "tragedy of the commons", is based on a model that assumes an open access regime (non-excludability), and that all agents are selfish, norm-free, and maximizers of short-term benefits. However, predictions based on this model are supported neither in field research nor in laboratory experiments. When agents are able to communicate, exclude others, or make rules, cooperation appears as an efficient solution to overcoming the tendency of agents to overuse the resource in question. Most of the examples observed of successful management involve local natural resources that are managed by a relatively large community who can restrict the access to the resource (common property regime). A significant characteristic of common property regimes is that the community either lacks the legal power to enforce social norms (cooperative norms) or it is too costly to rely on any kind of formal contract. However, those agents complying with the social norm may be able to place social pressure (e.g. social shunning or rejection) on those who do not adhere to it. Furthermore, in terms of sanctions, research finds that cooperation is higher when there is a threat of being excluded from the group. At the community level, many factors that influence cooperation

(i.e., trust, communication, social pressure) are very dependent on the underlying structure of social interactions, often formalized by a social network. Although the existing literature has recognized the importance of property rights in natural resource management, little attention has been paid to the types and patterns of interaction between the agents and the role they play in adherence to the social norms.

1.2 Aim of the research

The aim of this research is to assess social networks and their explicit role in the emergence and maintenance of cooperation in resource use. Moreover, the research also aims to contribute to the valuation approaches of intangible goods. Environmental economics contributed to the general economics with the foundation and formalization of methods to measure the value of intangible goods and services, for example, scenic value or existence value. In this work, we aim to extend the literature by defining a method to evaluate, in monetary terms, the effects social pressure has within a social network.

In particular, this research aims to answer the following research questions:

1. How can the value of the intangible good (social pressure) be measured? (**Q1**)
2. Are network effects able to trigger/sustain the socially optimal use of the resource? (**Q2**)[1]
3. How should traditional policy instruments be designed when network effects are taken into account? (**Q3**)
4. When is it best to apply the different policy options (network policy versus traditional policy instruments)? (**Q4**)

1.3 Methodology

Although cooperation is increasingly being recognized as a key determinant for overcoming the tragedy of the commons, there is much to be done in developing more sophisticated models that help us analyze the influence a network structure has on an agent's behavior and to design efficient policies that promote cooperation.

[1] The combination of **Q1** and **Q2** can be utilized for the formulation and specification of network-orientated policies.

In view of these considerations, this thesis suggests a new framework that combines the distinctive aspects of the three strands of the literature, i.e., an evolutionary game-theoretic approach based on the solutions to the differential games employed within a social network that accounts for the complexity of the interaction between agents.

With respect to the social network, we describe the structure of connections and analyze to what extent network effects support social norms in order to conserve natural resources. We focus on local commons and ask whether network effects are able to sustain the socially optimal use of the resource or at least to moderate or avoid the tragedy of the commons, i.e., the overuse or depletion of the natural resource. The characteristics of local commons (Ostrom [1990]) that may be important for management are:

1. Natural resources that are geographically bounded on an local or regional scale (i.e., coastal fisheries, forests, aquifers).

2. The community of agents exploiting the commons is often very large in size, ranging from several thousand or tens of thousands of agents.

3. The commons are degraded through intentional action. This means, resource use is conscious purpose because the resource provides major portion of livelihood.

4. Common property regime. The natural resource is owned by a community of agents. Access, use, and exclusion are controlled by the joint agents.

5. If the agents cooperate they can obtain cooperative benefits that cannot be obtained by non-cooperative behavior. However, the cooperative benefits can only be realized after a long and sustained period of cooperation while the non-cooperative benefits are immediate.

6. Learning from concrete experience is a feasible management strategy. It is feasible because the depletable resources regenerate on a short enough time scale to make learning possible and because the relevant properties of the resource are reasonably stable on that time scale.

We start from the observation that many social networks have common topological properties. However, traditional network generative models fail in one way or another when reproducing the observed topological properties of social networks. To quantify the exact influence a network structure has on cooperation, this research provides a new algorithm to generate comparable and realistic networks. The decision to comply with

the social norm is voluntary since resource rights are shared and the community has no legal power to enforce the social norm, however, the compliers may exercise social pressure (social shunning, social rejection) on members of the community that do not adhere to the social norm. Social pressure is applied by the compliers themselves, (i.e., without the presence of the authorities), and depends heavily on their structure and patterns of interaction. However, in some situations we observe that social pressure cannot maintain adherence to the social norm. Alternatively, or in combination with network policies (i.e., strategies that employ the characteristics of the network to achieve higher adherence to the social norm), the community may decide to employ traditional policy instruments such as taxes or subsidies. This research allows for policy options favoring the sustainable management of natural resources to be identified and targeted.

1.4 Main results

The main results of this thesis are:

1. New network generative model to simulate more realistic social networks. (**R1**)
2. Identification and ranking of factors impacting agent disposition to comply with a social norm. (**R2**)
3. Determination of resource management strategies that induce cooperation (community approach) and policies that improve the conservation of natural resources (policy approach). (**R3**)
4. Valuation, in monetary terms, of social pressure under variable social and environmental conditions. (**R4**)

1.5 Review of the literature

1.5.1 Social networks and their potential role in natural resource management

In many economic decision-making problems (i.e., decision-making in natural resource management), agent's acts are influenced by the group. Private outcomes dependent on group behavior are often referred to as peer effects (Ballester et al. [2006]). In situations of this kind, an extended model for rationality (Acemoglu et al. [2011]; Lamberson

[2009a]; Szabó and Fáth [2007]) is that agents not only take decisions depending on the payoff their given choice may yield, but also on the peer effects. A community of agents exploting a natural resource can be represented by a social network whose nodes are the economic agents and whose links represent their social interactions. The community is often very large in size, ranging from several thousand or tens of thousands of agents and links. Empirical observations (Barábasi and Albert [1999]; Clauset et al. [2009]; Faloutros et al. [1999]; Muchnik et al. [2013]; Newman [2003a]; Redner [1998]) have shown the complex structure of such social networks. Within the community, agents interact only with a subset of other agents (their peers), and peers tend to be heterogeneous across the members of the community. This results in agents having incomplete and asymmetric information about how all the other agents are acting which, in turn, means agents have to make assumptions and inferences about others' beliefs and what they are doing. As a consequence of its complex structure and an intricate decision-making process, collective behavior is difficult to predict.

Given the influence social interactions have on an agent's behavior, correctly understanding and describing social networks poses an important scientific challenge for the near future. In this direction, two new disciplines are attracting attention in the discussions concerning natural resource management, namely network science and economics of networks. Network science is well-suited to describe sociality in mathematical terms (Hyvonen et al. [2008]). Its strength lies in the inherent ability of networks to discard unnecessary details and capture the essence of social systems: the interactions between agents. The economics of networks (Bramoullé et al. [2014, 2016a]; Goyal [2007]) is a new field of network science that studies economic activities meditated by social relationships. Two important areas (Currarini et al. [2016]) here are (i) the emergence of a complex network structure as a result of agents' interaction, and (ii) the influence this underlying structure has on the collective behavior as a whole. The first question addressed here is related to what the incentives agents have to form a network by creating/modifying their interactions are. The second question appears to be a well-known characteristic of many economic problems, i.e. the role the network structure plays in the evolution of cooperation or the diffusion of new technologies.

Fortunately, social networks are observable phenomena that can be measured and analyzed using quantitative techniques. Advances in social networks analysis highlight that network structure cannot be characterized merely by the individual properties of agents, i.e. centrality. Most recent studies into social networks document patterns of interaction in the form of statistical properties (Newman [2002]). Interestingly, the

networks observed fall between the regularity of completely ordered lattices and the randomness of random networks (Erdős and Rényi [1960]). This finding reveals that there are mechanisms guiding social interactions and, ultimately, network formation. Furthermore, some statistical properties appear to be common in social networks: *small-world effect*, *scale-free*, *assortativity*, *transitivity* and *modularity*[2].

These properties play an important role in the economics of networks and the ways in which this discipline is linked to natural resource management. For example, *small-word* refers to topological distance. If a network is connected, there is a sequence of intermediate agents, or a path, between any two agents in the network. Small-world indicates that most pairs of agents within the network are connected by a short path. This property has direct implications on social learning, i.e. learning about the profitability of an innovation or how to use a new technology is predicted to be easier and faster in small-world networks. *Scale-free* implies few agents with a high number of links, often called *hubs*, and many other agents with a small number of links. In social networks, hubs have multiple alternative ways of finding information and thus they are relatively more advantaged (i.e., for innovation or learning). *Assortativity* is the result of *homophily*, or the tendency of agents to connect with similar agents. In the literature, this property usually refers to the level of interconnectivity between agents with similar number of links. Assortativity gives us information about network resilience. If a number of agents leave the network, the path length will increase, and ultimately some other agents that are still in the network will become disconnected. Isolated agents do not share information with the rest of network members. Disassortative networks are less resilient to such agent removal because hubs are more widely scattered across the network and many paths depend on them. Hence, assortativity has important implications on how communication flows and, finally, on the evolution of social learning. *Transitivity* (or local cohesiveness) sheds light on network formation. Unlike random networks, agents in social networks show transitive relations: "a friend of my friend tends to be my friend". The tendency of agents to tie in with closer agents breaks the network up into separate dense homogeneous subgroups. In the language of social networks, to be embedded within subgroups generates trust between the members. Trust promotes risk sharing and resource pooling, but also redundant information and negative lock-in. Subgroups are loosely connected to each other trough an excess of closure behavior. Cooperation, which is important in times of uncertainty or rapid change, can be accelerated by transitive relations, however, high

[2] An extensive explanation about statistical properties of social networks and how to measure them is given in Chapter 2.

levels of decentralization (*modularity*) slow down collective action within the network. High levels of separation between subgroups in the network can foster an attitude of "us against them", limiting their common ability to cooperate. Note that, with increasing decentralization, agents occupying bridging positions play an important role in cooperation.

The influence single aspects of a social network have on cooperation, such as the total number of cooperators, the density or size of the network, and the connectivity between agents, has been analyzed as isolated elements (Currarini et al. [2016]; Tavoni et al. [2012])[3], however, the influence and dynamics of a realistic network and its many facets has, as yet, not been studied in depth.

1.5.2 The evolution of social norms: Games played on networks

Natural resources and social norms are intrinsically dynamic. New approaches to natural resource management, such as adaptive management (Holling [1978]), cooperative management (Jentoft [2000]; Muse [1990]), collaborative management (Wondolleck et al. [2002]), and adaptive co-management (Olsson et al. [2004]), among others, share the same idea that social systems and natural systems are coupled and co-evolve in time. Berkes and Folke (McCarthy [2000]) develop the idea that the integrated social-ecological system must be the key analytical unit. This is because of the mutual feedback between the evolution of the social norms, the network structure, and the dynamic of the stock (Berkes et al. [2003]). In consonance with new approaches, we should describe natural resources as stocks whose laws of motion are affected by both natural factors and social behavior (Currarini et al. [2016]). On the other hand, one would expect that cooperative behavior not only spreads through the community according to social dynamics, but also according to stock dynamics. Consequently, cooperators would increase/decrease their pressure on non-cooperators in accordance with stock dynamics. However, the effects of stock dynamics on social pressure, and finally on cooperation, have not been thoroughly analyzed.

A first attempt to analyze the interplay between the emergence of cooperation and social networks was based on the evolutionary-game-theoretic approach. In its initial phase, the evolutionary game-theoretic approach was based on the premise that every agent can randomly meet any other agent, i.e., all agents are directly

[3]Factors other than the elements of a social network, but which favor disposition to comply with social norms, have been studied intensively in economics and other social sciences (Wenegrat et al. [1996], Hanaki et al. [2007]).

linked to each other. In terms of a social network, one would talk about a complete network. While this approach (Bowles [2004]) helped to understand the driving forces behind the emergence and preservation of cooperation, it does not take full account of the complexity, vicinity and segregation patterns that occur between agents when interacting in realistic social networks. For this reason, (Nowak and May [1992]) and (Szabó and Fáth [2007]) introduced a simple spatial structure where agents can interact only with their immediate neighbors. This new framework demonstrated that cooperation is evolutionarily viable within a narrow window of the specified parameters of the game. Nevertheless, this approach neglects empirical evidence (Amaral et al. [2000]; Jackson et al. [2017]) showing that agents are grounded in strongly heterogeneous networks with a great diversity among their neighborhood structure. To overcome the topological identity of the agents and to break up the underlying symmetry of the network structure, Santos et al. (Santos and Pacheco [2005]; Santos et al. [2006, 2012]) analyzed the emergence of cooperation in non-regular networks. Their results show that scale-free networks actively support the emergence of cooperation within a simple economic context.

In contrast to traditional ways of economic thinking, the evolutionary-game-theoretic framework assumes that the agents' rationality is limited and individual decisions are taken by comparing payoffs. The proportion of individuals choosing a particular behavior increases when the payoff for that behavior exceeds the average payoff in the population, and decreases when the reverse is true. Hence, behavior that performs badly from the individual's point of view is weeded out, while behavior that reaps benefits is imitated (Osés-Eraso and Viladrich-Grau [2007]; Sethi and Somanathan [1996]). Within the evolutionary-game-theoretic framework, little attention has been paid to how payoffs are determined. Payoffs could be based on short-term or long-term perspectives, depending on the degree of individual commitment to the interests of the collective. In a short-term perspective individual interests predominate, whereas a long-term perspective reflects the welfare of the collective. In the latter case, the payoff can be calculated as the outcome of a differential game. Finally, determining the optimal strategic response to, let us say, thousands of other agents (each of whom occupies a unique position in the social network) could, because of the complexity of the strategic decision problem, stretch the assumption of rationality beyond its limits. Therefore, the assumption of limited rationality seems reasonable to us if the social network is large and topologically complex.

Alternatively, economists have studied the behavior of agents constituting part of a social network within the framework of repeated games (Bramoullé et al. [2016b]; Haag

and Lagunoff [2006]). This strand of the literature establishes that cooperation can be maintained throughout the game if the defecting agents are sanctioned and excluded from cooperative benefits forever. The infinitely repeated games are framed as bilateral or multilateral prisoner dilemmas. While the results of these studies are interesting, their applicability to real life situations is limited because equilibrium is only found on the basis of grim trigger strategies within the set-ups of infinitely repeated prisoner dilemma type games (Bramoullé et al. [2016b]). Examples of successful cooperation (Sethi and Somanathan [1996]), however, show that these social networks are not based on grim strategies at all. Such repeated games are the repetition of static games and do not consider the evolution of a stock variable. Consequently, neither do they allow for the tragedy of the commons, where the evolution of a natural resource is a fundamental element of the problem being analyzed.

1.6 Outline

After this introduction (Chapter 1), the thesis is divided into three main chapters (Chapters 2-4) that address the research objectives, and a concluding chapter (Chapter 5). The four research questions (Q1-Q4) and the four main results (R1-R4) mentioned above, suggest the matrix shown in Table 1.1. Table 1.1 shows where each question and result are placed in the thesis. We now introduce the individual chapters.

In Chapter 2, "Influence of Fitness and Interaction Costs on Social Networks", we propose an efficient method for generating comparable and realistic networks. These networks will act as substrates for the evolutionary games proposed in Chapters 3 and 4. The aim of Chapters 3 and 4 is to analyze the influence social pressure within a network structure has on cooperation. Hence, in order to determine the exact influence network effects have on cooperation, we need to first generate an ordered sequence of realistic and comparable networks. In terms of realism, we observed that the complex structure of social networks is difficult to reproduce artificially and while traditional network generative models are recommended for analyzing the influence single properties of networks have on cooperation, they are, however, limited in terms of realism. In this chapter, we examine the mechanisms that determine how to generate realistic networks correctly. In terms of comparability, we propose an algorithm to simulate the evolution of social networks in time. The algorithm is based on *homophily*, or the tendency of agents to connect with similar agents (similar socioeconomic attributes). The resulting networks are scale-free networks with an increasing level of link correlations (assortativity, transitivity and modularity).

Chapter 3 is entitled "The Tragedy of the Commons and the Economics of Social Pressure". In this chapter, we study the effectiveness social sanctioning (social pressure) of resource overuse has in promoting sustainable extraction. Two types of agents, compliers (those who decide to follow the norm) and defectors (those who extract above the social norm) interact in realistic networks with increasing levels of link correlations (in accordance to Chapter 2). Both types of agents update their strategies based on utility differences. Compliers can reduce the utility of defectors using social pressure, and social pressure varies depending on the share of compliers in the neighborhood of agents, stock levels, and the level of cohesiveness between compliers. To quantify both network and stock effects in monetary terms, social pressure is multiplied by the extra benefits the defector gains as a result of incompliance. We refer to the economic loss compliers inflict on the defectors as *social punishment*. Social punishment allows us to analyze to what extent network effects contribute to overcoming the tragedy of the commons. It also allows us to determine the magnitude of error of a traditional "first-best" policy when network effects are not taken into account. Furthermore, our results suggest that one-time payments may help to overcome the tragedy of the commons.

Once factors and practices favoring cooperation have been identified, our aim is to answer the question of when different practices can be best applied. In Chapter 4, entitled "Tragedy of the Commons: Traditional Policy Instruments versus Network Policy", we study the three regimes of the stationary state of evolutionary dynamics: (i) all-defector equilibrium, (ii) all-complier equilibrium and (iii) the mixed equilibrium where both types of agents coexist; and how policies that disfavor defectors may lead to a stable cooperative stationary points. We use some representative types of networks (complete, scale-free and random networks) and identify three different policy corridors: (i) "no-policy", (ii) "network policy" and (iii) "traditional policy instruments". Corridors help us to determine the regions where different practices should be best applied. "Network policy" relates to initiatives that enhance the positive effects of social pressure, i.e., increasing the cohesiveness of compliers through seminars or workshops. "Traditional policy instruments" refers to traditional economic analysis (i.e., taxes or subsidies). Unlike network policy, economic incentives are focused on direct intervention in the form of initiatives that reduce/increase the payoff of a given choice. Results show large regions where both policies coexist, in other words, they can be applied indistinctly or in combination. The corridor "no-policy" means that there are sufficiently high levels of cooperation in the community to maintain sustainability.

Finally, Chapter 5 concludes by discussing the implications of this study and further research for the future.

Table 1.1 Framework of the thesis.

Questions	Chapter 2	Chapter 3	Chapter 4
Q1: Economic value of social pressure	**R1**	**R4**	**R4**
Q2: Network policy		**R2**	**R2**
Q3: Traditional policy instruments		**R3**	
Q4: Policy options			**R3**

Chapter 2

Influence of Fitness and Interaction Costs on Social Networks

Summary

Many social networks exhibit power law degree distribution with different levels of link correlations. Correlations are essential to understand spreading of information, trust or social pressure. However, the emergence of correlations is not well understood yet and thus there are no perfect network generative models reproducing the observed topology of social networks. In this study, we use socioeconomic information (fitness) of agents to drive their incentives for interaction. The distribution of fitness can be derived easily from empirical data where the parameter gamma of a power law cannot be observed. Thus, the study opens a door for modeling networks that can be empirically justified. In particular, we analyze the classes of fitness distribution over which a desired power law holds. We obtain that heavy-tailed fitness distributions generate power law networks efficiently. Moreover, existing links may be destroyed and new links may be created. If links are costly, one would expect that interaction costs would be lower between similar than dissimilar agents, implying that homophilous relations would be more stable and should be last longer. With our definition of link stability we provide new arguments to simulate the evolution of homophily in social networks. This study shows that homophily increases the levels of link correlations over time.

Keywords: Cost-directional rewiring; Evolving Networks; Fitness-based models

2.1 Introduction

Recent years have witnessed a burst in research on economics of networks (Bramoullé et al. [2014, 2016a]; Goyal [2007]), a new promising field of economics that analyzes the influence of social structure in economic activities, and how complex structure emerges in social systems (Currarini et al. [2016]).

The first question appears to be a prominent characteristic of many economic problems, i.e., evolution of cooperation or adoption of new technologies. The simplest way to represent the structure of a social system is the social network, whose nodes are the economic agents and links are their social interactions. Given that agents are involved in a wide variety of interactions, the totality of links in the social network characterizes the complex structure of the social system. Advances in network sciences have allowed to define social structure in the form of statistical properties of networks at different scales. At the macro-scale, the participation of an agent in the organization of the network is the most significant unit of analysis. The level of participation of an agent is often referred as her status, and measured by her degree (number of distinct links in the social network). Empirical observations (Barábasi and Albert [1999]; Clauset et al. [2009]; Faloutros et al. [1999]; Muchnik et al. [2013]; Newman [2003a]; Redner [1998]) have shown the power law pattern in the degree sequence of social networks. Contrary to random networks where most agents have comparable degree, in social networks a few highly connected agents (also called hubs) coexist with a large number of agents with small degree. At the micro-scale, some link correlations are observed. Agents tend to be linked to others who have *closer* characteristics, such as similar attributes (measured by assortativity[1] (Newman [2002])), and/or structural proximity (measured by transitivity (Newman [2003a])). Moreover, it has also been shown (Dorogovtsev et al. [2002]; Szabó et al. [2003]) an inverse proportionality between transitivity and degree, which means that hubs tend to have lower transitivity than the rest of agents. This inverse proportionality is often known as hierarchical clustering (Ravasz and Barabási [2003]). At the meso-scale, the tendency of agents to tie in with closer agents breaks the network up into separate dense and homogeneous communities (measured by modularity (Newman [2006])). The economic consequences of each of these properties can be reviewed in Jackson et al. (Jackson et al. [2017]).

The second question is motivated for the observed mode of organization. Social networks are in between the regularity of lattices and the randomness of random networks (Erdős and Rényi [1960]). This finding reveals the existence of distinct

[1] Assortativity, transitivity and modularity metrics are given in Appendix C.

ordering mechanisms behind complex structure, such as (i) network evolution, implying that social networks are not static and then agents may add/remove links to the network continuously in time; and (ii) microscopic dynamics, representing agent's preferences to connect to others with either high-attractive attributes or closer characteristics. Unfortunately, economics of networks has not yet given a satisfactory answer to the question of how complex structure emerge in a social system. As a consequence, traditional models of network formation fail in one way or another to reproduce at least one of the observed statistical properties. These models are useful tools for quantifying the influence of social structure in economic activities because artificial networks can be used for comparative purposes, however, they are limited in terms of realism.

In this study, we propose an extension of traditional models that helps to generate any number of *realistic* networks[2] which preserve the power law degree distribution and the hierarchical clustering, but present an increasing level of link correlations (assortativity, transitivity and modularity). To this extent, we revisit two popular approaches of network formation: preferential attachment (Barábasi and Albert [1999]; Price [1976]) and directional rewiring (Xulvi-Brunet and Sokolov [2004]). These approaches usually share a common trait; local rules for interaction are based on a macro-scale property (degree of agents) of networks. However, we argue that degree is a consequence and not a cause of network dynamics. In addition, we show that more flexible models can be constructed when local rules for interaction are based on a micro-scale property (fitness of agents) of networks.

The motivation behind our approach arises from the idea that fitness captures socioeconomic information of agents and may drive their incentives for interaction. Fitness is a numerical value that represents a large number of independent attributes of agents and its distribution within the population may be approximated by any statistical distribution. In our model, the original network is generated according to individual preferences to connect with higher fitted agents (preferential attachment) and then we perform successive link reconfigurations based on a cost function (cost-directional rewiring). Each of these reconfigurations generate a new network. The cost function is defined as the euclidean distance between fitness of linked agents, implying that links between similar agents (similar fitness) are more stable in time than links between dissimilar agents. In terms of stability, high-cost links have more probability to get cut and replaced. As a result of a dynamic process governed by the fitness of

[2]The term *realistic* is used to indicate that our model is able to generate artificial networks with statistical properties similar to those of real-world networks.

agents and the stability of links, the model generates comparable networks with an increasing level of link correlations.

Fitness-based network generative models are widely known in economic of networks literature (Bianconi and Barabási [2001]; Bianconi and Barabási [2001]; Caldarelli et al. [2002]; Nguyen and Tran [2012]; Servedio et al. [2004]), but little attention has been given to the necessary conditions to generate social networks efficiently. In this study, we analyze the range of densities (total number of links in the network) and the classes of fitness distribution over which the desired power law degree distribution holds. Once the classes of fitness distributions are identified, we analyze the effects of increasing fitness asymmetry in statistical and computational terms. A correct understanding of the restrictions of fitness distributions not only gives some insights on the microscopic dynamics that govern network evolution, but also allow us to improve the computational performance of network generative models. With our definition of link stability, we aim to provide new arguments to simulate the evolution of homophily ("like to associate with like") in a social system.

The study proceeds as follows. We discuss the related work in section 2.2. We describe the details of the model in section 2.3. The simulation results and possible applications are presented in section 2.4. We provide concluding remarks in section 2.5.

2.2 Related work

Since Price (Price [1976]) and Barabasi-Albert (Barábasi and Albert [1999]) models were published, it is commonly accepted that the power law degree pattern in social networks emerges as a result of a dynamic process in where networks grow monotonically and agents are involved in some sort of competition for links. The definition of social system as competitive system is motivated by the existence of hubs in social networks. In contrast to random networks, individual preferences for interaction seem to be biased[3], hence, not all agents are equally successful in acquiring links (Adamic and Huberman [2000]).

Althought competition is a good explanation for the emergence of the power law pattern, degree-based individual preferences lead to a correlation between the age[4]

[3]Similarly to biological systems, some agents seem to be more adapted to the social context. Those agents are more attractive to others. In the early models, attractiveness of agents is proportional to their degree; and the cumulative effects of preferential attachment increase the attractiveness of an agent because this agent is now more embedded within the network. This phenomenon is called "rich-get-richer" and induces the emergence of hubs.

[4]As the probability of selection increases linearly with degree, agents arriving earlier to the network become into the most attractive agents in the network and, finally, into hubs. Thus, when local

of the agents in the network and their degree (Krapivsky and Redner [2001]). Due to this correlation is not always realistic (Adamic and Huberman [2000]), different generalizations of the Barabasi-Albert model have been proposed during last years. One of the most interesting extensions of the model is the introduction of a fitness function that tries to represent the ability of agents to attract other agents. Thus, in this extension (Bianconi and Barabási [2001]; Bianconi and Barabási [2001]), fitness and degree jointly determine the preference of agents for interaction. However, further extensions (Caldarelli et al. [2002]; Nguyen and Tran [2012]; Servedio et al. [2004]) argue that often the information of agent's degree is hidden to agents or, when available, it is quite implausible that agents use this information when making connections. It is reasonable to expect, thus, there are many situations where link formation only depends on fitness[5].

High levels of assortativity, transitivity and modularity are usually observed in social networks, however, competition leads to dissortative networks. This means that competition is a necessary but not a sufficient driving force to generate more complex networks. To understand how link correlations appear in a social network one may think there are different types of agents in a population (high-attractive attributes, closer characteristics). Thus, the probability of interaction between agents depends not only on the attractiveness of agents but also on the individual preferences to connect with closer agents. However, link correlations do not clearly reflect the behavior of agents. Suppose the pair (ϕ_i,ϕ_j) represents the attributes of two linked agents i and j, for example, beliefs of climate change. In this case we cannot distinguish easily between different behaviors: (i) *homophily* (Jackson et al. [2017]) or link forming as a result of the pair (ϕ_i,ϕ_j) being similar, or (ii) *social influence* or the pair (ϕ_i,ϕ_j) becoming more similar as a result of the link. When attributes are either not malleable or else do not change appreciably on the time scale of interest, homophily is a good indicator of link formation (McPherson et al. [2001]). But, as recent studies (Bramoullé et al. [2012]; Jackson et al. [2017]) pointed out, we have an incomplete understanding of how homophily impacts network formation.

In absence of socioeconomic information, degree is a statistical property that is always available for every network (Newman [2003b]). Moreover, homophilous behavior based on degree has been proven as an efficient approach (Catanzaro et al. [2004];

rules for interaction are based on degree, the "rich-get-richer" phenomenon is equivalent to the "faster-get-richer" phenomenon.

[5]Following the analogy of biological systems, fitness represents the attributes of agents that are more associated with adaptation, i.e., experience. When attractiveness is proportional to fitness, the "rich-get-richer" phenomenon turns into the "fitter-get-richer" phenomenon. In this context, degree of agents has to be seen as a mere consequence of network dynamics.

Newman [2003b]) to increase the assortativity of networks. The downside is that these models fail when representing real transitivity trends (Liljeros et al. [2001]). For example, in Brunet et al. (Xulvi-Brunet and Sokolov [2004]) the rewiring step (Farkas et al. [2004]) produces networks with very small transitivity values, while Catanzaro et al. (Catanzaro et al. [2004]) cannot reproduce the power law degree distribution together with hierarchical clustering (Ravasz et al. [2002]).

On the other hand, correlation among nearby links (transitivity) is difficult to reproduce. The basic assumption when modeling cluster formation is closure behavior, an attempt to capture the evolution of agent interactions with structural constraints. This approach argues that the strong effect of individual preferences is mitigated in instances where agents are already proximate and then more available for interaction. Hence, the position of agents within the network may affect the ways in which they interact and this position depends in turn on choices they have made in the past. Note that structural proximity can be interpreted in different ways, (i) the shortest path length connecting agents or (ii) the "social interaction foci" (Feld [1981]) (group membership) that facilitates social interactions. In the simplest models, transitive relations arise by adding a "triad formation step" (Holme and Kim [2002]; Jin et al. [2001]) once the network has been constructed. If there exist a link between the pair of agents i and j, then one more link is added from i to a randomly chosen neighbor of j. Although triadic closure increases global transitivity of networks and allows closure of cycles greater than three (Kossinets and Watts [2009]), other aspects of closure behavior cannot be captured well (Jackson et al. [2017]). For example, link forming as a result of a chain of referrals or link forming as a consequence of group membership. The most important limitation in tiradic clousure models is that the power law degree distribution becomes increasingly weaker by adding new links to the network.

The interdependence between network properties, while non-trivial, may suggest that both homophilous and closure behavior are good candidates to explain community structure. However, high assortativity and/or transitivity values are not prerequisites to the existence of community structure, at least when considering modularity as an indicator of community structure.

Even though modularity optimization and other clustering techniques (Lancichinetti et al. [2008]) are efficient at discovering meaningful partitions within the network, there still is a disagreement on the necessary and sufficient conditions for the existence of community structure (Orman et al. [2013]). Thus, a formal definition of what a community is, and its possible identification in a specific network, will help to disclose unobservable mechanisms envolved in link formation.

This review focuses on limitations of some representative approaches to network formation suggesting that, while certainly useful, behavior of agents may have features that cannot be captured by the mechanisms described above. To this extent, Sendiña-Nadal et al. (Sendiña-Nadal et al. [2016]) recently proposed a new network generative model in which network structure emerges from exclusively microscopic growing assumptions, but individual preferences for connection are still based on degree.

2.3 The model

2.3.1 Network representation

Let (N, ω) be a link-weighted network, where $N = (A, L)$ is a simple connected network, and $\omega : L \to \mathbb{R}$ is a weight function. The network N consists of the finite set $A = \{1, ..., n\}$, $n \geq 2$, of agents and the set L of links, which are unordered pairs of elements of A. Link-weighted networks are widely used representations for numerous optimization problems, i.e., routing. One can find analogies to these networks when the stability of social interaction depends on a cost function. Even if it is not possible to derive a realistic cost function, heuristic considerations can be introduced to describe the ongoing cost of maintaining links. Let Φ_i be the fitness of any agent $i \in A$, $\omega(i, j)$ represents the cost of interaction between any pair of linked agents i and j, such that $\omega(i, j) =: \omega_{ij} = \sqrt{(\Phi_i - \Phi_j)^2} = |\Phi_i - \Phi_j|$, $(i, j) \in L$. Note that we are assuming that the cost of interaction is proportional to the social distance (measured as the euclidean distance) between connected agents. By definition, simple networks are undirected so that $\omega_{ij} \Leftrightarrow \omega_{ji}$. Moreover, agents are not linked with themselves (self-loops) and there is not more than one link between agent i and j (uniqueness of the link). For each agent i, $\mathcal{N}(i)$ denotes her neighborhood and $|\mathcal{N}(i)| = k_i$ her degree. If network N is connected, then for any pair of agents i and j there exist a finite sequence of agents $a_1, ..., a_M$ such that $a_1 = i$, $a_M = j$ and $a_{m+1} \in \mathcal{N}(a_m)$ for $m = 1, ..., M - 1$.

2.3.2 The power law degree distribution

Many social networks (Clauset et al. [2009]) are characterized by a degree distribution that can be approximated by the power law distribution, $p_k = k^{-\gamma}$, with scaling parameter $2 < \gamma < 3$ and k representing the degree of agents[6]. Despite the ongoing debate about the nature of the distribution that offers the best fit to empirical data, the

[6]In the reminder of this chapter, we use the term *scale-free regime* to mean that γ is in the range $(2, 3)$

power law pattern has arose much interest for its mathematical properties and physical interpretations. Among other distributions, the power law provides an attractive mathematical framework that helps to understand complex networks in simpler ways. Some properties of social networks, i.e., the ultra-small-world effect (Cohen and Havlin [2003]) and the degree differences between agents can be studied theoretically using the power law distribution because of their dependence to the scaling parameter and the size of the network.

Our model generates scale-free networks when the underlying fitness distribuion in the population is selected properly. We start from the observation that agent's attributes are an important factor for link formation (Jackson et al. [2017]). These attributes consist of biological and socioeconomic factors like gender, age, race, nationality, income, etc. The S attributes of each individual, denoted by Φ_i, can be expressed as a numerical value that falls within the interval of positive real numbers $(0, \infty]$. According to competition, the value of Φ can be understood as the ability of agents to attract links. Every agent i has individual attributes so that many agents differ from each other and form a heterogeneous population. In a heterogeneous population not all agents are equally attractive to others, which means agents with higher fitness tend to have higher degree[7].

The social network is generated link by link and the formation of a new link is decided by a stochastic decision rule. In contrast to other methods this network generation process has the advantage that it is endogenous, i.e., it depends on underlying distribution of the agents' attributes. As such it does not hamper the design of the micro-level structure of the network and provides sufficient freedom for variations at the micro-level structure as sought by this study.

The network generation process based on fitness is implemented by the following five steps:

1. Let N_0 be the initial (small) network which can be any network, and $|A_0| = n_0$.
2. Define as $0 < v \leq n_0$ the number of agents to whom a newcomer j may connect when she joins the network, and let $k_j = 0$ be the initial degree of a newcomer j.
3. At each step t of generation, $0 \leq t \leq n - n_0$, an agent i already present in the network is selected with a uniform probability $P_i = \frac{1}{n_0+t}$ that is independent of agent's i fitness Φ_i. If the newcomer j is already linked with agent i, repeat step 3.

[7] As it will be shown, degree of agents is very sensitive to: (i) the class of fitness distribution, (ii) the asymmetry of the fitness distribution, and (iii) the time at which agents arrive to the network.

4. With probability $P_i = \frac{\Phi_i}{\Phi_{max}}$ agent i connects to the newcomer j, where $\Phi_{max} = max\{\Phi_i\}_{i=1}^{n_0+t}$ denotes maximal value of the fitness of all agents in the network ($t \leq n - n_0$). Let us assign the value 1 to the decision to connect the newcomer to the existing network and 0 otherwise. For all randomly generated probabilities that are less than P_i the newcomer should be connected and otherwise not. To transform this decision rule into an operation rule we define the Bernoulli variable X that results from

$$X = \begin{cases} 1 & if \quad r \leq P_i \\ 0 & if \quad r > P_i \end{cases}$$

where r is randomly drawn number from the uniform distribution with $r \in [0, 1]$. This method is commonly known as the inverse transform method and is comparable with a forge coin where the probability to show up head (1) is P_i and tail (0) is $1 - P_i$. In case of rejection ($X = 0$), steps 3 and 4 are repeated. Likewise, steps 3 and 4 are repeated in case of acceptance in order to establish as many links as defined by v, i.e., until $k_j = v$.

5. Selection stops when $t = n - n_0$.

Although this algorithm is widely known, some requirements related to the outcomes have been less evidenced in the traditional models. Next, two complementary and necessary conditions are provided in order to generate networks according to the scale-free regime: (i) the sparsity of links, and (ii) the level of competition.

The sparsity of links

The choice of the parameter v allows defining the network density, d, and the average degree of the network, $\langle k \rangle$, since both parameters depend on v. More precisely, these properties are defined by $d = \frac{2(l_0+v(n-n_0))}{n(n-1)}$ and $\langle k \rangle = \frac{2(l_0+v(n-n_0))}{n}$, where $l_0 = |L_0|$ corresponds to the initial length of the set of links at $t = 0$. If the initial network is complete, it holds that $l_0 = \frac{n_0(n_0-1)}{2}$. As we are assuming that all agents add links at a constant rate v, it holds that $d = \frac{2v}{n-1}$ and $\langle k \rangle = 2v$. Each newcomer starts in the network with degree $k_j = 0$, however, as the network grows new links may be added so that the initial degree can be modified. Note that, at increasing v above a certain threshold the power law pattern becomes increasingly weaker. This threshold bounds the maximal number of links to be added at a constant rate by newcomers, v_{max}, and can be estimated using the natural cutoff of power law networks. Denote by $F(k) = Pr(K \geq k)$ the cumulative distribution function (CDF) of a power law

distributed variable, where again k represents the degree of agents. For instance, in the continuous case

$$F(k) = \int_k^{\infty} p(k)dk = \left(\frac{k}{k_{min}}\right)^{-\gamma+1} \tag{2.1}$$

and the integral of $p(k)$ over two different degrees

$$F(k) = \int_{k_1}^{k_2} p(k)dk \tag{2.2}$$

provides the probability that a randomly chosen agent has degree between k_1 and k_2. To calculate k_{max} we assume that in a network of n agents we expect at most one agent whose degree exceeds k_{max}, then

$$F(k) = \int_{k_{max}}^{\infty} p(k)dk = \left(\frac{k_{max}}{k_{min}}\right)^{-\gamma+1} = \frac{1}{n} \tag{2.3}$$

this yields

$$k_{max} = k_{min} n^{\frac{1}{\gamma-1}} \tag{2.4}$$

and by inverting eq. 2.4 in the limits, $2 \leq \gamma \leq 3$, we obtain

$$\begin{cases} \frac{k_{max}}{n} = k_{min} & \text{if} \quad \gamma = 2 \\ \\ \frac{k_{max}}{\sqrt{n}} = k_{min} & \text{if} \quad \gamma = 3 \end{cases} \tag{2.5}$$

Neither self-loops nor multiple links are allowed in our network so that $k_{max} < n$. Let $k_{max} = n - 1$ represent the extreme case in where all agents are connected to the highest-fitted agent (except herself). Let us assume that in a heterogenous population there always exist an agent with fitness very low and thus her ability to attract links nears zero. This agent with minimum degree has exactly v links, so $k_{min} = v$ in the network. Introducing $k_{max} = n - 1$ and $k_{min} = v$ in eq. 2.5, the number of links to be added at a constant rate by newcomers before power law becomes weaker falls into the range

$$1 \leq v < \sqrt{n} \tag{2.6}$$

In other words, if we want $2 < \gamma = \frac{ln(n)}{ln\left(\frac{k_{max}}{k_{min}}\right)} + 1 < 3$, we need $1 \leq k_{min} = m < \sqrt{n}$. Notice that $1 < k_{max} < n$. When k_{max} nears the network size, $k_{max} \to n$, the CDF of the degree sequence does not follow the power law distribution, however, it serves to

define the upper limits of density. As we can observe, scale-free networks are sparse networks with density very low $\frac{2}{n} < d < \frac{2}{\sqrt{n}}$.

The level of competition

The number and size of hubs are determined by the level of competition in the population. Without loss of generality, we use $v = 1$ at each time step; increasing v (within the range $v \in [1, \sqrt{n})$ would just result in higher density, neither changing the level of competition nor the emergence of power law pattern. By introducing $v = 1$ in eq. 2.5 we obtain that $\sqrt{n} < k_{max} < n$ and eq. 2.4 shows the larger a network, the larger the degree differences between the agent with the smallest degree k_{min} and the largest hub k_{max}.

Our first interest is in the largest hub satisfying $k_{max} > \sqrt{n}$. Note that an increasing level of competition makes the hubs smaller and less numerous, consequently the degree sequence $\{k_1, k_2, ..., k_n\}$ leaves the scale-free regime, $\gamma > 3$. The size of the hub is affected by the level of competition because the probability of highest-fitted agents being selected decreases as fitness becomes similar in the population. It results in agents having similar degrees and $k_{min} \sim k_{max}$ in the network. As described before, the probability of selection of any agent i in a single attempt equals $P_i = \frac{\Phi_i}{n'\Phi_{max}}$, where $n' = n_0 + t$ denotes the number of agents in the network at a given time step, however, several first attempts might fail thus we need to compute selection in unsepecified number of attempts as suggested in (Lipowski and Lipowska [2012])

$$P_i = \frac{\Phi_i}{n'\Phi_{max}}(1 + \tau + \tau^2 + ...) \tag{2.7}$$

where $\tau = \frac{1}{n'}\sum_{i=1}^{n'} 1 - \frac{\Phi_i}{\Phi_{max}} = 1 - \frac{\langle\Phi\rangle'}{\Phi_{max}}$ is the rejection probability and $\langle\Phi\rangle' = \frac{\sum_{i=1}^{n'}\Phi_i}{n'}$ is the average fitness in the network. Due to convergence $(0 < \tau < 1)$ we can compute the probability of selection of any agent i as

$$P_i = \frac{\Phi_i}{\sum_{j=1}^{n'}\Phi_j} = \frac{\Phi_i}{n'\langle\Phi\rangle'} \tag{2.8}$$

Define by $\Psi_i = \frac{\Phi_i}{\langle\Phi\rangle'}$ the intensity of attraction of agent i with respect to the others. When agents are equally fitted, we obtain $\Psi = 1$ for all agents and this value is constant over time. In this situation, the population is under symmetrical competition. The system behaves similarly to random networks and P_i follows the harmonic series $P_i = (\frac{1}{T}, ..., \frac{1}{n-1})$, $0 < P_i \leq 1$, where T is the arriving time, in other words, the time at

which agent i joins the network. When network grows, $t > T$, the probability of being selected decays proportionally to the network size. The expected degree of agent i, $\mathbf{E}(k_i)$, is a sum of $n - T$ independent but non-identical Bernoulli distributed variables that follows the Poisson's binomial distribution with mean and variance (Wang [1993])

$$\begin{aligned} \mathbf{E}(k_i) &= \mathbf{E}\left[\sum_{t=T+1}^{n} X_t\right] = \sum_{t=T+1}^{n} \mathbf{E}\left[X_t\right] = \sum_{t=T+1}^{n} P_t \\ \mathbf{Var}(k_i) &= \sum_{t=T+1}^{n} P_t\left(1 - P_t\right) \end{aligned} \tag{2.9}$$

Hence, we can estimate $\mathbf{E}(k_i)$ as the sum of the harmonic series such that $\mathbf{E}(k_i) = \sum_{t=T+1}^{n} \frac{1}{t} \simeq ln\left(\frac{n-1}{T}\right)$. Relative to T, agents with similar fitness but higher age (higher $n - T$ range) increase their probabilities to acquire more links.

Symmetrical competition cannot generate power law networks. The expected degree of any agent i in the population is $\mathbf{E}(k_i) \simeq v$ because the expected arriving time for any agent is $T_i = \frac{n}{2}$, and thus $P_i \approx 0$ at each time step. The expected largest degree is $\mathbf{E}(k_{max}) \simeq ln(n-1)$ because agent arriving at $T = 1$ maximizes her probabilities for k_{max}. The resulting degree sequence follows the exponential distribution with $k_{max} < \sqrt{n}$.

At the other extreme, when only agent i compete for links, there is complete asymmetrical (monopolistic) competition. In the monopolistic model, the expected largest degree is $\mathbf{E}(k_{max}) \equiv \mathbf{E}_k(\Phi_{max}) \simeq \frac{n}{2}v = \frac{n}{2}$, where $\mathbf{E}_k(\Phi_{max})$ represents the expected degree of the highest-fitted agent in the population. Although the size of the largest hub satisfies $k_{max} > \sqrt{n}$, the degree sequence does not follow the power law distribution because the rest of agents have degree $k = v = 1$.

It has been shown that fitness (Φ) and the arriving time (T) jointly determine degree and that, in contrast to degree-based models, in our approach it may occur that the later selected agents gain more links compared with the initially selected agents. Thus, fitness-based models reduce the positive correlation between age and degree in the network. The above examples of competition represent two ends of a continuum along which one can find a variety of dynamics influenced by the underlying fitness distribution that generates different number and size of hubs.

To determine the level of competition in any social system, we focus on the higher fitted agents in the population and when they join the network. Let us define $Q = \{q_1, ..., q_l\}$, $Q \subset A$, as the subset of higher fitted agents in the population. Each q agent is called *attractor* or potential leader. Let ξ be the number of time steps required for an attractor to join the network (success), then the probability that the $t - th$ time

step is the first success is $Pr(\xi = t) = (1-p)^{t-1}p$, each with success probability p. The average number of time steps required for first success is the expectation value of ξ

$$\mathbf{E}(\xi) = \sum_{t=1}^{\xi} t(1-p)^{t-1}p = p\left(\frac{1}{p^2}\right) = \frac{1}{p} \tag{2.10}$$

and $p = F(\Phi)$, where $F(\Phi)$ is the CDF that represents $F(\Phi) = Pr(\Phi > \Phi')$, Φ' is a threshold fitness, in any probability distribution $\rho(\Phi)$. In other words, and depending on the distribution, p may represent the fraction of outliers in $\rho(\Phi)$.

Let $\{\xi_1, \xi_2, ..., \xi_l\}$ be the number of time steps to different q successes. Each ξ_q is a geometric variable with success probability $p = F(\Phi)$. So, $\mathbf{E}(\xi_q) = \frac{1}{p}$ for each q. Now let Y be the number of the $l-th$ success, where $Y = \sum_{q=1}^{l} \xi_q$, then

$$\mathbf{E}(Y) = \mathbf{E}\left(\sum_{q=1}^{l} \xi_q\right) = \sum_{q=1}^{l} \mathbf{E}\left(\xi_q\right) = \frac{l}{p} \tag{2.11}$$

Attractors are expected to arrive to the network at a constant rate $t = (T, 2T, ..., lT)$, $T = \mathbf{E}(\xi_q) = \frac{1}{p}$. Given that scale-free regime requires few hubs coexisting with a large number of agents having small degree, our interest is in asymmetrical competition with $1 < l << n$ attractors. According to this, we can say that any particular fitness distribution $\rho(\Phi)$ supports the scale-free regime if and only if its outliers become hubs sufficiently large and numerous to have a significant impact on the degree sequence. While outliers represent a small fraction of the population, their number and attractiveness to others depend on the nature and restrictions of $\rho(\Phi)$.

Note that, moving away from the monopolistic model, $\hat{k}_{max} \equiv \mathbf{E}(k_{max}) < \frac{n}{2}$, and according to eq. 2.5 and eq. 2.6, parameter v is being reduced and thus $1 \leq v < \frac{\hat{k}_{max}}{\sqrt{n}} = \frac{\sqrt{n}}{2}$. This means that density is also reduced $\frac{2}{n} < d < \frac{1}{\sqrt{n}}$.

2.3.3 Increasing link correlations in the network

Based on homophilous behavior, Xulvi et al. (Xulvi-Brunet and Sokolov [2004]) proposed a method to generate networks with increasing correlation patterns. In their original algorithm, directional rewiring is drived by agent's degree and, at each time step, two links are selected in the network at random. With probability P, rewiring is applied only if it increases assortativity. Otherwise, with probability 1 - P, rewiring is random. However, this method generates small transitive relations and destroys the hierarchical clustering in the network.

Alternatively, we suggest that homophily would be related to a cost-link-minimization condition. According to Leenders (Leenders [1996]) and Kossinets (Kossinets and Watts [2009]) works, one would expect that the ongoing cost of maintaining connections would be lower between similar than dissimilar agents, implying that homophilous relations would be more stable and should be last longer. Lower costs are related to the fact that similarity of attributes simplifies the process of communicating with and predicting the behavior of others (Hamm [2000]).

In our algorithm, the social distance of connected agents helps us to define the cost of interactions and drive homophilous behavior. Cost-directional rewiring is applied after preferential attachment because competition leads to power law and dissassortative networks. In such networks, most of the links are connecting agents with large fitness differences (large social distance) and therefore have associated high costs of maintenance. At each time step, we simulate the tendency of agents to reduce their connection costs in the network over time. When two links are selected, there exist three possible configurations for rewiring. Denote by $C_\kappa = \{(i_\kappa, j_\kappa) : i_\kappa < j_\kappa\}$, $\kappa = \{1, 2, 3\}$, the set of all possible link configurations. We order them with respect to their aggregate cost e_{C_k}, where $e_{C_\kappa} = \sqrt{\sum_{(i_\kappa, j_\kappa) \in C_\kappa} (\Phi_{i_\kappa} - \Phi_{j_\kappa})^2}$.

Cost-directional rewiring is an extension of (Xulvi-Brunet and Sokolov [2004]) work in which we propose two main modifications from the original algorithm: (i) instead of stochastic acceptance, our algorithm selects the configuration of links C^*_κ that minimizes the aggregate cost function $e^* = min\{e_{C_1}, e_{C_2}, e_{C_3}\}$ of the selected agents; and (ii) homophilous behavior is based on fitness, not in degree, so the more similar the pair (Φ_i,Φ_j) the lower the cost function is.

Starting from the original power law network, cost-directional rewiring (Fig.2.1) works as follows:

1. At each rewiring step, two links connecting four different agents are selected with uniform probability $\frac{1}{|L|=l}$.

2. The original configuration of links is denoted by C_1 and its aggregate cost by e_{C_1}. The algorithm evaluates the other two alternative configurations, e_{C_2} and e_{C_3}, and selects the configuration with lowest aggregate cost e^*. After rewiring, C^*_k represents the most stable distribution of connections between agents such that the higher fitted agents are connected and the lower fitted agents are connected. In the case that one or both links already existed in the network, step 2 is discarded and step 1 is repeated.

3. Rewiring stops when the desired level of link correlations has been reached.

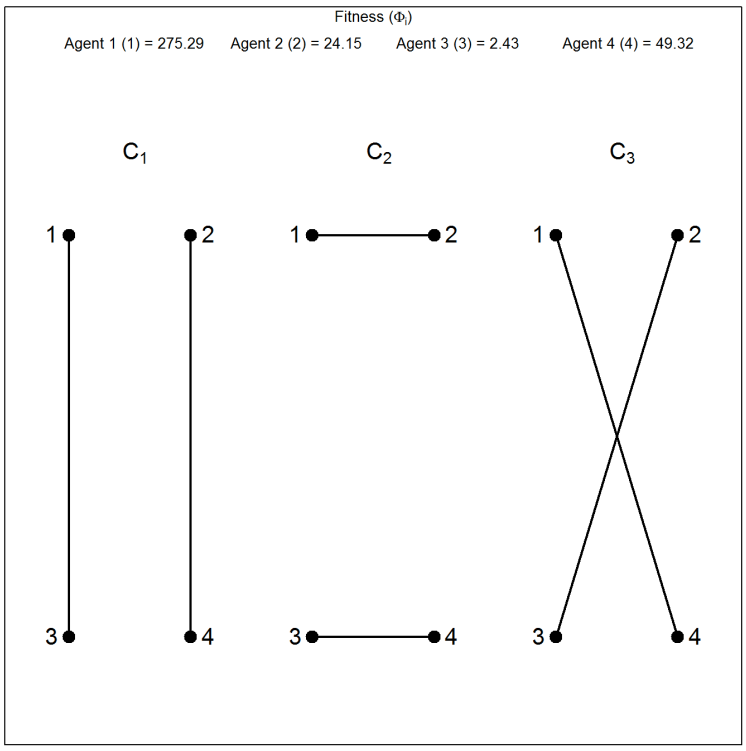

Fig. 2.1 Cost-directional rewiring.

Reconfiguration of links that reduces preferential attachment and increases the stability of connections. The plot shows all possible configurations (C_1, C_2, C_3) of two links connecting four agents $(1, 2, 3, 4)$. The first configuration C_1 corresponds to the pair of links with highest costs in the network. The other two configurations (C_2, C_3) are the alternatives for rewiring. Each configuration has associated an aggregate cost of connections $e_{C_1} = 274.02,\ e_{C_2} = 255.48,\ e_{C_3} = 227.01$. We select the configuration of links that minimizes that cost. In the example, the minimum aggregate cost is $e_{C_3} = e^*$ thus configuration $C_3 = C_k^*$ is selected.

Let $\theta = \sum_{u=1}^{\ell} \omega_u$ be the global cost function in the network, where $\ell = |L|$ is the total number of links. The evolution of θ over time can be described as $\theta(t+1) = \theta(t) - \Delta e(t+1)$, and $\Delta e(t+1) = e_{C_1}(t) - e^*(t)$. As we are minimizing the cost of interactions, we obtain that $\Delta e(t+1) \geq 0$ and then θ is a decreasing function $\theta(t+1) \leq \theta(t)$. Assuming there are no local minima, we have that $\theta(0) = max\left\{\theta\right\}_{t=0}^{t'}$ and $\theta(t') = min\left\{\theta\right\}_{t=0}^{t'}$, where t' represents the time at which the algorithm stops. This means we are obtaining more stable interactions in the network over time. The parameters t' and θ can also be used to stop the algorithm.

In section 4 we show that repeated application of cost-directional rewiring step leads to networks with increasing assortativity, modularity and transitivity. This process does not change the density and the degree pattern in the original network.

2.4 Simulation results

2.4.1 Influence of fitness distribution in competition

Following our model, we investigate the restrictions on the classes of fitness distribution which support the power law degree pattern. To measure the effect of fitness choices, $n = 10000$ random numbers are drawn from desired distributions. These numbers represent the fitness of agents and are used to generate the network. We perform 10000 repetitions of each desired distribution according to Appendix A, and generate the corresponding 10000 networks according to section 2.3.2. Once networks have been constructed, we anaylze statistically whether the resulting degree sequences can be succesfully fitted by the power law distribution. The statistical framework for quantifying the power law approximation is briefly presented in the Appendix B of this paper. Results are shown in Table 2.1 for the normal, uniform, exponential, stretched exponential, truncated normal, log normal and power law distributions.

Although network analysis provides guidance to the modeler, it is computationally very demanding, thus, we propose a complementary method to estimate the level of competition in a social system. The method proceeds as follows: for a given distribution, we select the agent $\hat{i}$ with the highest probability to become the largest hub in the network and use eq. 2.9 to make predictions, such that $\mathbf{E}(k_{max}) \approx \Psi_{\hat{i}} ln\left(\frac{n-1}{T_{\hat{i}}}\right)$ if $\Psi_{\hat{i}} < T_{\hat{i}}$; otherwise $\mathbf{E}(k_{max}) \approx \Psi_{\hat{i}} ln\left(\frac{n-1}{\Psi_{\hat{i}}}\right) + (\Psi_{\hat{i}} - T_{\hat{i}})$. To evaluate the quality of our predictions, the intensity of attraction and the arriving time of agent $\hat{i}$ are averaged over 10000 repetitions of each fitness distribution. Once $\langle \Psi_{\hat{i}} \rangle$ and $\langle T_{\hat{i}} \rangle$ are obtained from the entire population, the corresponding expected degree $\mathbf{E}(k_{\hat{i}})$ is compared to the average degree of the largest hub, $\langle k_{max} \rangle$, obtained from network simulations.

The selection of agent $\hat{i}$ depends on the nature of the fitness distribution, however, the ratio $\Psi_{\hat{i}}$ is always fluctuating while network is being constructed ($n' < n$). For the sake of simplicity, we prove that those fluctuations are small and decreasing with network's growth ($n' \to n$) and, thus, our predictions are not significantly affected.

Symmetric distributions

Many classes of fitness distributions display symmetry, such as normal, Cauchy, uniform or logistic distribution. Symmetric distributions have in common that they are never skewed distributions, thus, the intensity of attraction of all agents is of the same order of magnitude and competition is always close to be symmetrical too. In such distributions, agents can only increase their degree by decreasing their arriving time. Next, we study the normal distribution or, in other words, the effects of symmetry about the mean on competition. Normal distribution offers good economic interpretation of fitness values. We started assuming that fitness Φ_i of any agent i was defined by a reasonably large variety of socioeconomic arguments acting independently of one another. If additive effects on fitness are considered, then Φ_i will be normally distributed irrespective of the manner in which the individual arguments are distributed. The fitness can be written as $\Phi_i = \sum_{s=1}^{S} \phi_s$, $\forall i \in n$ and $\phi_s \in \mathbb{R}_+$. Arguments describe attributes like educational level, nationality, socioeconomic status, age, etc.

In the normal distribution, the majority of fitness values fall within two standard deviation of the mean. Moreover, in our model the fitness is restricted to be a positive real number, $\Phi \in \mathbb{R}_+$, such that the intensity of attraction of all agents is approximately bounded within the interval, $\Psi \in (0, 2]$, because $\Phi_{max} \simeq 2 \langle \Phi \rangle$. According to the fitness, agents with fitness about the mean are more numerous in the population and, thus, the first agent arriving to the network is likely to be one of those agents. According to the arriving time, the agent who arrives first to the network has on average higher probabilities to become the largest hub[8]. Fig.2.2 shows that degree of agents is not positively correlated to the fitness in the normal distribution. As expected, agents with fitness about the mean have larger degree.

[8]Note that, under symmetrical competition, the probability of being selected P_i is very sensitive to the size of the network and thus degree of agents is basically increased at early stages when the network is small ($n' << n$).

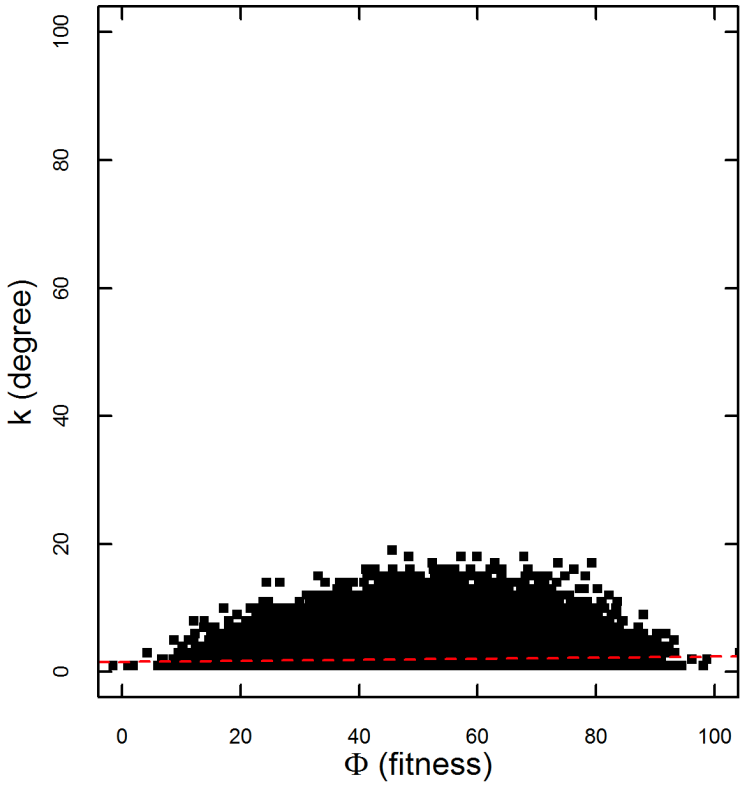

Fig. 2.2 Effect of fitness on degree.

Each data point gives the fitness of agents and their corresponding degree after the network has been constructed. The plot shows all data from 10000 simulations with the same fitness distribution ($Norm(\mu = 50, \sigma = 10)$). A trend is observed that degree of agents reaches maximum values when fitness of agents are about the mean. Read line indicates there is not positive correlation ($r^2 \simeq 0.05$) between the micro-level (fitness) and macro-level (degree) properties of networks.

To make predictions[9], we select the first agent arriving to the network as our agent $\hat{i}$, such that $\Psi_{\hat{i}} \approx 1$ and $T_{\hat{i}} = 1$, and therefore $\mathbf{E}(k_{max}) \equiv \mathbf{E}(k_{\hat{i}}) \approx ln\,(n-1)$.

[9]The restriction $\Phi \in \mathbb{R}_+$ bounds Ψ and makes the standard deviation of the population small. Consequently, the standard error of the mean, $SE_{\langle\Phi\rangle} = \frac{\sigma}{\sqrt{n'}}$, is also small even at early stages ($n' << n$). Let σ denote the standard deviation of the population and n' the number of agents already in the network once the key agent $\hat{i}$ joins the network. Even when $n' = 1$, if σ is small, $SE_{\langle\Phi\rangle}$ is also small. This means that fluctuations around the ratio $\Psi_{\hat{i}} = \frac{\Phi_{\hat{i}}}{\langle\Phi'\rangle}$ are of no significance because $\langle\Phi'\rangle \approx \langle\Phi\rangle$ at each time step. Note that fluctuations decrease as network grows because $SE_{\langle\Phi\rangle}$ decreases at each time step ($n' \to n$).

To test our predictions, we start generating 10000 normal distributions. We then choose every first agent in the list of numbers emulating how agents arrive to the network. As an example, we use $\rho(\Phi) = Norm(\mu = 50, \sigma = 10)$, and obtain that $\langle \Psi_{\hat{i}} \rangle = 0.99$, which in turn results in $\mathbf{E}(k_{max}) \approx 0.99ln\,(9999) = 9.12 \pm 2.85$.

After that, we generate 10000 power law networks according to our network generative model. Table 2.1 shows the results of our model when fitness of agents follows the same normal distribution as before, such that $\rho(\Phi) = Norm(\mu = 50, \sigma = 10)$. In Table 2.1, the degree of the largest hub is averaged over 10000 networks and results in $\langle k_{max} \rangle = 14.5 \pm 1.5$.

As it can be observed, our predictions and values from networks yield similar results about the size of the largest hub in the networks. Similar results can be obtained for other symmetric distributions, i.e., the uniform distribution (Table 2.1). Symmetric distributions cannot generate power law networks because attractors do not dominate competition and therefore $\mathbf{E}(k_{max}) < \sqrt{n}$ in all the cases.

Exponential distributions

The tail in exponential distributions goes to zero rapidly, which means that attractors have similar fitness and their fitness is only one order of magnitude higher than the population mean. Competition is now in a transition regime in where T (faster-get-richer) and Φ (fitter-get-richer) jointly determine the degree of agents. In this situation, one may expect that the first attractor joining the network has higher probability to become the largest hub in the network.

To make predictions[10], we first define attractors as the outliers of the exponential distribution. Their fitness has to be higher than a threshold fitness, which is defined as $\Phi_q > \Phi' = \langle \Phi \rangle + 3\sigma$. Second, we select the first attractor arriving to the network as our agent $\hat{i}$, and estimate the degree of the largest hub as $\mathbf{E}(k_{max}) \approx \Psi_{q_1} ln\left(\frac{n-1}{T_{q_1}}\right)$.

To test our predictions, we start generating 10000 exponential distributions. After that, we choose every first attractor in the list of numbers, emulating how they arrive to the network. As an example, we use $\rho(\Phi) = Exp(\lambda = 100)$, and obtain that $\langle \Psi_{q_1} \rangle \approx 5$ and $\langle T_{q_1} \rangle = 55$, which in turn results in $\mathbf{E}(k_{max}) = 26.1 \pm 5.1$. After that, we generate 10000 power law networks according to our network generative model. Table 2.1 shows the results of our model when fitness of agents follows the same exponential distribution.

[10]Like in the normal distribution, the standard error of the mean $SE_{\langle \Phi \rangle}$ is still small because σ although higher is still small. Again, fluctuations over the ratio $\Psi_{\hat{i}}$ are of no significance and decreasing with time.

In Table 2.1, the degree of the largest hub is averaged over 10000 networks and results in $\langle k_{max} \rangle = 31.0 \pm 5.7$.

As it can be observed, our predictions and values from networks yield similar results about the degree of the largest hub in the networks. Similar results can be obtained for the normal truncated distribution (Table 2.1). Our results suggest that none of those distributions can generate the desired networks because again $\mathbf{E}(k_{max}) < \sqrt{n}$.

Heavy-tailed distributions

The tail in heavy-tailed distributions decays slower that in exponential distributions, and one often encounters agents characterized by very large fitness values. Fig.2.3 shows that fitness of the highest-fitted agent in the log normal distribution is several order of magnitude higher than the population mean. Competition is now dominated by the fitter-get-richer phenomenon and, thus, the higher the fitness of agents the higher the probability is they become hubs, even when T is large. In this case, we use the highest-fitted agent in the population as the key agent $\hat{i}$, such that $\mathbf{E}(k_{max}) \equiv \mathbf{E}_k(\Phi_{max}) \approx \Psi_{max} ln\,(2)$, because the expected arriving time for this agent is $T = \frac{n}{2}$.

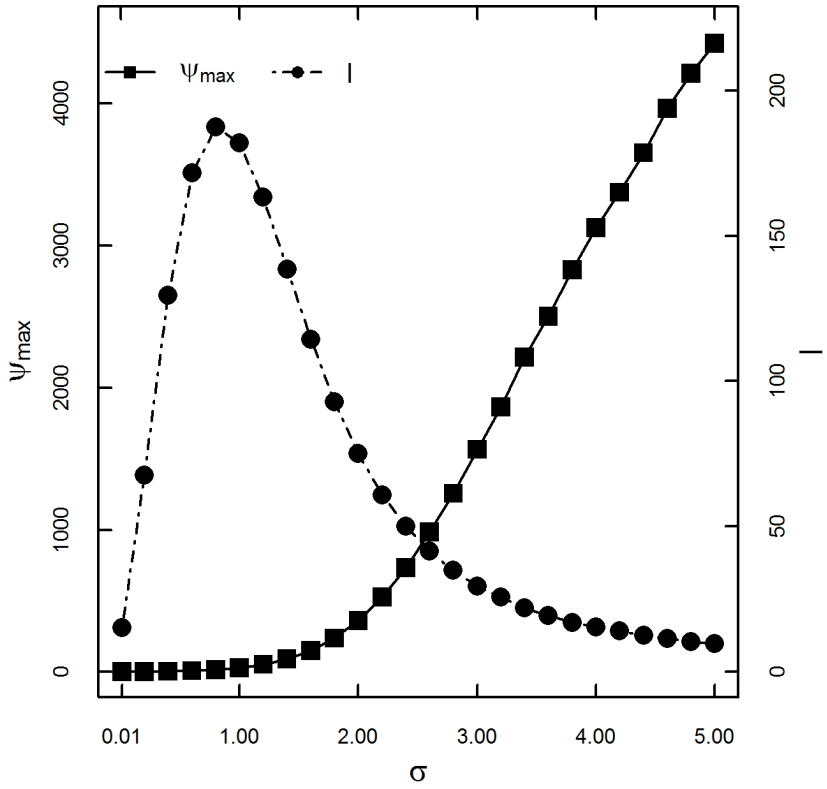

Fig. 2.3 Transition from symmetrical to monopolistic competition.

In log normal distribution, the higher σ (measured in log scale) the higher the ratio Ψ is, however, we decrease the fraction of attractors (l). When $\Psi_{max} > \frac{n}{2}$ and l too small ($\sigma \geq 5$), the system behaves as expected in the monopolistic model. On the other hand, when $\Psi_{max} \sim 1$ ($\sigma \leq 0.5$), the system behaves as expected in symmetrical competition.

In this study, we analyze three of the most representative heavy-tailed distributions: the log normal, the power law and the stretched exponential. We will focus on the log normal distribution because this distribution offers good economic interpretation of fitness values. Again, we assume that fitness Φ_i of any agent i is defined by a reasonably large variety of socioeconomic arguments acting independently of one another. If multiplicative effects on fitness are now considered, then Φ_i will be log normally distributed, irrespective of the manner in which the individual arguments are distributed. The fitness can be written as $\Phi_i = \prod_{s=1}^{S} \phi_s$, $\forall i \in n$ and $\phi_s \in \mathbb{R}_+$. Arguments describe attributes like educational level, nationality, socioeconomic status, age, etc.

When fitness is distributed according to $\rho(\Phi) = Lognorm(\mu = 0, \sigma = 2.5)$ we obtain that the intensity of attraction of the highest-fitted agent is on average $\langle \Psi_{max} \rangle \approx 830.6$, and her expected degree is $\mathbf{E}(k_{max}) \equiv \mathbf{E}_k(\Phi_{max}) \approx 584.1 \pm 22.7$. Likewise, when $\rho(\Phi) = Lognorm(\mu = 0, \sigma = 3.5)$, we obtain that $\langle \Psi_{max} \rangle \approx 2340.4$ and $\mathbf{E}(k_{max}) \approx 1622.2 \pm 32.9$. These values are averaged over 10000 repetitions. Similar values are obtained analytically for the same distributions, such that $\langle k_{max} \rangle \approx 792.3 \pm 607.4 (2093.9 \pm 1324.3)$. The degree of the largest hub is averaged over 10000 networks. Identical predictions can be done for the other two distributions.

Table 2.1 shows that these three distributions are good candidates to generate power law networks because not only the resulting hubs are large enough, $\mathbf{E}(k_{max}) > \sqrt{n}$, but also the degree sequence can be approximated well by the power law distribution (Table 2.1 and Fig.2.4A). Once we have identified the classes of fitness distributions that can produce the desired level of competition in the population, we need to provide arguments to generate power law networks efficiently.

Table 2.1 Basic parameters of fitness generation and the resulting degree distribution.

Null hypothesis (H_0) is power law a plausible fit to the degree distribution. Data show the results over 1000 simulations. We follow the methodology described in Clauset et al. (Clauset et al. [2009]), where high $p - values$ indicate that the null hypothesis is likely to be correct. The hypothesis is accepted only when $2 < \langle \gamma \rangle < 3$ and $\langle p - value \rangle > 0.1$. For the case of the truncated normal distribution ($NormT(\mu, \sigma, lower, upper)$) one can use the formula of normal distribution described in Table 2.2 (Appendix A) and then accept or reject random numbers if they falls in $lower \leq r \leq upper$ or not respectively. Repeating the process until a number is accepted gives Φ with the appropriate distribution.

$\rho(\Phi)$	$\langle \sigma_k \rangle \pm \sigma$	$\langle k_{max} \rangle \pm \sigma$	$\langle k_{min} \rangle \pm \sigma$	$\langle \gamma \rangle \pm \sigma$	$\langle p - value \rangle \pm \sigma$	H_0
$Exp(100)$	1.87 ± 0.03	31.02 ± 5.73	7.33 ± 2.35	4.22 ± 0.64	0.42 ± 0.34	Rejection
$ExpS(100, 0.3)$	7.01 ± 1.25	362.73 ± 181.85	2.34 ± 1.42	2.15 ± 0.04	0.21 ± 0.13	Acceptance
$Uni(0, 1000)$	1.47 ± 0.01	16 ± 1.18	7.33 ± 1.54	6.42 ± 1.40	0.53 ± 0.34	Rejection
$Lognorm(0, 1)$	2.23 ± 0.14	61.03 ± 26.20	5.63 ± 1.77	3.36 ± 0.28	0.40 ± 0.32	Rejection
$Lognorm(0, 1.5)$	3.93 ± 0.55	175.29 ± 74.48	2.71 ± 1.57	2.55 ± 0.16	0.29 ± 0.29	Acceptance
$Lognorm(0, 2)$	7.79 ± 3.10	486.82 ± 376.09	2.34 ± 1.09	2.38 ± 0.12	0.44 ± 0.35	Acceptance
$Lognorm(0, 2.5)$	12.21 ± 5.38	792.34 ± 607.38	3.48 ± 0.94	2.12 ± 0.05	0.57 ± 0.29	Acceptance
$Lognorm(0, 3)$	19.03 ± 7.86	1414.45 ± 907.47	3.71 ± 2.20	2.09 ± 0.36	0.57 ± 0.32	Acceptance
$Lognorm(0, 3.5)$	26.61 ± 11.68	2093.86 ± 1324.27	3.12 ± 1.78	2.41 ± 0.86	0.46 ± 0.37	Acceptance
$Pl(1, 1.75)$	22.83 ± 13.30	1712.00 ± 11486.33	1.23 ± 0.26	3.18 ± 0.29	0.01 ± 0.00	Rejection
$Pl(1, 2)$	22.61 ± 13.00	1930.57 ± 1346.62	1.14 ± 0.38	2.77 ± 0.18	0.01 ± 0.00	Rejection
$Pl(1, 2.25)$	11.62 ± 9.49	948.36 ± 998.39	2.09 ± 0.30	2.81 ± 0.09	0.11 ± 0.08	Acceptance
$Pl(1, 2.5)$	6.09 ± 4.74	450.06 ± 515.01	3.25 ± 0.57	2.98 ± 0.07	0.24 ± 0.14	Acceptance
$Pl(1, 3)$	2.66 ± 1.82	147.17 ± 203.64	4.44 ± 0.64	3.58 ± 0.13	0.49 ± 0.27	Rejection
$Norm(50, 10)$	1.41 ± 0.01	14.46 ± 1.49	7.27 ± 1.32	6.98 ± 1.38	0.51 ± 0.32	Rejection
$NormT(0, 125, 0, 1000)$	1.63 ± 0.02	20.5 ± 2.24	7.79 ± 1.8	5.611 ± 1.37	0.50 ± 0.35	Rejection

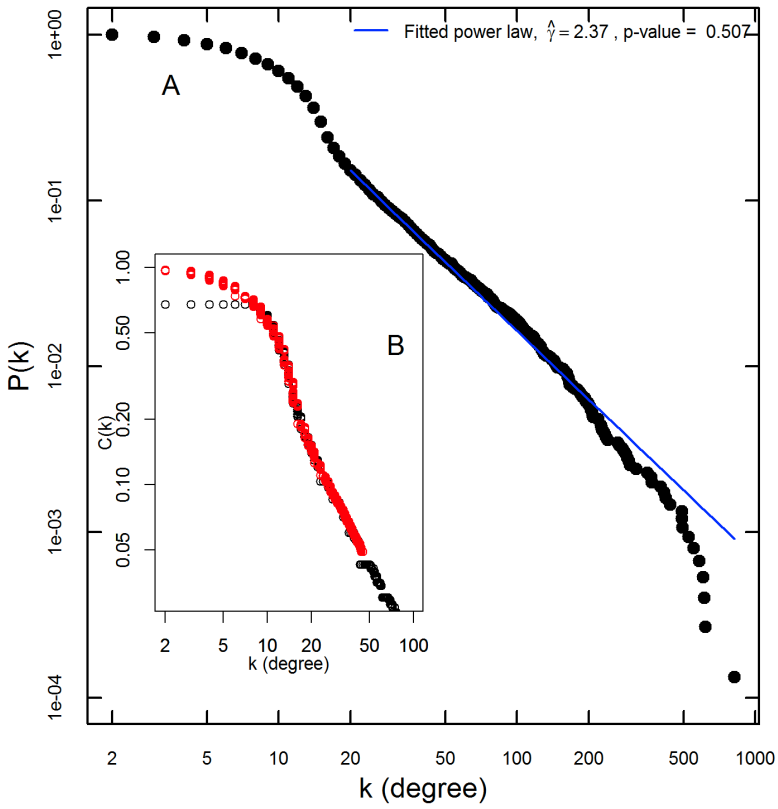

Fig. 2.4 Analysis of the power law hypothesis.

(A) CDF of the resulting degree sequence after preferential attachment. Fitness distribution follows the lognormal distribution with zero mean and variance of 2, $Lognorm(0, 2)$. Blue solid line represents the fitted discrete power law distribution with estimated parameters $k_{min} = 20$ and $\hat{\gamma} = 2.37$ according to the method described in Clauset et al. (Clauset et al. [2009]). The goodness-of-fit test, via bootstrapping procedure, generates a p-value = 0.507 (greater than 0.1), thus the power law is a plausible fit to the data. (B) The figure compares the CDF of hierarchical clustering in the original network (black dots) to the latest network after rewiring (red dots). The figure shows that transitivity of low-fitted agents is being increased as rewiring is repeated.

2.4.2 Influence of fitness asymmetry in competition

We investigate statistically and computationally the impact of varying the asymmetry (skewness) of heavy-tailed distributions in competition. In order to unambiguously correlate the influence of fitness asymmetry in competition, we have kept all parameters

fixed except the parameter σ, γ, or β in log normal, power law and stretched exponential respectively. These parameters control the fitness differences in the corresponding distributions. Again, we focus on the log normal distribution.

Fig.2.3 shows that parameter σ can be used to generate different levels of competition in the population. By increasing σ (measured in log scale) we increase asymmetry, in other words, the ratio Ψ_{max} increases but the fraction of attractors (l) decreases. When σ is very small ($\sigma \leq 0.5$), agents have similar probability to obtain links and system behaves as expected in symmetrical competition. On making σ large enough ($\sigma \geq 5$), we can see how only few agents compete for links (l nears zero) and system behaves as expected in the monopolistic model (Ψ_{max} very large).

Note that, when $n = 10000$ and $\sigma \geq 5$, $\Psi_{max} \geq \mathbf{E}(T_{\Phi_{max}}) = \frac{n}{2}$. We use this argument to define monopolistic competition. Competition is monopolistic when the intensity of attraction of the highest-fitted agent in the population is greater than her expected arriving time. As Ψ_{max} increases, parameter gamma of the power law decreases, such that $\gamma \to 2$.

As shown in Fig.2.3, the transition from symmetrical to monopolistic competition is not discontinuous. Between the two extreme cases ($0.5 < \sigma < 5$) the level of competition seems to be adequate to generate power law networks. Thus, for each value of σ in the range $(0.5, 5)$ we generate 10000 networks and the corresponding degree sequences are approximated by the power law distribution. Fig.2.5 shows the fitting exponent $\hat{\gamma}$ and the goodness-of-fit (p-value) as a function of σ only when the scale-free property is observed.

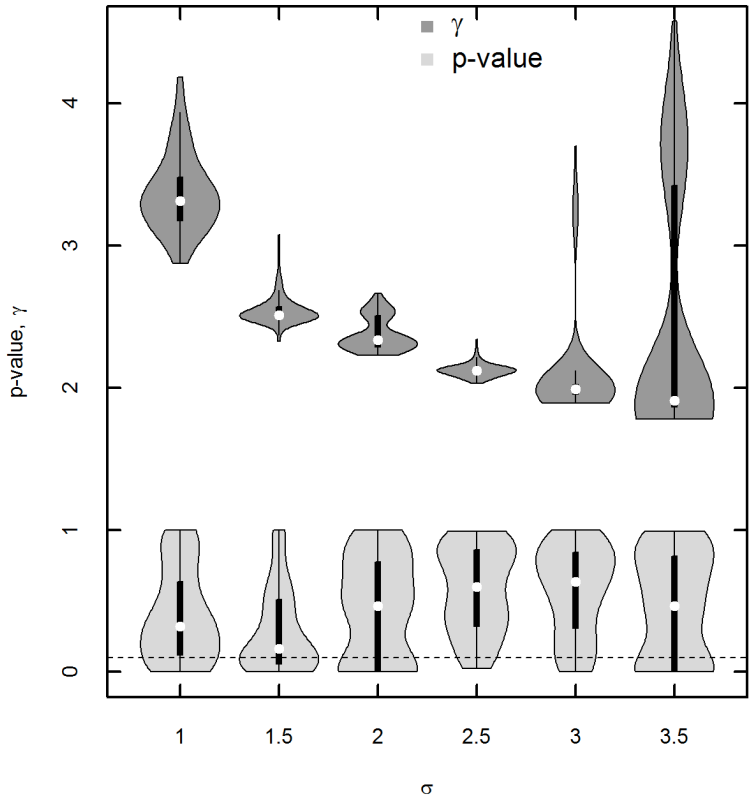

Fig. 2.5 Influence of increasing fitness asymmetry in competition.

According to the log normal distribution, $Lognorm(0, \sigma)$, with zero mean, $\mu = 0$, and tunable variance $1 \leq \sigma \leq 3.5$ we increase the order of magnitude differences in fitness between the lowest-fitted agent Φ_{min} and the highest-fitted agent Φ_{max}. The resulting degree distribution is approximated by the power law. We generate $n = 10000$ networks for each value of σ. Dark violin plots represent the estimates of the scaling parameter $\hat{\gamma}$ for the power law degree approximation. We are interested in variances that generate scale-free regime. Light violin plots represent the goodness-of-fit between the resulting networks and the power law approximation. If the p-value is greater than 0.1 (dotted line) the power law is plausible hypothesis for the model, otherwise is rejected. In both cases, white points inside the violin plots indicate the median values of the 10000 simulations.

Results are not shown for the cases $\sigma < 1$ and $\sigma > 3.5$. In the first case, $(\sigma < 1)$, because there is a transition from power law to exponential distribution when $\sigma \in (0.5, 1]$. In the second case, $(\sigma > 3.5)$, because there is a transition from power law to monopolistic competition when $\sigma \in [3.5, 5)$. As a consequence of the transitions,

there is an increase in the fluctuations seen at exponent $\hat{\gamma}$ (represented by violin plots), which means that only a small fraction of the resulting networks are consistent with the scale-free regime. It is important to remark that when the scale-free regime is observed ($1 \leq \sigma \leq 3.5$), the median values (represented by white points inside the violin plots) are monotonically decreasing with parameter σ.

Based on statistical analysis, our results suggest that networks generated with parameter σ in the range $[1.5, 3]$ are suitable for our interest[11]. In this range, the fitting exponent is scale-free ($2 < \hat{\gamma} < 3$) with p-values greater than 0.1 (represented by a dotted line in Fig.2.5), which means that the power law approximation is plausible hypothesis for the resulting degree sequences. A wider range $\sigma \in (1, 3.5)$ is obtained by Nguyen et al. (Nguyen and Tran [2012]), but they do not analyze their results statistically.

Additionally to statistical analysis, we provide a computational argument that helps to improve the performance of fitness-based network generative models. This argument refers to the increasing complexity of the algorithms when σ is increased. Similarly to eq. 2.7, we can calculate the average number of attempts λ needed for a single selection of any agent (Lipowski and Lipowska [2012]) as follows

$$\lambda = \frac{1}{n}\sum_{i=1}^{n}\frac{\Phi_i}{\Phi_{max}}(1 + 2\tau + 3\tau^2 + ...) = \frac{\Phi_{max}}{\langle\Phi\rangle} \tag{2.12}$$

Complexity is linked to the level of competition in the population in such a way $\lambda = \Psi_{max}$ if the highest-fitted agent is already in the network, which is expected to be at $T = \frac{n}{2}$. Before that moment the algorithm runs faster because the intensity of attraction of agents already in the network is smaller than Ψ_{max}. As we have seen in Fig.2.3, the higher σ the higher $\lambda = \Psi_{max}$ and consequently computational performance is decreased. The algorithm is on average 10 times more efficient when we use $\sigma = 1.5$ ($\lambda \equiv \Psi_{max} \approx 100$) rather than $\sigma = 2.5$ ($\lambda \equiv \Psi_{max} \approx 1000$) to generate networks. According to complexity, we recommend the choice of parameter σ in the range $[1.5, 2.5]$ for the case of log normal distribution when $n = 10000$.

In the interest of simplification, our examples consider fitness as fixed but the model allows fitness variations. For efficiency, we recommend fitness variations to be of the same orders of magnitude. However, efficiency is very sensitive to network size (n) because the ratio Ψ_{max} does not increase linearly with n when generating the fitness

[11] In this case, the standard error of the mean is $SE_{\langle\Phi\rangle} = \frac{\sigma}{\sqrt{\frac{n}{2}}}$ but now fluctuations strongly depend on the asymmetry of $\rho(\Phi)$. In the optimal range $\sigma \in [1.5, 3]$ we observe that fluctuations are small and therefore our predictions are not significatively affected.

distribution. We can easily prove that our first condition $\mathbf{E}_k(\Phi_{max}) \approx \Psi_{max} ln\,(2) > \sqrt{n}$ is not satisfied when network is very large ($n >> 10000$) and the optimal range $\sigma \in [1.5, 2.5]$ is maintained. In those situations, we need to select fitness distributions with greater asymmetries or reduce the arriving times for attractors.

Although we have focused on log normal fitness distribution for its economic interpretation, similar analysis can be done for power law and stretched exponential fitness distributions to generate social networks efficiently.

2.4.3 Cost function as a driving mechanism for homophily

We next analyze to what extent our definition of link stability helps to simulate the evolution of homophily in a social system, and the consequences in social structure.

Fig.2.6 shows how the statistical properties of networks and the type of attachment (from preferential attachment to similar attachment) change as more and more agents are disconnected and reconnected, such that the new connection decreases the value of the cost function. As a consequence, the cost of maintaining links in the whole network is reduced monotonically as homophily evolves. Fig.2.6 also shows that cost-link minimization leads to increasing values of assortativity, modularity and transitivity, and a positive relation between them. Only assortativity shows an stationary behavior after repeated rewiring, suggesting that reconnection among hubs are more frequent at first steps. Hubs are connected more intensely than low-degree agents thus the probability of selecting links pointing to a hub is very high.

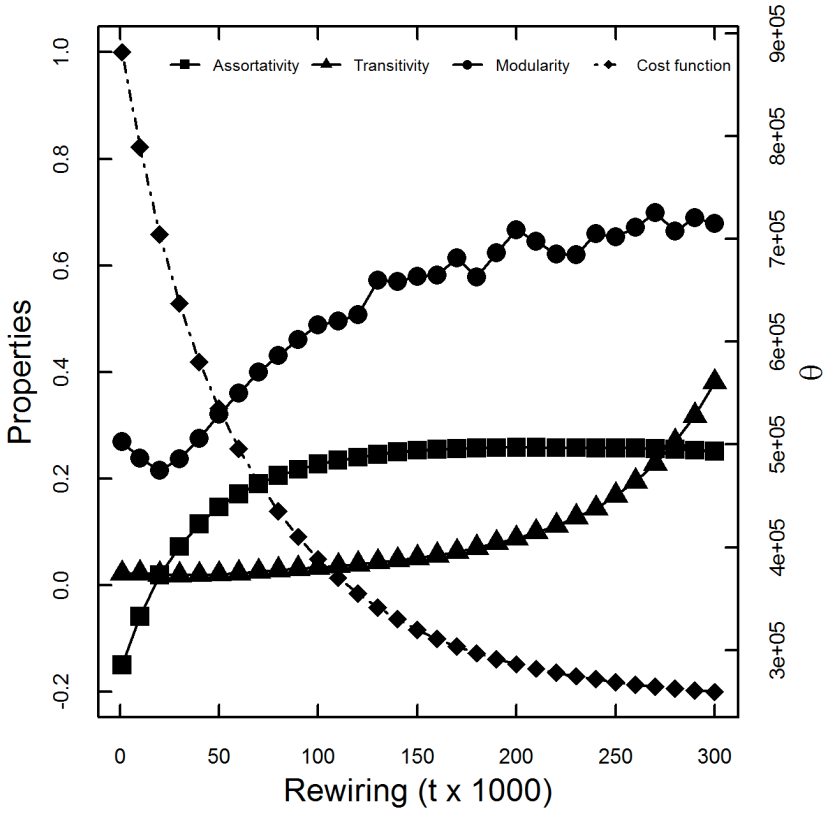

Fig. 2.6 Structural properties and global cost function evolution.

The figure shows assortativity, modularity, transitivity and link costs after repeated application of rewiring. All networks are scale-free and have 7500 agents with average degree of 15.

Given that agents with higher fitness tend to be hubs and hubs are a small group (Fig.2.3), links among hubs represent the most stable distribution of connections when rewiring is applied. In their study, (Xu et al. [2010]) demonstrate that values of assortativity are largely controlled by connections among hubs. Thus, when a new link connects two hubs the global assortativity is increased significativelly more as it does when a link connects two agents with low fitnesses.

While dissortative networks may present community structure (Orman et al. [2013]), we observe how modularity of networks increases as assortativity and transitivity increases. Unlike assortativity, transitivity is increased more in the last rewiring steps. This dynamic suggests that transitivity is very dependent on low-low connections. Low-fitted agents tend to have small degree thus their neighborhoods are close to be

complete after many reconnection. Note that our algorithm does not change degree of agents but it does change the connections within their neighborhood. This result is confirmed by Fig2.4.B which shows how hierarchical clustering increases as rewiring is repeated. In heavy-tailed distributions low-fitted agents are numerous but fitness differences are very small, this means low-low connections are unstable compared to high-high connections. In Fig2.6, the evolution of the global cost function θ confirms the trends. In the early steps, θ is rapidly decreased suggesting that high-cost links are cut. These links can only represent connections between hubs and low-fitted agents. In the last steps, θ remains practically constant indicating that low-low connections are being cut and replaced. In this case, rewiring is less significant in terms of costs but it is important for increasing transitivity of networks.

2.5 Concluding remarks

Network generative models may help us to understand how social interactions shape agents' behavior.

This study shows that fitness of agents can be used to generate realistic networks with power law degree distribution, hierarchical clustering and high levels of link correlations (assortativity, transitivity, modularity). In contrast to traditional network generative models, in our model the individual preferences for interaction are based exclusively on fitness. Hence, network structure emerges as a consequence of two ordering mechanisms: (i) network grows according to individual preferences to connect with highest-fitted agents (preferential attachment); and (ii) network evolves following a cost-link minimization condition (cost-directional rewiring). In absence of realistic cost functions, we use the euclidean distance between fitness of connected agents to determine the ongoing costs of maintaining links. Link stability is based on homophily, implying that links connecting similar agents (similar fitness) are more stable and should be last longer. Lower costs between similar agents can be explained by the fact that similarity of attributes increases trust and thus simplifies the process of communicating with neighbors. As a result of a dynamic process governed by the fitness of agents and the stability of links, the model generates comparable networks with tunable levels of link correlations.

In this study, we provide a useful tool for generating comparable networks that can act as substrates for games, i.e., evolutionary games played on networks. An ordered sequence of networks help us to quantify to what extent network properties affect agents' behavior in games.

Although fitness-based network generative models are widely known in the literature of networks, little attention has been given to the necessary conditions to generate realistic networks efficiently. In this study, we prove that power law networks are always sparse networks with density $\frac{2}{n} \leq d \leq \frac{1}{\sqrt{n}}$. Moreover, we prove that only heavy-tailed fitness distributions support the power law degree pattern. When fitness of agents follows other statistical distributions, such as symmetric or exponential distributions, attractors are less numerous and do not dominate competition. It means that hubs are not sufficiently large to generate the power law degree distribution.

When competition is very asymmetrical, we provide an argument to define whether competition is monopolistic or not. Concretely, if the intensity of attraction of the highest-fitted agent in the population is higher than her expected arriving time, we define competition as monopolistic.

Finally, we have shown that the complexity of our algorithm is linked to the level of competition in the population, thus, we provide statistical and computational arguments for the selection of optimal levels of asymmetry in heavy-tailed distributions. In particular, we recommend the selection of parameters σ, γ, β for log normal, power law and stretched exponential respectively according to the size of the network. For example, if the size of the network is $n = 10000$ we have shown that the optimal range of asymmetry for the case of log normal distribution is $\sigma \in [1.5, 2.5]$. If n increases, we need to increase σ, or alternatively arriving time of attractors may be reduced.

2.6 Appendices

2.6.1 Appendix A: Generating Random Fitness with Specified Distributions

In this study, we have used independent fitnesses drawn from desired distributions (exponential, normal, etc.) to test how accurate we can generate scale-free networks with a particular scaling parameter. In most cases we use the inverse transform method for continuous distributions.

Let $F(x)$, $x \in \mathbb{R}_+$, denote any continuous cumulative distribution function (CDF). Define $F : \mathbb{R} \to [0, 1]$ as continuous, non-negative and non-decreasing (monotone) function such that $F(\infty) = 1$ and $F(0) = 0$. We want random deviates Φ distributed as F thus $Pr(\Phi \leq x) = F(x)$. Let $F^{-1}(r)$, $r \in [0, 1]$, be the generalized inverse of F. As F is continuous, the F is invertible which means $F^{-1}(r) = min\{x : F(x) = r\}$ is the ordinary inverse function. In general it holds that $F(F^{-1}(x)) \leq x$ and $F(F^{-1}(r)) \geq r$. As $F^{-1}(r)$ is a non-decreasing (monotone) function in r, it is possible to find a simple method for simulating random deviates Φ distributed as F.

Proof: Define $\Phi = F^{-1}(r)$ and let Pr denote the underlying probability. $r \sim Unif(0, 1)$ means $Pr(r \leq y) = y$ for $0 \leq y \leq 1$. Then,

$$Pr(\Phi \leq x) = Pr(r \leq F(x)) = F(x).$$

For the case of the exponential distribution, F(x) is given by $F(x) = 1 - e^{-\lambda x}$, where $\lambda > 0$ is a constant. Solving the equation $r = 1 - e^{-\lambda x}$ for x in terms of $r \in [0, 1]$ yields $x = F^{-1}(r) = -\frac{1}{\lambda} ln(1 - r)$. This yields $\Phi = -\frac{1}{\lambda} ln(1 - r)$. Note that $(1 - r) \sim Unif(0, 1)$ since $r \sim Unif(0, 1)$ and thus we can simplify the equation as

$$\Phi = -\frac{1}{\lambda} lnr \tag{2.13}$$

This simplification can be done for other F(x), i.e., power law distributions (Table 2.2). The algorithm for generating an exponential Φ at a given rate λ works as follows

- Define $A = \{1, ..., n\}$ as the set of agents in the network and a value for λ
- Generate $r \sim Unif(0, 1)$

- Set $\Phi_i = -\frac{1}{\lambda} lnr$, where $\Phi(i) =: \Phi_i : A \to \mathbb{R}_+$ represents the fitness of an agent $i \in A$.
- Repeat the process n times such that each agent in the network have an associated fitness drawn from the exponential distribution.

A standard approach to generate random deviates according to the uniform distribution is provided by multiplicative linear congruential generators (MLCG). A linear congruence sequence is a series of integers $n_1, ..., n_m$ based on the relation

$$n_{i+1} = an_i \ mod \ m \tag{2.14}$$

where m is called the modulus, a is called the multiplier and n_0 the seed. Numbers $r_i \in [0, 1]$ are defined by $r_i = \frac{n_i}{m}$, $\forall i \in m$. Note that r_i are periodic in the cycle $[1, m-1]$. Since this method is deterministic and entirely reproducible, a longer cycle length allows for sequences that appears more random because there is no immediately discernible pattern. If nature of the method is to be stressed, one refers to r_i as $pseudo - random$ numbers in the range $(0, 1)$.

The inverse transform method can also be used to generate random deviates from other distributions, i.e. power law or stretched exponential distributions, though not all, since in normal and log normal distributions there are no closed-form expressions neither for F nor for its inverse F^{-1}. For both cases we apply a standard transformation method in $\mathbb{R}^2$, also known as Box-Muller transformation. Note that we modify the usual algorithm to produce non unit-variance normal and log normal distributions. Typically, the algorithm converts a two-dimensional uniform distribution (r_1, r_2) to a normal distribution (Φ_1, Φ_2) with zero mean and unit variance

$$\Phi_1 = \sqrt{-2lnr_1} sin(2\pi r_2)$$
$$\Phi_2 = \sqrt{-2lnr_1} cos(2\pi r_2)$$

We modify the algorithm as follows

$$\hat{\Phi} = \Phi\sigma + \mu$$

setting $\mu = 0$ again, we obtain

$$\hat{\Phi}_1 = \sqrt{-2lnr_1} sin(2\pi r_2)\sigma$$
$$\hat{\Phi}_2 = \sqrt{-2lnr_1} cos(2\pi r_2)\sigma$$

In Table 2.2 we recall $(\hat{\Phi}_1, \hat{\Phi}_2)$ as (Φ_1, Φ_2) and show only one of the two possible random deviates generated with this method.

Table 2.2 Formulas for generating random fitness Φ drawn from continous distributions. Fitness of agents is generated given a source of random numbers r following the uniform distribution in the range $0 < r < 1$.

Distribution	Notation	CDF	Transformation method
Exponential	$Exp(\lambda)$	$1 - e^{-\lambda x}$	$\Phi = -\frac{1}{\lambda} lnr$
Stretched exponential	$ExpS(\lambda, \beta)$	$1 - e^{-\lambda x^{\beta}}$	$\Phi = \left[-\frac{1}{\lambda} lnr\right]^{\frac{1}{\beta}}$
Log normal	$Lognorm(0, \sigma)$	$\frac{1}{2}\left[1 + erf\left(\frac{lnx-\mu}{\sqrt{2}\sigma}\right)\right]$	$\Phi = e^{\sqrt{-2lnr_1} sin(2\pi r_2)\sigma}$
Power law	$Pl(\gamma)$	$\left(\frac{x}{x_{min}}\right)^{-\gamma+1}$	$\Phi = \Phi_{min} r^{\frac{-1}{\gamma-1}}$
Normal	$Norm(0, \sigma)$	$\frac{1}{2}\left[1 + erf\left(\frac{x-\mu}{\sqrt{2}\sigma}\right)\right]$	$\Phi = \sqrt{-2lnr_1} sin(2\pi r_2)\sigma$

2.6.2 Appendix B: Fitting power law to empirical data

Our simulation study was based on the algorithm described above using Python to generate the networks and the library *poweRlaw* developed in R to test the results. The fitness of agents was generated according to the following distributions: uniform, exponential, stretched exponential, normal, truncated normal, log normal and power law. Following the model, we generated 10000 networks for each distribution, all having $n = 10000$ agents. Without loss of generality, we assumed that the number of links added at each time step was $v = 1$, increasing v would just result in higher density, not changing the power law pattern. Each distribution has an associated parameters for generating random fitness. By tuning the parameters according the transformation method described in Table 2.2, we wanted to investigate the impact of the nature of fitness and its restrictions on the power law degree pattern.

Once the fitness of agents has been generated and after the network has been constructed, we validate and quantify statistically whether power law is a good approximation to empirical results. According to (Clauset et al. [2009]) the first step is to estimate γ and k_{min}. Before calculating the scaling parameter γ, we need to select the scaling region in the tail by discarding all values $\{k_j\} = \{k_1, .., k_n\}$ that are under the lower bound $k_j < k_{min}$. k_{min} is the smallest value for which the power law holds. If k_{min} is too small, we will be trying to fit a power law to any other distribution. If k_{min} is too large, we will be increasing the statistical error on the scaling parameter. Choosing k_{min} means minimize discrepancy between the fitted model and the empirical distribution and it is measured as follows which results in

$$\hat{k}_{min} = \underset{k_{min}}{argmin} D(P(k|\hat{\gamma}, \hat{k}_{min}), S(k)) \tag{2.15}$$

where D is the Kolmogorov-Smirnov (KS) statistic that measures the largest deviation in cumulative density functions between the theoretical model ($P(k|\hat{\gamma}, \hat{k}_{min})$) and the empirical data ($S(k)$). This step is repeated for each data point and stored in a vector. Finally, we select the minimum value of D from the vector and designate the corresponding k_i to be the parameter k_{min}. For a given value k_{min}, the scaling parameter is estimated numerically optimizing the logarithm of the likelihood

$$\hat{\gamma} = 1 + \frac{n}{\sum_{i=1}^{n} ln\left(\frac{k_i}{k_{min}}\right)} \tag{2.16}$$

where $k_i > k_{min}$ and the standard error is computed as follows

$$\hat{\sigma} = \frac{(\hat{\gamma} - 1)}{\sqrt{n}} + \mathcal{O}\left(\frac{1}{n}\right) \tag{2.17}$$

Since it is possible to fit a power law distribution to any empirical data, as suggested in (Clauset et al. [2009]), we use a statistical hypothesis test to determine whether the power law is a plausible fit to the data. The selected approach to answer the question is the goodness-of-fit tests via bootstrapping procedure. Such approach is based on repeated Kolmogorov-Smirnov (KS) tests between synthetic data and empirical data. A large number of synthetic data is generated with the chosen $\hat{k}_{min}$ and $\hat{\gamma}$. The test generates a $p - value$ that can be used to quantify plausibility of the hypothesis. Null hypothesis assumes data is generated from a power law distribution. If $p - value$ is greater than 0.1, we fail to reject the null hypothesis and conclude that power law is a good fit. Otherwise, another distribution may be more appropriate. With the purpose of deriving robust results we perform 5000 KS tests and evaluate the cumulative estimate of the $p - value$ and its standard deviation.

2.6.3 Appendix C: Assortativity, Transitivity and Modularity metrics

To compute the assortativity of a network, we use the Pearson correlation coefficient between the degrees of agents joined by a link (Newman [2002]):

$$r = \frac{l^{-1}\sum_i j_i k_i - \left[l^{-1}\sum_i \frac{1}{2}(j_i + k_i)\right]^2}{l^{-1}\sum_i \frac{1}{2}(j_i^2 + k_i^2) - \left[l^{-1}\sum_i \frac{1}{2}(j_i + k_i)\right]^2} \tag{2.18}$$

where $l = |L|$ is the number of links in the network, and j_i and k_i denote the agent degree of the two agents connected by the i^{th} link. The measure lies in the range $-1 \leq r \leq 1$, where 1 means maximal assortativity. For random networks, since agent interaction is placed at random without mixing behavior, it follows that $r = 0$ when networks are large, $n \to \infty$.

Transitivity or local cohesiveness coefficient τ_i measures how close the neighborhood $\mathcal{N}(i)$ of agent i is to be a complete network. If agent i has k_i neighbors, there can exist at most $\binom{k_i}{2} = \frac{k_i(k_i-1)}{2}$ links connecting agent i neighbors. If we define a transitive relation in the neighborhood of i as $\forall i \in A$, $\forall u, v \in \mathcal{N}(i) : (uRi \wedge iRu) \Rightarrow uRv$, where $\mathcal{N}(i) = \{a_u : l_{iu} \in L \vee l_{ui} \in L\}$, the local clustering can be quantified as.

$$\tau_i = \frac{2\,|\{l_{uv} : a_u, a_v \in \mathcal{N}(i), l_{uv} \in L\}|}{k_i(k_i - 1)} \tag{2.19}$$

Transitivity lies in the range $\tau_i \in [0, 1]$ with the upper limit attained only a fully interconnected neighborhood, in where everyone knows each other. The network clustering coefficient $\tau \equiv \langle \tau_i \rangle$ is defined as the average of τ_i over all agents in the network:

$$\tau = \frac{1}{n}\sum_{i=1}^{n} \tau_i \tag{2.20}$$

When $\tau = 1$, all possible links exist and the network is a clique. On the contrary, when $\tau = 0$ there are not triangles in the network, i.e. n-agent cycles usually represented by C^n.

Given a partition $\mathcal{P}$, the network N is divided in m communities, $N' = (A', L')$, embedded within the network such that $\forall i, j \in m$, $N'_i \subset N$ and $N'_j \subset N$, and $A'_i \cap A'_j = 0$. Let us define a $m \times m$ symetric matrix e, the element e_{ij} represents the fraction of links connecting agents in community i to agents in community j.

The fraction of intra-community links is $\sum_i e_{ii}$. Let $e_{i+} = e_{+i}$ be the fraction of links connecting at least one agent from community i. (Newman and Girvan [2004]) proposed modularity as a measure to quantify the community structure based on the difference between e_{ii} and the expected such fraction in a network with the same community divisions if links were distributed at random. The modularity of the network given partition $\mathcal{P}$ is defined as:

$$Q_{\mathcal{P}} = \sum_{i=1}^{m} (e_{ii} - e_{i+}^2) \tag{2.21}$$

To approximate the best partition and largest $Q_{\mathcal{P}}^* = Q$, an information-based algorithm is performed. If the number of intra-community links is not higher than random, we get $Q = 0$, and values approaching $Q = 1$ indicate strong community structure. Note that, if network is connected, communities are not totally isolated from others and therefore $Q < 1$.

While not clear definition for high values, in practice social networks show considerably higher assortativity, transitivity and community structure than those obtained in random networks.

Chapter 3

Tragedy of the Commons and the Economics of Social Pressure

Summary

This chapter revisits the problem of the tragedy of the commons. We analyze the influence the interaction between agents has on their behavior and determine the economic value of social pressure. For a socially optimal management of the resource, an initially high share of compliers is necessary but is not sufficient. The analysis shows the extent to which the state of the resource, the share of compliers and the size, density and local cohesiveness of compliers of the network contribute to overcoming the tragedy of the commons. It also determines the magnitude of how imprecise a single aspect of the network is for predicting cooperativeness. Likewise, it shows the magnitude of error if a "first-best tax" on the extracted amount of the resource is applied without fully taking into account the interaction between the agents involved. The study suggests that the origin of the problem – short-sighted behavior - is also the starting point for a solution in the form of a one-time payment. A numerical analysis of a social network comprising 7500 agents and a realistic topological structure is performed using empirical data from the Western La Mancha Aquifer in Spain.

Keywords: Natural resource management; evolutionary game; social network; social punishment; one-time payment

---

3.1 Introduction

The tragedy of the commons (Hardin [1968]) is often explained by the fact that a natural resource is exploited by many agents and they all have open access to the resource. However, such social trap is not inevitable when property rights are shared by the members of a community and cooperative behavior is promoted efficiently within the community (Ostrom [1990]). At the community level, many factors impacting cooperation (i.e., trust, communication, social pressure) are very dependent on the underlying structure of social interactions (Bodin and Crona [2009]), often formalized by a social network.

For a better understanding of underlying forces of the tragedy of the commons we analyze to what extent macro and micro characteristics of social networks support social norms that help to conserve natural resources (Jackson et al. [2017]). In our model, macro and micro characteristics of social networks lead to social pressure that depends on the share of compliers, the state of the resource and the local cohesiveness of compliers.

This study analyzes agents' behavior by taking into account that they are interacting in a large, complex network that is close to real social networks. This requires, among other elements, that the network structure is highly asymmetric, that the distribution of the number of the agent's links follows a power law, and that there is a large number of agents. Among the single aspects analyzed in the literature, cohesiveness and the share of compliers stand out. The definition for cohesiveness is most frequently based on links between agents. However, in the case of cooperativeness or the exercise of social pressure, not only are the links between agents important, but so too are the agents' chosen strategies. If two compliers are linked, one can expect they will experience greater social pressure than if every complier were linked to a defector but not linked between themselves. For this reason, we propose a new connectivity measure that is based on links and the strategy chosen. We have called it "local cohesiveness of compliers" and it considers the links between the compliers in the neighborhood of an agent. The share of compliers is another single aspect that is often seen as an important driving force behind the dynamics of the network. That said, the share of compliers is independent of network size and density. As such, its indicative power to foresee a possible propagation of compliers within social networks is limited. The previous arguments suggest that merely focusing on the single aspects of the network does not offer a reliable instrument to accurately analyze the tragedy of the commons. The results of the study confirm this supposition and determine the magnitude of imprecision. Likewise, the study shows the magnitude of error if a "first-best tax" on

the amount of the resource extracted is applied without fully considering the effects the social network has.

The results of a numerical study based on empirical data from the western La Mancha aquifer show that a critical level of the initial share of compliers is necessary to achieve a more socially-optimal management of the resource. Yet, our calculations demonstrate that the range of the critical level of share of compliers is between 0.31 and 1. Given this wide range, the share of compliers alone is not a good indicator of cooperativeness in the community. The results show to what extent the critical level depends on the size and density of the network, the state of the resource and the strength of local cohesiveness of compliers. Thus, one may find that a certain initial share of compliers is necessary, but not sufficient, to overcome the tragedy of the commons. While a higher network density may contribute to greater acceptance of the social norm, this increase in density is only relevant if the additional links strengthen local cohesiveness of compliers, otherwise they are redundant. The fact that new links might be redundant demonstrates that density alone is a poor indicator of the network characteristics that support cooperation. Moreover, if all other characteristics are equal, then the analysis shows that large networks are less capable than smaller networks in engendering adherence to a social norm. Yet, this shortcoming may be redressed by favoring the creation of new connections between compliers. New strategy-dependent links can be supported when workshops are organized, meetings or courses are run or new institutions, such as complier associations, are set up. Another policy option to secure higher cooperation may consist of a one-time payment to defectors if they change their strategy. The rationale for a single payment is the fact that defectors are short-sighted. Once they have changed sides, the increased number of compliers hampers them from reverting. In this respect, although short-sightedness of defectors is often considered as the origin of the tragedy of the commons, it also offers a starting point for its solution.

Environmental economics contributed to general economics by establishing a foundation for and formalizing methods to measure the value of intangible goods and services, such as nature's aesthetic values or a particular environmental resource's existence value. This work aims to contribute to the literature by analyzing the monetary value of social pressure using the case of the western La Mancha Aquifer in Spain.

The reminder of this study is structured as follows: section 3.2 introduces the different elements of the economic model based on an integrated social-ecological system. In Section 3.3, we define a concept for equilibrium and analyze possible equilibria. Then, in Section 3.4, we analyze the economics of social pressure and discuss

policy instruments for overcoming the tragedy of the commons. In Section 3.5, to analyze the effect the social network has on the tragedy of the commons, we present a numerical analysis for our groundwater resource case. The study then closes with some concluding remarks (section 3.6).

3.2 The economic model

The economic model is based on three different components: the social network that defines the interaction between agents, the resource demand strategies and the agent's chosen strategy. In the following, we present the three components.

3.2.1 A social network as a graph

Our interest is in the interaction between different members of a social network that can be described by a simple graph $N = (A, L)$ which consists of a finite set $A = 1, ..., n, n > 2$ of agents and a set L of links that are the unordered pairs of elements from A. The elements in set L consist of the values of the indicatrix link function $l : A \times A \to \{0, 1\}$:

$$l(i,j) \equiv l_{ij} = \begin{cases} 1; (i,j) \in L \\ 0; (i,j) \in L \end{cases}$$

For any pair of agents, i and j, the expression $l_{ij} = 1$ indicates that the two agents are neighbors, otherwise $l_{ij} = 0$, i.e., they know and relate to each other. By definition, simple graphs are undirected so that $l_{ij} = 1 \Leftrightarrow l_{ji} = 1$[1]. If every agent is connected to all other agents, N forms a complete network. For each agent i, $\mathcal{N}(i)$ denotes their neighborhood, i.e., the set of all neighbors. The degree $k_N(i) = k_i = \sum_j l_{ij}$ of an agent i is the number of links at i, i.e., the number of neighbors i has. Denote by $P(K = k) = p_k$ the degree distribution of N, that is the probability that an agent i in N chosen uniformly at random has exactly k neighbors. If the links of all the agents were formed assuming the same probability p, we would obtain a random network whose degree distribution approximately follows a Poisson distribution. However, empirical studies (Jeong et al. [2000]; Liljeros et al. [2001]) have shown that the degree distribution of large social networks does not follow a Poisson distribution and therefore recent research (Barábasi and Albert [1999]; Clauset et al. [2009]) has focused

[1]Moreover, agents are not linked to themselves (self-loops), i.e., $l_{ii} = 0$, and there is no more than one link between agent i and j (uniqueness of the link).

on scale-free topology. These networks are characterized by a degree distribution that follows the power-law $p_k = k^{-\gamma}$ with $2 < \gamma < 3$ (Nguyen and Tran [2012]). Scale-free networks have more weight in the tails than do random networks where there are few central agents of high degree and many other agents of small degree and thus offer a better match with the social networks observed (Jackson [2008]). Finally, and very importantly, compared to random networks, scale-free networks allow for some organizing principles to be considered (Réka and Barabási [2002]).

3.2.2 Evolving networks

To analyze the effects of network structure on social pressure, and finally on cooperation, a game will be played on comparable and realistic networks. Each of these networks corresponds to a sequence of weighted networks with an increasing level of homophily (see Chapter 2). More precisely, let $\{N^{[v]}\}_{v=1}^{V} = \left(A, \{L^{[v]}\}_{v=1}^{V}, \{\omega^{[v]}\}_{v=1}^{V}\right)$ be the sequence of weighted networks evolving in discrete time. Here, the number of agents and links, $|A| = n$ and $|L| = \ell$, are fixed but the evolution in time is given by the change in the configuration of the set of the links, $L^{[v]}$, and the corresponding weights, $\omega^{[v]}$. With this notation, the sequence of networks is an ordered sequence of time points $\{t_v\}_{v=1}^{V}$ in such a way the level of homophily in the network in t_{v-1} is lower than the level of homophily in t_v. Let $\theta(t_v) = \sum_{u=1}^{\ell} \omega_u$ be the global level of homophily in the network at time t_v. The evolution of θ over time can be described as $\theta(t_{v+1}) = \theta(t_v) + \triangle\theta(t_{v+1})$, where $\triangle\theta(t_{v+1}) \geq 0$ such that $\theta(t_{v+1}) \geq \theta(t_v)$.

3.2.3 Resource demand strategies

Each member of the social network has access to a common property resource. However, extraction based on the maximization of each member's private net benefits would, in the long-run, lead either to the depletion of the resource or to very low annual private net benefits. To overcome the tragedy of the commons, the members of the social network have reached a common understanding of the characteristics of a sustainable extraction path. Let us interpret this common understanding as a social norm. Adherence to the social norm is voluntary and every member of the social network may choose to follow the sustainable extraction path or not. Let us label the behavior of the agents that follow the sustainable extraction path as *compliers* and the behavior of all other agents as $defectors$.

Each member or agent either employs the extracted resource as the input to produce a single good or commercializes it on the market. Let $w_i(t)$ denote the amount of

the resource extracted at calendar time t by agent i. The available amount of the resource is denoted by $s(t)$ with $s(0) = s_0$. We assume that all members adjust all other inputs to the extracted amount of the resource such that their net benefits are maximized. Adherence to the social norm by agent i will support sustainable extraction, whereas non-adherence will lead to a non-sustainable extraction path. Non-coordinated individual behavior would result in a sustainable extraction path if all members were to consider stock dependent costs when determining the privately optimal extraction path. These costs will be fully considered if all the agents have a private planning horizon of an infinite length. Consequently, we define compliers, denoted by C, as far-sighted agents with an infinite planning horizon of $T \to \infty$ years, whereas defectors, denoted by D, are short-sighted and their planning horizon is $T \to 0$ year. We assume that the underlying reason for this short-sightedness is related to socioeconomic factors (e.g. age, personal commitment to the community, risk aversion etc.). Each agent determines the privately optimal extraction path (resource demand function) based on the solution of the following decision problems. The resource demand function at time t is given by:

$$w_i^K(t, T, s(\xi)) = arg \max_{w_i^K(\xi)} \int_t^T e^{-r\xi} \pi^K(w_i^K(\xi), s(\xi)) d\xi, \;\; K = C, D \tag{3.1}$$

where r denotes the private inter-temporal discount rate and π the private net benefits of the agent. We assume that compliers and defectors differ only in respect to the length of their planning horizon, but not to their private discount rate. For the case of compliers equation (1) is also subject to

$$\dot{s}(\xi) = g(s(\xi)) - \sum_{i}^{cn} w_i^C(\xi) - \sum_{cn+1}^{n} w_i^D(\xi), \;\; s(\xi) = s_t \tag{3.2}$$

where a dot over a variable denotes the operator $\frac{d}{dt}$, c the share of compliers within the population of all agents and $g(s(t))$ is the reproduction or growth function of the resource. We assume that the compliers' expectation of the defectors' future extraction at time t, $\bar{w}_i^D$, is based on their current level of extraction, i.e., $\bar{w}_i^D = w_i^D(t)$. The resource demand function (eq. 1) is the solution to an open-loop strategy. Based on the circumstance that agents can frequently observe the level of stock remaining, we propose that they are allowed to modify their extraction profile after $T - t$. In other words, the agents determine a new open-loop extraction profile based on the amount of the natural resource they observe. This profile is maintained until the next revision period when new information about the level of the remaining stock is obtained. Since

compliers take account of the stock dependent costs in terms of inter-temporal or user costs, denoted by $\eta(t)$, their marginal extraction costs are higher than those of the defectors. Thus, it holds for a given stock $s(t)$ that defectors extract at least as much as compliers and their net benefits are never less than those of the compliers, i.e.,

$$w_i^D(t, T, s(t)) \geq w_i^C(t, T, s(t))$$

and

$$\pi^D(w_i^D(t), s(t)) \geq \pi^C(w_i^C(t), s(t))$$

3.2.4 Strategy choice - an evolutionary game-theoretic approach

Given our focus on the interaction between agents, we analyze how an arbitrary initial distribution of compliers and defectors evolves over time and how this changing distribution affects the evolution of the resource. At every moment of time, agents can change their strategy, i.e., from complier to defector, or vice versa. Strategy choice is based on the evolutionary game-theoretic approach (Osés-Eraso and Viladrich-Grau [2007]; Sethi and Somanathan [1996]). We assume that this decision is influenced by the following factors:

- the difference between the net benefits of a defector and a complier (i.e., the defector's extra benefits) and
- the interaction with other agents (network effects)

In the case of the first point, we assume that the larger the difference is between the maximal net benefits of complying with the strategy, given by $\pi^C(w_i^C(\cdot), s(t))$ and not complying with the strategy, given $\pi^D(w_i^D(\cdot), s(t))$, the greater the chance at moment a complier will become a defector and a defector will not become a complier. The difference between $\pi^D - \pi^C$ is not only important for the agent's strategy, but also presents the magnitude of the loss defectors inflict on those members of the network who are adhering to the social norm. In the absence of an institution that is technically and legally in a position to punish defectors, compliers may retaliate for the defectors' abstraction of the common property resource through social shunning (ostracism) (Ali and Miller [2016]).

In terms of social pressure, we assume that all agents are perfectly informed about the strategy choice their neighbors have made (complete monitoring) and that there is

no time delay between detecting non-compliance and retaliation[2]. To concentrate on the first-order dilemma of public goods (provision of cooperation), we suppose that retaliation is costless for the compliers. In doing so, we avoid the second-order dilemma of public goods since compliers do not have to agree on how to divide the costs of retaliation among themselves.

Social pressure and social punishment

If an agent defects, they will be exposed to social pressure from the compliers[3]. However, making use of the social network suggests that social pressure on defector i depends on the number of compliers and defectors within their local neighborhood $\mathcal{N}(i)$. Let us define the set of compliers within the neighborhood $\mathcal{N}(i)$ by $\mathcal{N}_C(i)$. Thus, the share of compliers in the neighborhood of agent i, c_i, can be defined by $c_i = \frac{|\mathcal{N}_C(i)|}{|\mathcal{N}(i)|}$. This relationship is considered an important factor in determining social pressure because it measures the direct influence the neighborhood has on defector i (Haag and Lagunoff [2006]; Jackson et al. [2012]). The higher the number of compliers of neighborhood $\mathcal{N}(i)$ is, the greater the social pressure on agent i. However, not only is the share of compliers, c_i, important in determining social pressure, but so too is the relationship between the agents who form part of the set $\mathcal{N}_C(i)$. In the case that none of these agents is linked to another agent in this set, one can assume that the social pressure on defector i will not be as high as when each and every agent in set $\mathcal{N}_C(i)$ is linked. In the first case, local cohesiveness between the agents in set $\mathcal{N}_C(i)$ would be zero, whereas in the latter it would be one. Let us denote the cohesiveness among the compliers in the neighborhood by $\tau_{c_i} \in [0, 1]$ (see Appendix E of Chapter 4). This measures the degree of connectivity between the compliers in set $\mathcal{N}_C(i)$. (Haag and Lagunoff [2006]) and (Jackson et al. [2012]) employed a different metric, independent of the agents' strategy choice, for connectivity. However, we used a more stringent measure of connectivity since the cohesiveness of compliers is important to analyze the tragedy of the commons. We denote the connectivity of all agents (compliers and defectors) in the neighborhood of agent i by $\tau_i \in [0, 1]$ (also known as transitivity). This measures how close the neighborhood of agent i is to a complete network. Thus, if, $\tau_i = 1$, all neighbors of agent i are connected to each other. Alternatively, the measurement of cohesiveness for nodes or agents can also be measured on a network level. On this scale, we define average transitivity or average local cohesiveness, as the

[2]Social pressure is the application of the principle of reciprocity as the response to non-compliance of the social norm by defectors.

[3]Instead of the male and female possessive pronoun we use plural form to facilitate the reading.

average value of local cohesiveness, i.e., $\bar{\tau} = \frac{1}{n}\sum_i^n \tau_i$. Finally, we assume, if the resource is abundant, the set of compliers $\mathcal{N}_C(i)$ will exert less social pressure on defector i than if it were scarce.

Once the three key elements of social pressure have been introduced, we can then write the social pressure function as $\omega(s(t), c_i(t), \tau_{c_i}(t)) \geq 0$. As explained above, an increase in the stock reduces social pressure (i.e., $\frac{\partial \omega}{\partial t} < 0$), an increase in number of compliers in the neighborhood of defector i increases social pressure (i.e., $\frac{\partial \omega}{\partial c_i} > 0$), and an increase in the strength of social ties between compliers in the neighborhood of defector i raises social pressure (i.e., $\frac{\partial \omega}{\partial \tau_{c_i}} > 0$).

In line with (Tavoni et al. [2012]) we model social pressure, ω, using a Gompertz growth function. This asymmetric sigmoid function is given by $\tilde{\omega}(c) = ae^{-de^{-gc}}$. The social pressure function is limited above by the parameter a (i.e., $0 \leq \omega \leq a$), the slope can be adjusted by the parameter g, and the social pressure function can be displaced along the origin by the parameter d. The parameter d indicates the minimum threshold for the responsiveness of defectors to social pressure. Since the strength of social pressure exerted highly depends on the specification of the function ω we suggest introducing a more flexible specification and allow to consider irregular networks. For this purpose we substitute the share of compliers in the network, c, for the share of compliers in the neighborhood of agent i, c_i and the parameters a and g with the functions $a(\tau_{c_i})$ and $g(s)$, $g'(s) < 0$, respectively. Hence, the modified Gompertz function depends on the characteristics of the neighborhood with respect to its share of compliers, its cohesiveness between compliers and the depth of the water table, and is given by

$$\omega(s, c_i, \tau_{c_i}) = a(\tau_{c_i})e^{-de^{-g(s)c_i}} \tag{3.3}$$

We assume that social punishment is directly related to the difference between the net benefits of the defector and the complier $\pi^D - \pi^C$. Since these extra benefits present the loss defectors inflict on compliers, any social punishment can be viewed as redemption for the privation suffered by the compilers. However, social punishment is not independent of social interaction among the agents and, therefore, we assume that the loss defectors inflict on the compliers is attenuated or aggravated by the strength of social pressure $\omega(s, c_i, \tau_{c_i})$. More precisely, the social pressure produced and the extra benefits the defector gains as a result of incompliance, define the social punishment imposed and is written as:

$$\omega(\cdot)(\pi^D(\cdot) - \pi^C(\cdot)) \tag{3.4}$$

Agent utility and a probabilistic model of strategy choice

We assume that the utility of agent i adhering to the social norm at moment t is given by:

$$U^C(t) = \pi^C(\cdot), \tag{3.5}$$

and the utility of the same agent i not adhering to the social norm at moment t is given by:

$$U^D(t) = \pi^D(\cdot) - \Big[\omega(s(t), c_i(t), \tau_{c_i}(t)(\pi^D(\cdot) - \pi^C(\cdot)))\Big] \tag{3.6}$$

Eq. 3.5 indicates that the utility of a complier is equal to their private net benefits[4]. This depends on the amount of the extracted resource and the level of the stock. Eq. 3.6 shows that the utility of a defector consists of the net benefits from resource exploitation minus social punishment and, likewise, depends on the amount of the resource extracted and the stock levels. However, it also depends on the position the defector holds within the social network and the characteristics/topology of the social network within their neighborhood.

At each time step, every agent decides whether to maintain their current strategy or not. For this purpose, every agent i compares the utility associated with their current strategy $U(t)$ with that of the alternative strategy $U'(t)$. The utility of a complier is independent of their position in the network or the characteristics/topology of the social network within their neighborhood. However, the decision to maintain or to change their current strategy depends on these very elements as they influence the alternative strategy's utility. The agent will probably adopt an alternative strategy if it proves more beneficial, $U'(t) > U(t)$, whereas if $U'(t) \leq U(t)$, the agent will maintain their current strategy. These inequalities also form our tie-breaker rule in the reminder of the study. In mathematical terms, the probability of a change in the current strategy adopted by agent i for a given level of stock, is considered proportional to the difference in the utilities. Let the probability that agent i changes from complier to defector be denoted by $p_i^C(t)$ given by:

$$p_i^C(t) = \left\{ \begin{array}{l} \frac{U^D(t) - U^C(t)}{max\{U^D(t) - U^C(t)\}}, \text{if } \; U^D(t) - U^C(t) > 0 \\ \\ 0 \qquad\qquad , \text{if } \; U^D(t) - U^C(t) \leq 0 \end{array} \right\}, \tag{3.7}$$

[4]Although this formulation implies that agents are risk neutral, we opted for this specification to simplify the model and to concentrate on the interaction between agents in a social network.

and let the probability that agent i changes from defector to complier be denoted $p_i^D(t)$ given by:

$$p_i^D(t) = \left\{ \begin{array}{ll} \frac{U^C(t)-U^D(t)}{max\{U^D(t)-U^C(t)\}}, & \text{if } U^C(t) - U^D(t) > 0 \\ \\ 0 & \text{, if } U^C(t) - U^D(t) \leq 0 \end{array} \right\}, \tag{3.8}$$

The denominator of eq. 3.7 and 3.8 refers to the maximal difference between the utility of the different strategies for a given level of stock at time t. Since the value of U^C is independent of the neighborhood and varies only with the level of stock, $U^D(t) - U^C(t)$ is maximal if U^D is maximal. For a given level of stock, the maximum of U^D transpires, if social punishment is zero. In other words, there are no compliers in the neighborhood and consequently local cohesiveness is zero and $U^D = \pi^D$. The decision to maintain the current strategy or to adopt the alternative one is a $0-1$ decision in probabilities. For this purpose, using the inverse transform method we generated a random number that takes only the values of 0 or 1[5]. If the random number drawn is a 1, the defector will change their strategy. Otherwise they will not.

All agents simultaneously decide which strategy to choose based on the current distribution of compliers and defectors within the social network, with the probability being p_i^C or p_i^D (i.e., see eq. 3.25 in Appendix B). We assume that agents do not act strategically, i.e., they do not consider the possible strategy choices of their neighbors when deciding on their own. Given the large size of the social network and the resulting huge set of possible constellations each player needs to consider to make a strategic choice, it would seem to be more realistic to base individual strategy-choice on non-strategic behavior as in (Gale and Kariv [2003]).

3.3 Equilibrium concept

For the dynamics of a resource and a non-structured population, (Sethi and Somanathan [1996]) and (Osés-Eraso and Viladrich-Grau [2007]) identified equilibrium conditions. In the absence of a natural resource, (Santos and Pacheco [2005]; Santos et al. [2006, 2012]) used Monte Carlo techniques to identify a window of parameter values for an equilibrium of the dynamics of a population embedded in an asymmetric social network.

[5] A number u is drawn randomly from the uniform distribution $Uni(0 \leq P_i \leq 1)$. If u is less than or equal to P_i, the outcome is associated with a 1 or with a 0 otherwise. This method is comparable to a forged coin where the probability of landing heads up (1) is P_i and tails up (0) $1 - P_i$. Put simply, if $P_i = 0.8$, there is an eighty percent probability this method will generate a 1 and a twenty percent probability it will generate a 0.

Proposition 1: (Equilibria conditions):

Any steady state equilibrium concept requires the following three equilibria, a) equilibria with respect to the dynamics of the resource, b) changes in the choice of strategy adopted by the agents and c) the demand the agents make of the resource must be incentive-compatible with the equilibria with respect to the dynamics of the resource.

Equilibria a) demands that $\dot{s}(t) = 0$ which, in turn, requires that

$$g(s(t)) = \sum_{i}^{c} w_i^C(t) + \sum_{c+1}^{n} w_i^D(t) \tag{3.9}$$

Additional to eq. 3.9, none of the agents change their strategy, or the share of compliers c is constant must also hold[6]. Hence, an equilibrium b) in expected values is achieved if:

$$\sum_{i}^{cn} p_i^C - \sum_{cn+1}^{n} p_j^D = 0. \tag{3.10}$$

Finally, equilibrium c) holds if there is a $w_i^C(t)$ and $w_i^D(t)$ that satisfies eq. 3.1, and 3.9. In other words, the amount of extracted resource required satisfies the balance between reproduction and extraction (eq. 3.9) also has to be optimal from an economic point of view for compliers and defectors, i.e., none of the agents changes their strategy.

Hence, an equilibrium is defined by eq. 3.1, 3.9 and 3.10. Given the great number of agents and the large degree of freedom to satisfy conditions 3.9 and 3.10, an equilibrium, if it exists, is likely to be not unique and stable. In this case, while it is possible that the number of compliers and defectors is maintained for a certain period of time, the new constellation in some neighborhoods will induce agents to change their strategies. Thus, the equilibrium is likely to be only temporary.

From a social point of view, the all-defector equilibrium or any mix equilibrium would not be efficient because the social optima can only be achieved with the all-complier equilibrium. Therefore, the more compliers there are, the more efficient the

[6]The share of compliers can be kept constant if none of the agent changes, i.e., $p_i^C = 0, p_j^D = 0, \forall i, \forall j, i \neq j, i \in I : \{1, ..., cn\}, j \in J : \{cn+1, ..., n\}$. Moreover, there may be a dynamic equilibrium if $p_i^C \neq 0, p_j^D \neq 0, p_k^C = 0, p_l^D = 0, \forall i, \forall j, \forall k, \forall l, i \in I, k \in I, i \neq k, j \in J, l \in J, j \neq l$ and the share of compliers of all agents is constant. This implies that strategy changes from compliers to defectors, or vice versa, cancel each other out for agents i and j, meanwhile agents k and l maintain their current strategy. None of these two equilibria are necessarily steady state equilibria.

resource management is. Consequently, low probabilities of the all-defector equilibrium or any mix equilibrium must be evaluated positively from a social point of view[7].

3.4 Economics of social pressure

Assume now that an equilibrium is not achieved by the bioeconomic system on its own. For instance, if the number of compliers is low, then little social pressure can be exercised. Hence, there is a strong likelihood that the number of defectors will rise and the biophysical system will drift along an unsustainable path which may lead to inefficient equilibrium or resource depletion.

3.4.1 Traditional policy instruments

As a first-best policy instrument economists would traditionally advocate for imposing a tax on the amount of the resource extracted by the defectors. According to economic theory, this tax $\hat{\theta}$ should be equal to the socially optimal path of the user costs $\eta^*(t)$ (Perman et al. [2011]), i.e.,

$$\hat{\theta} = \eta^*(t). \tag{3.11}$$

However, since the traditional approach does not consider the social interaction between the agents the tax $\hat{\theta}$ is inefficient. The first-best policy instrument where social interactions are taken into account is defined by the resource-extraction tax θ_i that is given by

$$\theta_i = \eta^*(t) - \omega(s, c_i, \tau_{c_i})(\pi_i^D - \pi_i^C) = \eta^*(t) - a(\tau_{c_i})e^{-de^{-g(s)c_i}}(\pi_i^D - \pi_i^C). \tag{3.12}$$

This takes into account the state of the resource, the local cohesiveness of the compliers and the share of compliers in the neighborhood of agent i. Eq. 3.12 differs from previous literature about network effects and pigouvian taxes where only a single aspect of the network, like the share of compliers among all the members of the community in question, c, is taken into account (Greaker and Midttømme [2016]). Instead, eq. 3.12 shows, in particular, that taking account of a single aspect of the structure of social network, like c, may actually lead to a poor approximation of the first-best policy

[7] One should bear in mind that the interpretation of equilibrium employed in evolutionary game theory is different from that employed in non-cooperative game theory. In the latter, equilibrium provides guidance for the agent with respect to the choice of the strategy. In evolutionary game theory, however, an equilibrium simply describes a temporary or permanent steady state without offering directions for the choice of the strategy.

instrument. Depending on the value of the local cohesiveness of the compliers and the state of the resource, the use of a single aspect of the network may magnify or diminish the error of the tax $\hat{\theta}$. In Section 3.7 we determine the quality of the approximation of social interactions by using the single aspect c. In particular, we determine the lower and upper limit of indefiniteness of the share of compliers for its future evolution. The size of the interval indicates that using the single indicator c is likely to introduce a significant error when calculating the tax θ_i. Eq. 3.12 also shows that the tax varies over time and is specific for every agent because the local cohesiveness of the compliers τ_{c_i} and the share of compliers c_i are defined for the neighborhood of agent i which, together with the state of the resource, changes over time.

The imposition of a personalized and time-dependent tax might be complicated to implement. In this situation, the community may decide to impose a one-time payment (ν_i) on the defector whose behavior has inflicted a loss on the compliers, so that the number of compliers rises which, in turn, induces more defectors to change their strategy and adhere to the social norm. Given that there is now a higher number of compliers, the resource is managed in a more sustainable way.

Proposition 1: (Equilibria conditions):

One-time payments can immediately increase the number of compliers. Likewise, an increase in the number of links between compliers increases local cohesiveness. Provided that the number of compliers and/or the increase in local cohesiveness of compliers resulting from such an action is high enough, the increased social pressure allows for the new number of compliers to be maintained, thus favoring the sustainable management of the resource[8].

For this argument to be plausible, one should bear in mind that the short-sighted behavior of defectors obstructs the emergence of cooperative behavior. The short-sightedness of defectors is the origin of the tragedy of the commons. However, at the same time it offers a solution. Such short-sightedness enables the number of compliers to be increased at relatively low costs. Since defectors abandon their strategy as soon as their utility is less or equal to the one of compliers, only a one-time payment is required. Further payments are not necessary if enough defectors change sides which, in turn, increases the element of social punishment and eliminates the incentive to

[8]Nyborg and Rege (2003) and Blanco et al. (2009), suggested an increase in the number of compliers such that an all-complier equilibrium can be achieved. However, their proposal does not consider network effects or determining the one-time payment.

revert to a defection strategy. If defectors had a planning horizon longer than a year, the payment would have to be larger to compensate not only for the forgone extra benefits of the current period, but also for those of future periods. In the case of a one-year planning horizon a defector is willing to become a complier if their new utility is greater than before, i.e.,

$$\pi^D - \omega_i(s, c_i, \tau_{c_i})(\pi^D - \pi^C) < \pi^C + \nu_i, . \tag{3.13}$$

where ν_i denotes the minimal one-time payment.

Alternatively, or in combination with a policy aimed at increasing the number of compliers, the community may employ the characteristics of the network to achieve a higher adherence to the social norm. In particular, it may aim to increase the number of links between the compliers, for instance through specific actions such as organizing workshops, creating institutions, running training courses or providing other additional benefits exclusively for compliers. Newly created links between compliers, as a result of these actions, increases local cohesiveness which, in turn, increases social pressure. The choice of policy to be implemented will depend on the number of compliers and the strength of local cohesiveness required for the sustainable management of the resource. How to identify the missing number of compliers and how to determine the additional strength of cohesiveness that complies with eq. 3.13 is discussed in sub-section 3.7.4. If the community wants to comply with eq. 3.13 at minimal costs, it will need to identify the agents with the lowest costs and the neighborhoods with the lowest local cohesiveness of compliers. For this purpose, the experience gained from designing reverse auctions as payment schemes for environmental services could be used to target one-time payments (Schomers and Matzdorf [2013]), along with undertaking surveys to better target link-building activities.

3.4.2 The economic value of the different elements of social punishment

As discussed in Section 3.4, individual social pressure, ω_i , is often not equal to the social pressure, $\bar{\omega}_i$, needed to support a network equilibrium. Missing or excessive social punishment could be substituted by a tax or a subsidy so that the sum of each defector's social punishment and the amount of an individual tax/subsidy $ł_i$ is equal to

the social punishment equilibrium $\bar{\omega}_i(\cdot)(\pi^D - \pi^C)$[9]. Mathematically, the tax/subsidy is given by

$$\omega_i(s, c_i, \tau_{c_i})(\pi^D - \pi^C) + \text{ł} = \bar{\omega}_i(\cdot)(\pi^D - \pi^C). \tag{3.14}$$

Although, as mentioned above, the imposition of an individual tax/subsidy that varies over time is not a realistic policy option eq. 3.14 is, however, very informative in other ways as it allows the economic values of a change in the share of compliers in the neighborhood of agent i, c_i, the strength of local cohesiveness among the compliers in the neighborhood of agent i, τ_{c_i}, and the stock to be determined. Based on a comparative static analysis, we obtain:

Observation 1: (The marginal economic value of social punishment) An increase in the share of compliers or local cohesiveness of compliers will increase the economic value of social punishment, whereas an increase in stock will lead to a increase or decrease in the economic value of social punishment.

The mathematical details for Observation 1 can be found in the Appendix A. While the effect of an increase in the share of compliers or the local cohesiveness of compliers leads unambiguously to more social punishment, an increase in the stock leads only to an increase in social punishment if the stock-dependent costs are important. For the opposite case social punishment decreases with an increase in the stock.

3.5 A numerical analysis based on the groundwater extraction case

The social-ecological system defined by eq. 3.1 - 3.6, form the basis for the agents' strategy choice within the social network $N = (A, L)$ which consists of 7500 agents. All the networks considered are scale-free and have an average degree of 15. The structure of the social network and its current state enters the system via the social pressure function ω, which depends on the depth of the water table, the share of compliers and the cohesiveness of compliers of the neighborhood of agent i. Given the complexity of this system, it is not possible to provide an analytical solution and therefore we offer a numerical analysis. For the numerical study, we focus on a case of

[9] A subsidy would be required if the social pressure is too high so that even a defector that is not required to change would like to do so. Only a subsidy can compensate for strong social pressure and make the defector stick to their current strategy.

groundwater extraction to irrigate agricultural land, more precisely the Western La Mancha Aquifer (Spain). The two resource demand functions were determined by a mathematical programming model that was programmed in GAMS (General Algebraic Modeling System). More details on this part of this model are provided in Appendix C - Numerical Analysis and Specification of the Functions Employed.

We start our analysis with the limiting cases where i) all agents are compliers or ii) all agents are defectors. Moreover, we assume that none of the agents change their strategies over time. In this case, there is no interaction between agents, i.e., there are no network effects. To analyze the evolution of the water table of the aquifer, the social-biophysical system is based on eq. 3.1 - 3.6 with $\omega = 0$. Figure 1 presents the drop in the water table assuming an initial water table depth of 0 m and 135 years as the hypothetical lifetime of the well.

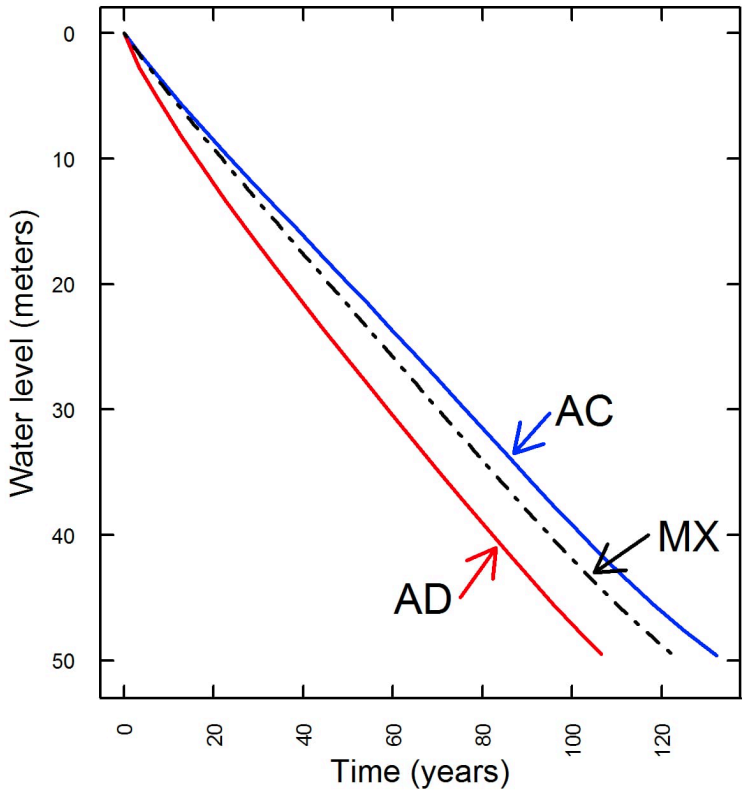

Fig. 3.1 Evolution of the water table.

Evolution of the water table for different strategies, where AD = all defector population, AC all compliers population and MX = mixed population.

Fig. 3.1 shows that the water table declines constantly and if all agents were compliers, (AC), the aquifer would be depleted in 135 years. Conversely, if all agents were defectors, (AD), the extraction rate would be higher and the aquifer would be depleted within 106 years. Finally, if the population of agents consists of compliers and defectors (case MX) for at least some period of time, the aquifer would be depleted sometime between 106 and 135 years. Furthermore, our calculations indicate that an identical qualitative pattern of extraction (not presented in Fig. 3.1) is obtained if the initial depth of the well were lower and the economic lifetime were 25 years. In both cases, it is always optimal to decrease the water table constantly until (whichever comes first) the bottom of the well is reached or the economic lifetime of the well concludes.

The estimated marginal benefits and the calculated extraction cost (Appendix C) explain why both types of agents extract down to the full depth of the well. Once the bottom of the well has been reached, the current social norm cannot be maintained since natural recharge is not sufficient to satisfy the demand of the agents, even if they were all compliers[10]. Thus, the members of the social network need to agree on a shift in the regime and stipulate a new social norm that allows supply and demand to be met once the aquifer has been depleted. Alternatively, the members could have defined a more stringent social norm right from the beginning that would have guaranteed a sustainable level of extraction at an earlier point in time, i.e., when the level of water table was higher than the depth of the well. For our analysis, however, these considerations are not of real importance since we are studying social punishment and the factors that influence an agent's decision to comply or not with the social norm. The factors we consider are related to the structure and state of the social network, and to an agent's strategy, but not to the formulation of the underlying social norm. In this respect, the results of our study are also valid if the social norm were redefined.

3.5.1 Cooperation vs. non-cooperation

Given the specification of the social-biophysical system (eq. 3.1 - 3.6) we start our analysis for the entire network - the macro-perspective. Fig. 3.2a and 3.2b show the evolution of the share of compliers c and defectors over time for two different initial values (0.5 and 0.65) of the share of compliers c_0, the two different initial values (15m and 40m) of the depth of the water table $s(0)$, and three different degrees (0.05, 0.15

[10]The water table constantly decreases over the entire planning horizon, even if all agents were compliers. This implies that the natural recharge is always less than the agents' demand. In other words eq. 3.9 in general terms or eq. 3.21 from Appendix C cannot be met for the case of the aquifer.

and 0.35) of the average local cohesiveness of the entire social network τ. Given the evolution of the share of compliers in Fig. 3.2a and 3.2b, the corresponding evolution of social punishment $\omega(\cdot)(\pi^D - \pi^C)$ can be observed in Fig. 3.2c and 3.2d. Additionally, the last two figures also show the corresponding evolution of the defector's extra benefits $(\pi^D - \pi^C)$ for an average local cohesiveness of 0.35[11].

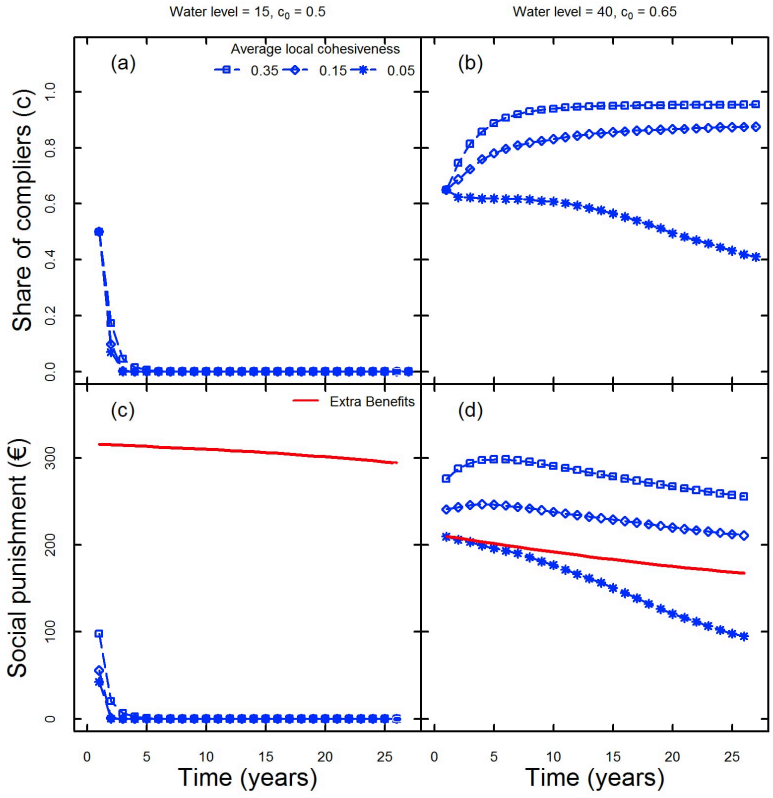

Fig. 3.2 Evolution of the share of compliers

Fig. 3.2a – 3.2b: Evolution of the share of compliers for different degrees of average local cohesiveness with $\tau = 0.05$, 0.15, and 0.35. Fig. 3.2a: $c_0 = 0.5$, $s(0) = 15$, Fig. 3.2b: $c_0 = 0.65$, $s(0) = 40$. Fig. 3.2c – 3.2d: Evolution of social punishment (SP) and of the defectors extra benefits for differing degrees of average local cohesiveness with $\tau = 0.05$, 0.15, 0.25 and 0.35. Fig. 3.2c: $c_0 = 0.5$, $s(0) = 15$, Fig. 3.2d: $c_0 = 0.65$, $s(0) = 40$.

[11]While average local cohesiveness does not affect $(\pi^D - \pi^C)$ directly it does indirectly through its effect on the evolution of the depth of the water table which, in turn, affects net benefits. However, $(\pi^D - \pi^C)$ is relatively insensitive to changes in the average local cohesiveness and thus, we graph the extra benefits only for the value of 0.35.

With an initial value $c_0 = 0.5$ for the share of compliers, Fig. 3.2a shows that even higher values of average local cohesiveness cannot delay the decrease in the share of compliers in the network if the initial water depth is 15m. The relatively little scarcity of groundwater leads to ineffective social punishment of defectors and so compliers abandon their current strategy and become defectors within 5 years. A reversed result is obtained in Fig. 3.2b, where the scarcity of groundwater ($s(0) = 40$), an initial value $c_0 = 0.65$ and values of average local cohesiveness above 0.05, lead to appropriately high social pressure that the number of compliers increases over time. Only very weak average local cohesiveness, $\tau = 0.05$, is not sufficient to accumulate the social pressure required to maintain and expand the initial number of compliers. Fig. 3.2b also reveals that even though the share of compliers increases, it does not reach one. There is always a certain (albeit small) number of defectors that receive no or very little social pressure. In the cases where the defectors' neighborhood consists mainly of other defectors or local cohesiveness of compliers is very low, social pressure is very weak or does not even exist. In other words, defectors can survive if they live in a fairly isolated community where compliers are absent or less cohesive. Fig. 3.8a and 3.8d in Appendix D (Evolution of Social Pressure) illustrate this phenomenon since social pressure does not attain its maximal value. This observation is analogous to a finding in the non-cooperative game literature where (Bramoullé [2007]) observed that agents have an incentive to anti-coordinate if they are embedded in a bipartite network. Although these findings are obtained in very distinct frameworks, the underlying force in both cases is the social network heterogeneity that leads to segregation. Fig. 3.2a and 3.2b show that, overall, sufficiently strong network effects and the state of the resource can modify or even reverse the effect of the share of compliers. Fig. 3.2c and 3.2d show that as long as the defector's extra benefits are greater than social punishment, the agent will likely maintain their strategy. Once this relationship is reversed, however, the agent will likely become a complier. Thus, the evolution of the difference between the defector's extra benefits and social punishment explains the evolution of the share of compliers observed in Figures 2a – 2b.

Moreover, Fig. 3.2c and 3.2d provide information about the tangible monetary value of social pressure (social punishment) on the scale of the network. Fig. 3.2c, for instance, shows that an increase in average local cohesiveness has virtually no monetary value since the three lines are nearly identical after the first three years. When comparing the level of social punishment between Fig. 3.2c and 3.2d, the same degree of average local cohesiveness offers information about the monetary value of a drop in the water table (from 15m to 40m) and of an increase in the initial share of

compliers. Thus, the comparison between Fig. 3.2c and 3.2d allows the monetary value of social punishment attributable to the change in the water table and the initial share of compliers to be determined. Likewise, the distance between the different trajectories of the social punishment in each of the four figures allows for the monetary value of the social punishment attributable to a change in the degree of average local cohesiveness to be established.

The results can be summarized in the following observation:

Observation 2: (Critical mass of compliers and limited substitutability between the share of compliers and average local cohesiveness on the macro level)

Fig. 3.2c and 3.2d show that the resource can only be managed in a sustainable way if the initial number of compliers in the network exceeds a "critical mass". The value of this "critical mass" depends on the strength of the average local cohesiveness of the network and the depth of the water table. The share of compliers, network effects and the state of the resource are substitutes within certain limits. Thus, for a given share of compliers, average local cohesiveness and the state of the resource can be decisive for the agents' strategy choice. An all-complier equilibrium does not emerge if an isolated group of defectors, who are hardly exposed to any social pressure, evolves.

Finally, Fig. 3.2c and 3.2d also illustrate the inefficiency when a traditional "first-best" tax $\hat{\theta}$ on the extracted amount of the resource by defectors is chosen to be equal to the socially optimal path of user costs $\eta^*(t)$ as defined in eq. 3.11. This inefficiency is quantified in eq. 3.12 and corresponds to the vertical difference between the extra benefits and the social punishment in Fig. 3.2c and 3.2d. Likewise, this difference presents the minimum amount of the one-time payment ν_i as defined in eq. 3.13.

3.5.2 The share of compliers as a catalyst for sustainable management

The share of compliers as a catalyst for sustainable management Fig. 3.2a and 3.2d have highlighted the importance of the depth of the water table, average local cohesiveness and the share of compliers for a sustainable and socially efficient management of the resource. For the choice of the values of local cohesiveness, however, one has to take to into account that the share of compliers conditions the maximal magnitude of local

cohesiveness of compliers. By definition, the fewer compliers in the neighborhood there are, the lower the maximum value of local cohesiveness of compliers $\tau_{c_i}^{max}$ is, since the set of compliers in the neighborhood is a subset of the set of neighbors. For this reason, there is a functional relationship between the share of compliers in the neighborhood and the maximum local cohesiveness of compliers that can be achieved. It can be approximated by $c_i^2 \approx \tau_{c_i}^{max}$ and is denoted by $c_i^2 \approx \tau_{c_i}^{max}(c_i)$.

Fig. 3.2a and 3.2d show, in particular, that initial values of the share of compliers, the state of the resource and local cohesiveness are driving factors behind the agents' decision to adhere to the social norm. This echoes the idea that these factors shape the individual's incentives to become a complier. One of the critical factors for the evolution of the resource is the share of compliers. For the values considered for the state of the resource and local cohesiveness, Fig. 3.2a and 3.2d seem to suggest that the critical mass of the share of compliers is situated somehow between 0.5 and 0.65. These critical mass values can be related to the social pressure function as defined in eq. 3.3. If social pressure is equal to 1, the utility of defectors and compliers are identical and thus, agents have no incentive to change their strategy. However, if the social pressure is below 1, the defectors obtain extra benefits and consequently compliers are likely to change their strategy to non-compliance. If the social pressure is above 1, defectors obtain negative extra benefits and are likely to change their strategy to compliance. The more the social pressure differs from 1, the more likely the agent is to switch from their current strategy to the alternative one. Thus, a social pressure of 1 allows the critical mass c_i^{crit} of the share of compliers to be determined.

The minimal-required initial share of compliers denoted by $\underline{c}_i^{crit}$, and which excludes a decrease in the number of compliers over time for different values of s, is given by the set

$$\underline{c}_i^{crit}(s) = \left\{\omega(s, c_i, \tau_{c_i}^{max}(c_i)) = 1\right\}. \tag{3.15}$$

As illustrated in Fig. 3.3, the set provides for different values of the stock and the maximum value of the local cohesiveness of compliers $(\tau_{c_i}^{max}(c_i))$, the minimal initial number of compliers, denoted as $\underline{c}_i^{crit}$, that allows for a negative evolution of the population of compliers to be discarded. Likewise, we determine for different values of the stock and the minimal value of local cohesiveness of compliers, $\tau_{c_i}^{min} = 0$, the maximal initial share of required compliers, $\bar{c}_i^{crit}$, that will lead to a positive evolution of the number of compliers over time. In other words, if the initial share of compliers is above $\bar{c}_i^{crit}$, the number of compliers will increase over time. The critical level of the

initial share of compliers $\bar{c}_i^{crit}$ is determined by the set

$$\bar{c}_i^{crit}(s) = \left\{\omega(s, c_i, \tau_{c_i}^{min} = 0) = 1\right\}. \tag{3.16}$$

Hence, we can conclude that the evolution of the share of compliers is always negative if the initial number of compliers is smaller than $\underline{c}_i^{crit}$, but will always be positive if the initial number of compliers is larger than $\bar{c}_i^{crit}$. As shown in 3.3, is equal to one. The two values, $\underline{c}_i^{crit}$ and $\bar{c}_i^{crit}$, are the limiting values of the critical mass, i.e., $c_i^{crit} \in (\underline{c}_i^{crit}, \bar{c}_i^{crit})$. Fig. 3.3 provides a graphical representation of the sets $\underline{c}_i^{crit}$ and $\bar{c}_i^{crit}$. For the sake of brevity, we have put the mathematical details for the detailed specification of the social pressure function allowing the sets to be determined in Appendix C (Numerical Analysis and Specification of the Functions Employed). For a given value of the stock the initial share of compliers that is above $\bar{c}_i^{crit}$ guarantees a positive evolution of the share of compliers over time, whereas values below $\underline{c}_i^{crit}$ guarantee a negative evolution. For any initial share of compliers within the interval $c_i^{crit} \in (\underline{c}_i^{crit}, \bar{c}_i^{crit})$ the evolution of the share of compliers is undetermined and depends on the precise values of the local cohesiveness of compliers. The range of the indeterminacy is depicted by the shaded area in Fig. 3.3. Although the assumption of $\tau_{c_i}^{min} = 0$ is extreme, it does allow the complete range of indeterminacy to be ascertained. In reality, one expects that at least some compliers are linked to each other and thus for $\bar{c}_i^{crit}$ to be below 1 and slightly curved downward.

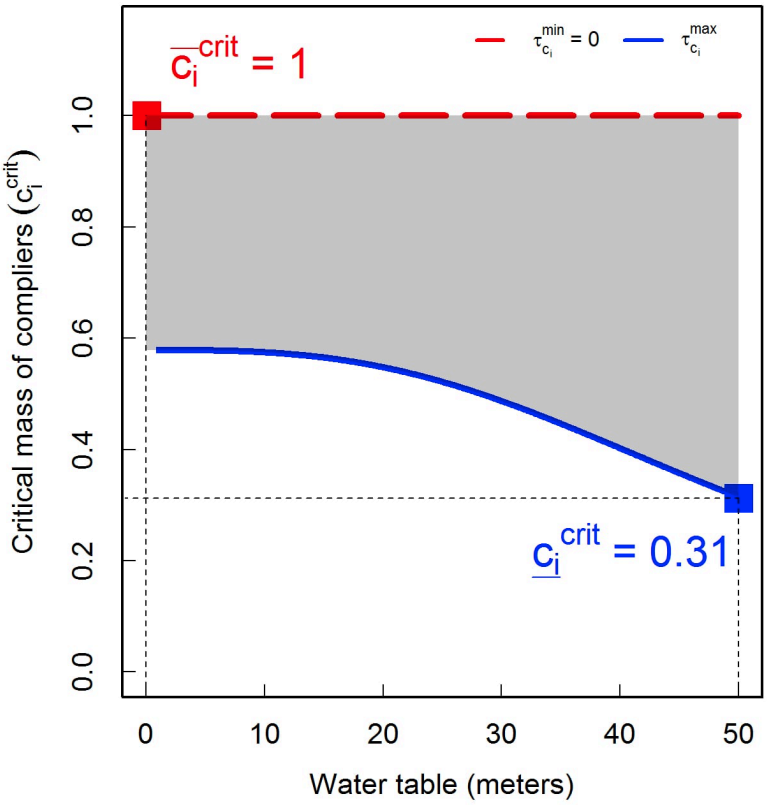

Fig. 3.3 Maximal and minimal initial share of compliers

Maximal and minimal initial share of compliers that condition either a negative or positive evolution of the share of compliers.

The size of the interval $(\underline{c}_i^{crit}, \bar{c}_i^{crit})$ corresponds to the vertical distance between the two continuous lines and reflects the influence that the strength of the local cohesiveness of compliers (network effect) has on the evolution of the critical values of the share of compliers. Likewise, the changes in the vertical distance between the two continuous lines indicate the influence the depth of the water table exerts on the interval $(\underline{c}_i^{crit}, \bar{c}_i^{crit})$. The possible (wide) range of $(\underline{c}_i^{crit}, \bar{c}_i^{crit})$ also indicates that the share of compliers alone is an inaccurate indicator of cooperativeness and to be correctly interpreted needs to be accompanied by other characteristics of the social network such as the local cohesiveness of compliers or the state of the resource.

The results have, so far, been framed in terms of the neighborhood of agent i. As far as the neighborhood of agent i is representative of the network, the results can be generalized. For the case where this condition does not hold, the results cannot be

carried over directly. In this case, the specific values of the points $\underline{c}_i^{crit}$ and $\bar{c}_i^{crit}$ are likely to be different, but the elements and principal conclusions of the analysis will not be affected.

Fig. 3.2 shows that a critical mass of compliers is necessary for the sustainable and efficient management of the resource, however, this is not actually sufficient to ensure this is so. The population dynamics themselves are important but need to be accompanied by the dynamics of the network and the state of the resource. Fig. 3.3 highlights these dependencies. In the absence of the local cohesiveness of compliers and the scarcity of the resource, even an extremely high share of compliers is not sufficient to prevent the degradation of the resource and the proliferation of defectors over time. These results are summarized in the following observation:

Observation 3: (Critical mass of compliers, state of the resource and network effects)

3.3 shows that a sufficiently high share of compliers is necessary, but is not sufficient for the sustainable management of the resource. The necessary share of compliers depends on the state of the resource and the strength of local cohesiveness of compliers.

3.5.3 Social pressure and the density and size of the network

The influence the local cohesiveness of compliers has on the critical mass of compliers that supports cooperativeness, c_i^{crit}, is presented more explicitly in Fig. 3.4a for a given depth of the water table: $s = 15$. It shows that the critical value decreases as the network effect increases. The graph is bounded to the right because the local cohesiveness of compliers is limited by the number of compliers; more precisely by $\tau_{c_i}^{max} = c_i^2$. Fig. 3.4a is linked to Fig. 3.4b through the strength of the local cohesiveness of compliers τ_{c_i} which in turn is related to the number of links between the neighbors (compliers and defectors) of agent i, denoted by τ_i. An increase in the number of links (increase in density) between the neighbors can be allocated randomly or directionally. In the latter case, new links are only formed between the neighbors who are compliers. Directional formation of new links leads to a one-to-one increase in local cohesiveness. Hence, the slope of this directional-formation line is 1, along which it holds that $\tau_i = \tau_{c_i}$. The term τ_{c_i} increases until $\tau_{c_i}^{max}$ is reached. From there on, additional links between neighbors do not strengthen the local cohesiveness of compliers any further because its value is limited by $\tau_{c_i}^{max}$. For the graph in Fig. 3.4b and without loss of generality we consider a share of compliers of 0.57 as an example so that $\tau_{c_i}^{max}$ is approximately given

by 0.325. A random allocation of new links between the neighbors of agent i also leads to an increase in the local cohesiveness of compliers, but requires far more new links for the same amount of increase. Only if nearly all the neighbors are randomly connected is the value of $\tau_{c_i}^{max}$ reached. Any value located in the blue area presents links between defectors and between compliers and defectors that are inefficient with respect to the local cohesiveness of compliers because the same degree of local cohesiveness could be achieved with fewer links. Likewise, any value in the red area indicates that links are redundant because the degree of local cohesiveness has already reached its maximal value with fewer links.

The fact that links are redundant sheds new light on the findings in the previous literature (Coleman [1988]; Karlan et al. [2009]), where an increase in τ_i (denser networks) favors the compliance to a social norm. Fig. 3.4b shows that an increase in links only favors compliance to the social norm up to the point where τ_i is equal to the value of the maximal local cohesiveness of compliers, $\tau_{c_i}^{max}$. Beyond this point an increase in density does not contribute to higher social pressure.

Many authors have highlighted the importance the share of compliers (Osés-Eraso and Viladrich-Grau [2007]; Sethi and Somanathan [1996]; Tavoni et al. [2012]) has for the socially efficient management of the resource. However, the share of compliers is independent of the size of the community, which questions the widespread hypothesis (Ostrom et al. [1999]) that a small community exercises more social pressure than a large community does. Fig. 3.4b offers an explanation for this apparent contradiction. For this purpose, we compare a small and large community where the share of compliers is identical.

In a small community, it is often the case that agents know each other well and so the density and local cohesiveness of all neighbors τ_i is high. For example, consider a complete network where by definition $\tau = \tau_i = 1$. This equation holds simply because all agents are connected with each other so that all the agents have the same neighborhood. Thus, given a share of compliers, for example 0.57, a small community presented by a complete network is always located in Fig. 3.4b at the point $(\tau_{c_i}^{max}, 1)$.

In more general terms with respect to the network structure, recent research (Barábasi and Albert [1999]; Clauset et al. [2009]) has shown that agents can only maintain a limited number of links ($k <<< n$), which results in a sparse (low density), scale-free social network as the number of agents n of the network increases. Thus, as the network grows, the total number of actual links increases to a lower degree than

the possible number of links[12]. Consequently the density of the network decreases with an increase in size[13]. As the density of the network is reduced, the probability of transitive relationships between agents is severely constrained. Moreover, for scale-free networks (Dorogovtsev and Mendes [2002]) and (Szabó et al. [2003]) found that the local cohesiveness of all neighbors decreases with the degree of agents by approximately $\tau_i \approx k_i^{-1}$, which means that high-degree agents tend to have a low cohesiveness coefficient. These findings suggest that the probability of having $\tau_i \geq \tau_{c_i}^{max}$ decreases rapidly with the network size and degree of the agents. Fig. 3.4b shows that large networks, characterized by the fact that the density of higher-degree agents is significantly lower than $\tau_{c_i}^{max}$, cannot build up sufficient local cohesiveness between compliers to attain the value of $\tau_{c_i}^{max}$. In a particular neighborhood, $\tau_{c_i}^{max}$ may be achieved, especially for agents with small degrees, but not the maximal average local cohesiveness on the scale of the network.

Observation 4: (Social pressure in relation to the size and degree of the network)

Given the same size network, denser networks favor compliance to the social norm, but only up to the point where the maximal strength of the local cohesiveness of compliers is reached. Beyond this point higher density is redundant. The density of a network is an imprecise indicator for cooperativeness because it considers not only links that help to tighten local cohesiveness of compliers but also redundant links. Given the same share of compliers and same degree, smaller networks with high densities facilitate attaining the maximal local cohesiveness of compliers, whereas larger networks with low densities and scale-free structure cannot reach the maximal local cohesiveness.

Observation 4 provides a conceptual interpretation of the oft-cited finding that closely knit networks favor social norm compliance more than loosely knit networks do. Yet, this finding has to be considered with caution since it is the type of knit, more than the tightness of the knit that is important. Likewise, this explains why, given a degree,

[12]The total number of links increases as a linear function of the number of agents given by $|L| = \sum_{i=1}^{n} k_i$. However, the possible number of links increases with the square of the network size given by $L^{max} = \frac{n(n-1)}{2}$. Thus, the network density, $d = \frac{2|L|}{n(n-1)} < 1$, decreases with the network size.

[13]Although the following example is not based on a scale-free network it illustrates the relationship between density and degree. Assume that every agent knows exactly 100 other agents. Thus, if the network consists of 100 agents we have a complete network with degree 100. However, if the network would consist of 1000 agents the agents only knows 10% of all agents and the density of the network would decrease while the degree remains 100.

smaller networks comply to the social norm more than larger networks do. Thus, while the share of compliers is important, so too is the size and density of the network as these two factors exercise a very significant influence on the strength of social pressure.

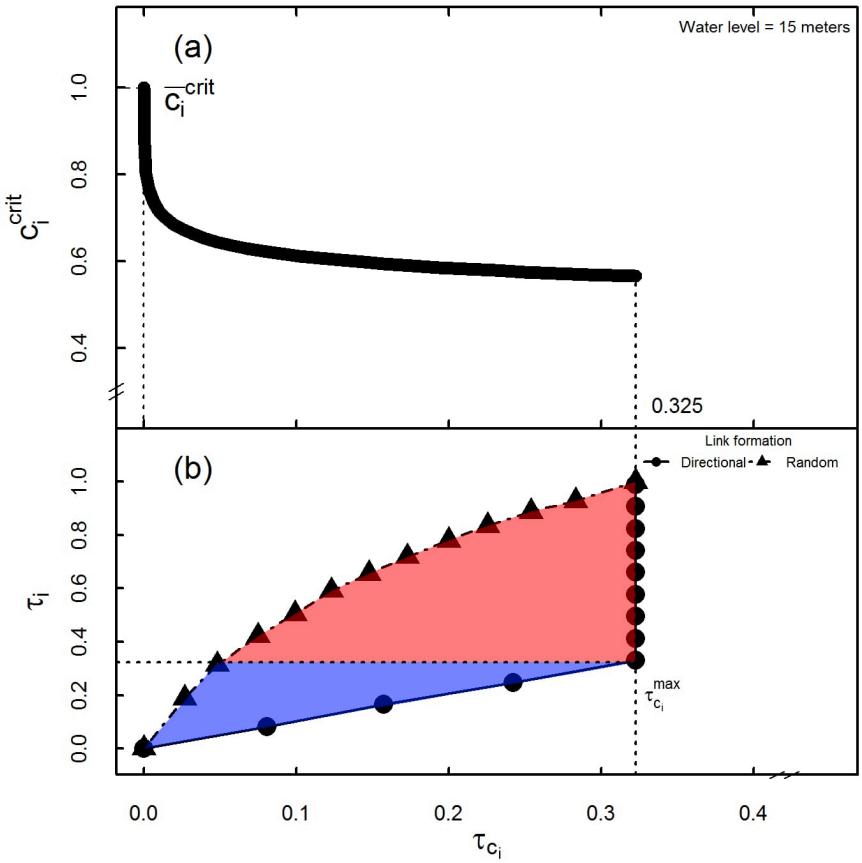

Fig. 3.4 Critical share of compliers, density and local cohesiveness

Fig. 3.4a: The critical share of compliers as a function of local cohesiveness of compliers (level curves) with $\tau_{c_i}^{max} = 0.325$. Fig. 3.4b: The relationship between density and local cohesiveness with $\tau_{c_i}^{max} = 0.325$.

3.5.4 Social punishment and the social network characteristics on the micro level

Our previous analysis focused mainly on the overall structure of the network (i.e., a macro perspective). For the remainder of the analysis, we concentrate on the structure of agent i's neighborhood (i.e., a micro perspective). Fig. 3.2a – 3.2d allowed the monetary value of social pressure as a function of time, the average local cohesiveness

of compliers and of the depth of the water table at the macro level to be determined. Fig. 3.5 provides information about the economic value of the share of compliers and local cohesiveness of compliers in the neighborhood of agent (i.e., at the micro level). As explained above, to interpret Fig. 3.5 one should keep in mind that the value of the share of compliers introduces an upper limit of local cohesiveness of compliers. For this reason, the part of the c_i, τ_i plane that is not admissible has been left blank.

Based on eq. 3.13, we determine the one-time payment as the difference between the defector's and complier's utility. Thus, if the community were to offer this one-time payment to a defector, they would abandon their current strategy and would become a complier. This one-time payment is determined by the solution of the following equation:

$$\nu_i = U^D - U^C = \pi^D - \omega_i(s, c_i, \tau_{c_i})(\pi^D - \pi^C) - \pi^C = (1 - \bar{\omega}_i)(\pi^D - \pi^C). \qquad (3.17)$$

with respect to the three unknown s, c_i, τ_{c_i}. The three-dimensional plane in Fig. 3.5 shows the level curves of social punishment for different values of the share of compliers, of the local cohesiveness of the compliers at time 0 and given a water table depth of 15 m. The defector's extra benefits, $\pi^D - \pi^C$, amount to €316.36 and are presented by the line in bold. These extra benefits are marked by a straight line because, for a given moment in time, they depend only on s, and not on c_i or τ_{c_i}. If social punishment is below the line in bold ($\omega_i < 1$), the defector's extra benefit $\pi^D - \pi^C$, is greater than social punishment. In this case, a one-time payment of $(1 - \omega_i)(\pi^D - \pi^C)$ is needed to offer the agent an incentive to abandon their current strategy and to adhere to the complier's strategy. The difference between the defector's extra benefits $\pi^D - \pi^C$ and the three-dimensional plane for the monetary value of social punishment determines the amount required for the one-time payment.

Fig. 3.5 also shows the level-curves of social punishment. The distance between the level curves indicates an €80 decrease or increase in social punishment. To keep Fig. 3.5 simple, we have only marked the level curve whose value is equal to the defectors' extra benefits of €316. The form of the level curves indicates that the substitution elasticity between the share of compliers and the local cohesiveness of compliers is relatively close to 0. Only within a small range of the values of the share of compliers and of local cohesiveness of compliers can both arguments for social punishment substitute each other. The level curves are not evenly spaced, indicating that the greater the distance between the level curves, the lower the effect an increase in the share of compliers or local cohesiveness of compliers has on the social punishment. We also solved eq. 3.17 for s=40m.

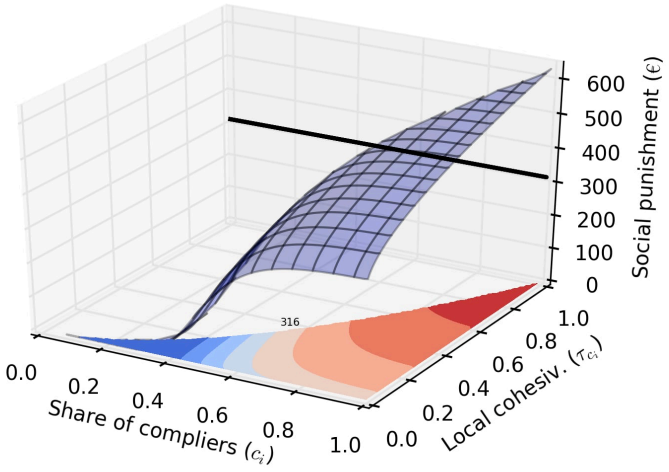

Fig. 3.5 Economic value of Social Punishment

Social punishment as a function of the share of compliers c_i and local cohesiveness of compliers τ_{c_i} with $s(0) = 15$.

Fig. 3.5 is the result of a snapshot at time 0 and, as such, it does not provide any information about the evolution of the social punishment over time. Figures 2a – 2d show the evolution of compliers and of social punishment over time. Thus, the only missing information to determine the social punishment over time is the evolution of the defector's extra benefits. This information is presented in Fig. 3.9a – 3.9d in the Appendix D (Evolution of Social Pressure).

3.6 Concluding remarks

This study defines a social norm based on the socially-optimal management of a renewable natural resource owned by a community. In contrast, the non-compliance of the social norm is linked to short-sighted behavior where agents maximize the net benefits of the current time period. Based on these two extraction strategies, we define compliers (in compliance with the social norm) and defectors (non-compliance with the social norm). Agents can revise their strategy within an evolutionary game-theoretic approach, i.e., the probability of changing from their current strategy to the alternative one increases the higher the perspective gains become. Although agents are free to choose their preferred strategy, we consider the case where compliers exercise a

social punishment that reduces the defector's utility. Social punishment depends on the remaining level of the natural resource, the number of compliers and their local cohesiveness in the neighborhood of agent i. This formulation aims to answer the question as to what extent network effects (share of compliers, local cohesiveness of compliers, size and density) and stock effects (resource) provide incentives for individual agents to comply with a social norm, to what extent compliance with a social norm is a self-enforcing process and what exactly are the social and physical conditions required to either initiate this process or choke it off.

If all equilibrium conditions hold, an overall equilibrium (with respect to the dynamics of the resource, the network and the resource demand) may emerge. However, given the asymmetry and complexity of the network, no analytical solution can be provided. In contrast with the previous literature, the emergence of an all-complier-network equilibrium is extremely unlikely since isolated communities of defectors immune to social punishment may emerge.

Given the limitation of an analytical solution, the study analyzes the case of the Western La Mancha Aquifer in Spain. There, the social network consists of approximately 7500 farmers. Given the economic conditions and the maximal depth of the aquifer, an economic equilibrium does not exist. The results show that, while a sufficiently high share of compliers is required for the efficient management of the resource this is not sufficient in itself. The magnitude of the critical mass of compliers depends on the state of the resource, the density, the size and local cohesiveness of compliers of network. The wide range of the critical mass leads to an indeterminacy that highlights the fact that the share of compliers or any other single aspect of the network alone is not a precise indicator for evaluating cooperativeness. To narrow down the range of indeterminacy additional information about the characteristics of the social network and the state of the resource is indispensable. For instance, a higher density is likely to favor cooperativeness but on its own it is an imprecise indicator for cooperativeness since it does not distinguish between links that tighten the local cohesiveness of compliers or those that are redundant. The results also show that, given the same share of compliers and average degree, smaller networks better support cooperativeness than larger networks do.

Moreover, the analysis allows for practices favoring the sustainable management of natural resources to be identified and targeted. An example of such a practice would be the one-time payment to defectors based on the condition that they adopt the complier's strategy. As a result of the increase in social pressure, one would expect defectors not to revert to their former behavior. The critical mass of the initial share

of compliers indicates how many compliers are needed to implement such a policy. Moreover, the study allows the magnitude of error to be determined for a traditional "first-best" tax on the amount of the resource extracted compared to a tax that takes into account of the interaction between the agents. Finally, the study provides a monetary valuation of the intangible good – social pressure – in the case of the Western La Mancha Aquifer.

There seem to be two promising directions in which the analysis of the study could be extended. First, the current work can be considered as a building block to developing a metric for the cooperativeness of a social network. This implies analyzing and extending the relationships between the metrics employed for the different characteristics of the network. The second line of research is related to changes in the underlying economic forces. The assumption that social pressure is costless for the compliers or the defector's extra benefits are independent of the state of the social network could be revised. A change in the later assumption, for instance, may lead to an anti-coordination behavior if the defectors' extra benefits were to increase as the number of compliers increases.

3.7 Appendices

3.7.1 Appendix A: Observation 1

Based on eq. 3.14 the analysis shows that

$$\frac{\partial ł_i}{\partial c_i} = -\frac{\omega_i(\cdot)(\pi^D - \pi^C)}{\partial c_i} < 0, \frac{\partial ł_i}{\partial \tau_{c_i}} = -\frac{\omega_i(\cdot)(\pi^D - \pi^C)}{\partial \tau_{c_i}} < 0 \tag{3.18}$$

Eq. 3.15 indicates that, an increase in the number of compliers in the neighborhood of agent reduces the tax/subsidy required to maintain the steady state equilibrium pressure. It also specifies that an increase in local cohesiveness between the compliers within the neighborhood of agent i leads to a decrease in the proposed tax/subsidy. Since the tax/subsidy $ł_i$ in eq. 3.14 is complementary to individual social punishment, a decrease amounts to an increase in the economic value of social punishment: $\omega_i(\cdot)(\pi^D - \pi^C)$. The comparative static shows further that

$$\frac{\partial ł_i}{\partial s} = -\frac{\omega_i(\cdot)(\pi^D - \pi^C)}{\partial s} = \frac{\partial \omega_i}{\partial s}(\pi^D - \pi^C) - \omega_i \frac{\partial(\pi^D - \pi^C)}{\partial s} \lessgtr 0. \tag{3.19}$$

The sign of eq. 3.19 cannot be determined unambiguously because $\frac{\partial \omega_i}{\partial s} > 0$ and $\frac{\partial(\pi^D - \pi^C)}{\partial s} > 0$ have opposite sign[14]. Yet, if stock-dependent extraction costs are not important for the overall net benefits, then the second term of eq. 3.19 is not dominant and $\frac{\partial ł_i}{\partial s} > 0$.

In this case, social punishment decreases with an increase in stock due to the complementarity of the tax/subsidy and social punishment. However, if stock-dependent extraction costs are dominant in eq. 3.19, social punishment will increase with an increase in the stock. Eq. 3.18 and 3.19 present the marginal monetary values of social punishment with respect to an increase in the share of compliers, local cohesiveness of compliers and stock. A comparative static analysis, based on eq 3.14, 3.18 and 3.19 with $ł_i = 0$, further reveals that the share of compliers in the neighborhood of agent i decreases with an increase in the strength of the local cohesiveness of compliers or

[14]The positive sign of $\frac{\partial \omega_i}{\partial s}$ is based on the assumption that social pressure increases with an increase in s which implies that the sign of $\frac{\partial g}{\partial s}$ is positive. The negative sign of $\frac{\partial(\pi^D - \pi^C)}{\partial s}$ is based on the observation that the lower the stock, the higher the extraction costs for both strategies. Thus, the difference between the extraction profiles and corresponding net benefits decreases. This hypothesis is also confirmed by our empirical analysis – see Table B1, Figures C2a –C2d in Appendix C and D respectively.

in the stock, i.e., $\frac{\partial c_i}{\partial \tau c_i} < 0$, $\frac{\partial c_i}{\partial s} < 0$. Thus, the local cohesiveness of compliers and the state of the resource are substitutes for the share of compliers.

3.7.2 Appendix B: Methodological and Technical Aspects of the Implementation of the Social Network

In Chapter 2 we have described the network generative model based on the fitness of agents. In this appendix, we describe how the game is initialized in the different networks. We randomly assigned the desired number of compliers and defectors within the network, simulated the evolution of the network and calculated the social pressure function after one year. Let us denote that this results in $\hat{\omega}$. However, depending on the initial distribution of compliers and defectors within the network, the value of $\hat{\omega}$ may vary greatly. To evaluate the magnitude of this bias, we used the Monte Carlo method and repeated the calculations for $\hat{\omega}$ n-times. The variance of the n-times repeated calculations, $\sigma^n_{\hat{\omega}}$, is employed to determine the magnitude of the bias. Following (Vose [2012]), we determined the required number of repetition n that guarantees that $\sigma^n_{\hat{\omega}}$ is less than an acceptable error φ given a confidence interval $(1-\alpha)$.[15] For a confidence interval of 95% and an acceptable error of 0.004, the required number of repetitions is 96.04. For this reason, we repeated all our calculations presented in this study with 100 different initial assignments. The results presented throughout the article are the average values over those 100 repetitions.

One may think that the required number of repetitions is low. However, this can be explained by the large number of agents (7500) that diminish the effect of the initial assignment to the final value of $\hat{\omega}$.

The differential equation $\dot{s} = g(s) - \sum_i^{cn} w_i^C - \sum_{cn+1}^{n} w_i^D$ was solved analytically for the case of pure strategies: all agents are compliers or all agents are defectors. However, for the case of mixed strategies, an analytical solution cannot be provided because the share of compliers c changes over time. Hence, the value of $s(t)$ was determined numerically by the Euler method at each moment of time.

[15] It would have been possible to evaluate the social pressure function in later years. However, the effect of the initial assignment is diluted over the years, thus, limiting the error term of the first year depicts the stringent test. The formula for the calculation of the necessary simple size is given by $n = \frac{(1.96\sigma^n_{\hat{\omega}})^2}{\varphi^2}$.

3.7.3 Appendix C: Numerical Analysis and Specification of the Functions Employed

As an example of high policy relevance, we focus on the Western La Mancha Aquifer situated within the upper Guadiana basin (inland region of Castilla La Mancha, Spain) and extending over $5000km^2$ (see Fig. 3.6). The constant overdraft of this aquifer has led to a variety of policy measures designed to curb its deterioration and comply with the European Union Water Framework Directive (Gutiérrez et al. [2011]).

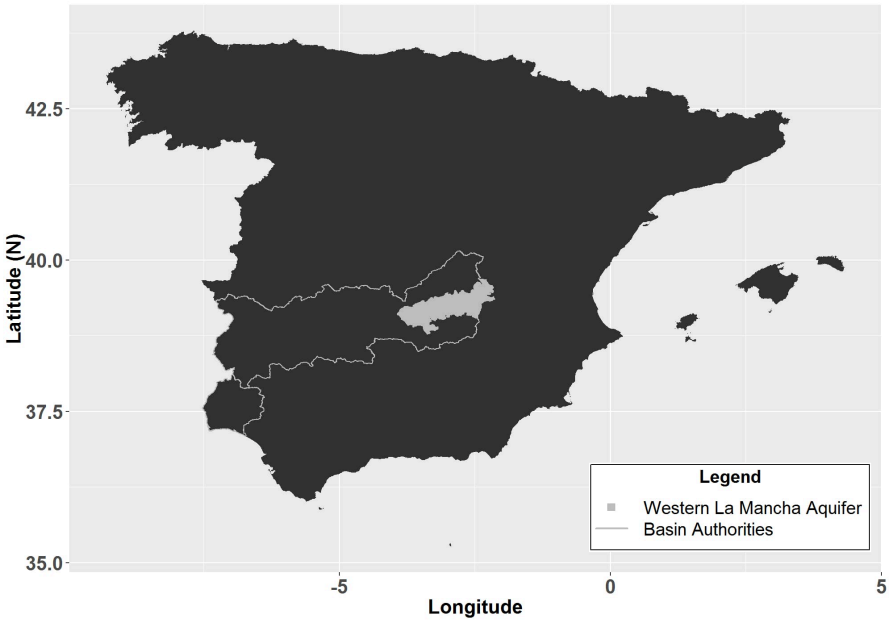

Fig. 3.6 Geographical location of the Western La Mancha Aquifer

The Western La Mancha Aquifer is the largest aquifer in Spain.

Hydrological model

We start out with the specification of the dynamics of the aquifer, $\dot{s}(\xi) = g(s(\xi)) - \sum_i^{cn} w_i^C(\xi) - \sum_{cn+1}^{n} w_i^D(\xi), s(\xi) = s_1$. In the case of an aquifer, natural replenishment is independent of the stock and thus the term $g(s(\xi))$ is equal to R which denotes natural replenishment. The stock $s(t)$ indicates the depth of the water table in meters, and $w_i^C(t)$ and $w_i^D(t)$ indicate the water extracted in m^3/ha. Since the extraction is measured in m^3 and the depth of the water table in m, we introduce the conversion factor φ that expresses the change in the depth of the water table as a result of the

water extraction. Moreover, a part of the water extracted for irrigation percolates back into the aquifer. Following (Encarna and Albiac [2011]), we set this return rate, denoted by ψ, equal to 20%. Thus, the dynamics of the natural resource are now given by

$$\dot{s}(t) = \varphi\left(R - \psi\left(\sum_{i}^{cn} w_i^C - \sum_{cn+1}^{n} w_i^D\right)\right). \tag{3.20}$$

(Encarna and Albiac [2011]) reported that in 2007 the land cultivated for agricultural production comprised 191,400ha. (Encarna and Albiac [2011]; Esteban and Albiac [2012]) calculated that the irrigation practices lead to a gross extraction of $1km^3$ of water from the aquifer and extended the irrigated area by 62,000ha. Consequently, the water table dropped by 32m, i.e., a decrease of $2.6666m$ per year. The gross extraction per m^3 of water per ha is given by 1,000,000.000m^3/253400ha= 39,463,299,131.807m^3/ha. To keep the model more manageable, but without losing any important characteristic related to the hydrological processes, we scaled the aquifer down to 7500 ha which implies that all agents own exactly one hectare. Hence a drop of $2.6666m$ per year is caused by a total extraction of 39,463,299,131.807m^3/ha times 7500ha. In other words, a decrease in the water table in meters per m^3 of extraction is given by the conversion factor $2{,}66666m/29597474{,}34885525m^3 = 0.00000009009778m/m^3$. Although we down-scaled the aquifer, we kept the number of agents approximately identical. However, we had to adjust the number of stakeholders and so we assume that every agent owns exactly one hectare.

According to (Encarna and Albiac [2011]), the overall recharge is $0.36km^3$. Hence, per cultivated ha we obtain a recharge of 360.000.000/253400=1420,678768m^3. This number links well with the reported rainfall of $415mm$/ha (Martínez-Santos et al. [2008]). In terms of cubic meters, it results in 10,000m^2 times $0.415m = 4150m^3$/ha.

Water extraction costs

We calculated the extraction costs as a function of the overall depth of the well (annualized construction and maintenance costs) and of the lifting costs. They are denoted by $c(w, s)$. Based on average values for the area of the Western La Mancha Aquifer, the cost of wells with a lifetime of 25 years and a depth of $46.83m$ are €371 per ha. is €7.94 per lineal meter of the constructed well depth. Assuming an average price rise of 4% p.a. over 10 years (2013 onwards), the nominal costs per lineal meter for 2014 are €11.75 per lineal meter. As reported by Llamas and Garrido (2007), it takes 0.004 kWh to draw $1m^3$ of water per meter. At €0.12 per kWh, water drawing

costs per m^3 are € 0.00048 per lineal meter.

Net benefits of agricultural production and water demand

(Ortega et al. [2011]) developed a mathematical programming model for four different types of farm characterizing the variety of production systems and farm types found around the Western La Mancha Aquifer. Using economic, agronomic and policy constraints, the authors calculated the net income for a farm under different water allocation schemes. In other words, they calculated the best response the farmer would make to changes in the amount of water allocated per ha. for the upcoming agricultural campaign, i.e., the changes in inputs other than water or changes in the type of crop to be planted (to adjust to allocated water changes) to maximize the farm's net income. The best response function with respect to changes in the amount of water is given by the composite input $x^*(w)$. The reported results by (Ortega et al. [2011]) allow us to relate the maximal net income for a farm, with respect to optimal use of the composite input x^*, as a function of the water assigned per ha, i.e., $\pi(x^*(w))$. Optimal farm income and the water assigned to it are reported in Table 3.1 of their work (Ortega et al. [2011]). For the empirical estimation of this relationship, we calculated the weighted average of a farm's net income and water consumption for the four different types of farm. Unfortunately, the data that was collected and presented only reflects the upward sloping section of the farm-net-benefit function. Yet, the same authors report that prior to water restrictions being implemented at the beginning of the 21st century, the economic optimum corresponded to extracting $4300m^3$ of water per ha per year. By adding this information as a decrease when consumption surpassed $4300m^3$ in the farm-net-benefit function, we were able to estimate the net benefits of the farm as a function of water consumption. Additionally, we incorporated water extraction costs. The function that best fitted the data was a quadratic function with an R^2 adjusted of 0.94. This is given by

$$\pi(x^*(w)) = 70,3547448 + 0,5061w - 0,000060w^2 - 7,94s - 11,75s - 0,00048ws \quad (3.21)$$

In the next step we need to obtain the solution of the dynamic optimization problem detailed in eq. 3.1 and 3.2. For this purpose we amend eq 3.1 by introducing the specification of the term $x^*(w)$ explicitly as defined in eq. 3.21 and substitute the general resource dynamics $\dot{s}$ by its specifications given in eq 3.21. Thereafter, the dynamic solution problem is solved numerically in GAMS. The compliers' and defectors' strategies differ by the length of their planning horizon. Compliers adhere to the social

norm by having a farsighted perspective of 25 years, whereas defectors deviate from it as they focus on a planning horizon of a mere year.

The choice of a planning horizon of 25 years is obviously debatable, but this period of time coincides with the current farming generation leaving the farm to the next and with the economic lifetime of the investment itself[16].

The data obtained from the solution the dynamic optimization model provided for different initial values of s_0, allowed us to estimate the water demanded by the compliers and defectors to maximize their net benefits, $w_i^C(t, T, s(t))$ and $w_i^D(t, 1, s(t))$, as a function of the depth of the water table. Likewise, the optimal water demand for each strategy for different initial values of s_0 allowed us to calculate the farms' optimal net benefits, $\pi(x_i^*(w_i^C(\cdot), s(t)), w_i^C(\cdot), s(t))$, and $\pi(x_i^*(w_i^D(\cdot), s(t)), w_i^D(\cdot), s(t))$ as a function of the depth of the water table[17]. The results from both estimations are presented in Table 3.1.

Table 3.1 Water demand and optimal farm net benefits as a function of the depth of the water table.

Functions	Defector	Complier
Water demand	4004,032258 - 3,870967742 s(t)	3910,124356 - 18,28383925s(t) + 0,855521467 $s(t)^2$ - 0,012022391$s(t)^3$
Farm net benefit	924,2879956 - 13,86127128s(t)	529,5613916 - 0,989226044 s(t) - 0,81859727$s(t)^2$ + 0,023769413$s(t)^3$ -0,000212445$s(t)^4$

Although the compliers maximize their net benefits over 25 years, both compliers and defectors may change their strategy at each moment of time. For this purpose, every agent compares the usefulness of their current of strategy with the effectiveness of the alternative strategy. The probability of a change in strategies is given by eq. 3.7 and 3.8, and takes into account, among other elements, a farm's optimal net benefits π^C and π^D.

Cooperative behavior and groundwater management

As mentioned above, the social pressure exercised by the compliers is an informal mechanism to enforce the social norm. It allows compliers to retaliate for the defectors'

[16]Alternatively, we could have distinguished the behavior of compliers and defectors by the choice of different time preferences. Yet, the choice of different discount rates would have been more difficult since there is no natural orientation for its specification like generational succession or economic lifetime of an investment.

[17] For the case of the compliers, we used the average water demand and the farm's average discounted net benefits over 25 years. In this way, the compliers' water demand can be considered as the expected annual water demand. Moreover, taking the average value moderates the end-value problem toward the end of the planning horizon.

higher extraction rates of the groundwater which cause a faster decrease in the water table level, higher pumping costs and scarcity for all agents.

After having specified the optimal net benefits per farm for each strategy, π^C and π^D, we specify social pressure as a function of the depth of the water table, the number of compliers and the cohesiveness of compliers in the neighborhood $\mathcal{N}(i)$ of agent i. As described in the article, the social pressure function depends on the characteristics of the neighborhood with respect to its share of compliers, its cohesiveness and the depth of the water table, and is given by

$$\omega(s, c_i, \tau_{c_i}) = a(\tau_{c_i})e^{-de^{g(s)c_i}}. \tag{3.22}$$

Fig. 3.7a shows its form as a function of the share of compliers for a given depth of the water table (15 m and 40 m) and $a(\tau_{c_i} = 0) = 1$. Fig. 3.7b illustrates the scaling factor that determines the upper limit of the social pressure function. While higher values of local cohesiveness of compliers lead to higher values of the upper limit (asymptote), the shape of the social pressure function remains unchanged. The specification of the functions and parameters is explained in detail below.

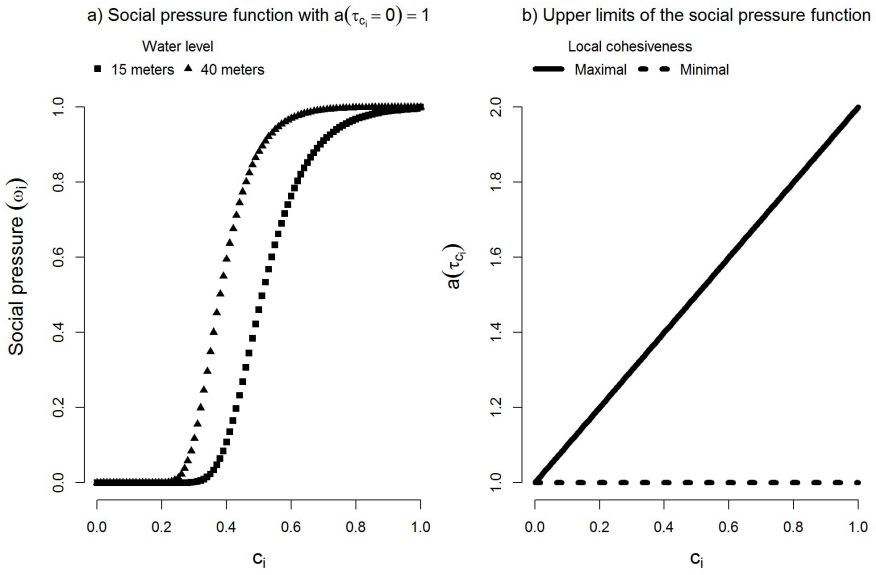

Fig. 3.7 The social pressure function

a) Social pressure as a function of the share of compliers for a given depth of the water table (15m and 40m) and minimal local cohesiveness of compliers $\tau_{c_i} = 0$, b) Upper limits of social pressure as a function of the share of compliers c_i.

Social pressure is then characterized as incremental sanctioning driven by the four parameters: the share of compliers in agent i's neighborhood (c_i), the stock levels(s), the effectiveness of sanctioning (d) and the number of compliers in the agent's neighborhood who are connected (τ_{c_i}).

Compliers are well aware of the evolution of the stock and increase their pressure on defectors as s falls. The function $g(s)$ induces ω to grow faster as the water table s approaches the maximal depth of the well, s_{max}, in particular if $s > \frac{s_{max}}{2}$. The precise formulation of g is given by

$$g(s) = A + (B - A)\left(\frac{s}{s_{max}}\right)^n. \tag{3.23}$$

and is bounded between $A < g(s) < B$. We set the parameter $A = 10$, $B = 20$ and $n = 3$ so that $10 < g(s) < 20$. Higher values of the parameter d displace the social pressure function to the right so that higher values of c_i are needed to exert the same pressure as before on defectors. Thus, the parameter d describes the ability to exercise social pressure, i.e., the ability to sanction defectors (Tavoni et al. [2012]). In the model, we set $d = 150$ in accordance with the study of (Tavoni et al. [2012]).

Since the function $a(\tau_{c_i})$ defines the upper asymptote, it reflects the maximal social pressure that compliers can exercise. Provided that agent i is a defector, the social pressure agent i experiences increases if the compliers in the neighborhood of agent i coordinate their action against agent i. Thus, the cohesiveness of the compliers in the neighborhood of agent i is a precondition to their cooperation and is liable to increases the social pressure placed on defectors. For this reason, we introduced the function $a(\tau_{c_i})$ which measures to what extent compliers in the neighborhood of agent i are connected to each other. The specification of the cohesiveness function $a(\tau_{c_i})$ is given by

$$a = 1 + \left(\frac{\tau_{c_i}}{\tau_{max}}\right)^{\alpha} = 1 + \sqrt{\tau_{c_i}}. \tag{3.24}$$

If all neighbors of agent i were compliers $c_i = 1$ and connected to each other, we would have $\tau_{c_i} = \tau_{max} = 1$. However, if not all neighbors are compliers, it holds that $0 < \tau_{c_i} < \tau_{max} = 1$ and consequently the function a is bounded by $1 \leq a \leq 2$. Moreover, we stipulate to set $\alpha = 0.5$. This choice affects only the behavior of the function within its boundaries but not the boundaries itself. Given that the term $e^{-de^{g(s)c_i}}$ of the social pressure function is bounded by $0 < e^{-de^{g(s)c_i}} \leq 1$, we know that the social pressure function is limited as well, more precisely by $0 < \omega \leq 2$.

The defined boundary of the social pressure function is of utmost importance since it limits social punishment to be at most twice the difference between the benefits of defectors and compliers, i.e., $\omega \leq 2(\pi^D - \pi^C)$.

Obviously, the choice of the parameters and the specification of the social pressure function ω is debatable and we cannot defend its choice on the grounds of the literature or experiments previously conducted. However, the choice of limiting ω to be smaller or equal to two seems rational in terms of economic reasoning. The main objective of social punishment is to deter agents from defecting from the social norm. Once social punishment outweighs the non-compliance benefits it would be best for rational agents to adhere to the social norm. However, since social punishment of agent i depends on the structure and state of the network, we allowed $0 < \omega \leq 2$ so that effective social punishment, $\omega > 1$, occurs regardless if all the neighbors of agent i are compliers and perfectly connected to each other.

The definition of the social pressure function, however, is not only motivated by economic reasoning but also allows the structure and state of the network to be linked to the decisions taken by each agent. Finally, the choice of boundaries for ω are also decisive for limiting the probability of a change from the agent's current strategy to an alternative strategy. Denote the utility of the agent's current strategy by U_i and their alternative strategy by U_i' . Thus, based on eq. 3.5 - 3.8, we observe that the probability of a change in the agent's current strategy to the agent's alternative strategy is given by

$$p_i(t) = \frac{U_i'(t) - U_i(t)}{max\{U^D(t) - U^C(t)\}} = 1 - \omega. \tag{3.25}$$

If $U_i'(t) - U_i(t) \geq 0$, we have $0 \leq p_i(t) < 1$ and if $U_i'(t) - U_i(t) \leq 0$, we have $0 \geq p_i(t) \geq -1$. Thus, eq. 3.25 shows that the probability is limited by $-1 \leq p_i(t) < 1$ and links to the mathematical conception of probability. In eq. 3.7 and 3.8 we set the probability of a change in strategies equal to zero if it leads to an economic loss, i.e., if $U_i'(t) - U_i(t) \leq 0$. Consequently, it will not be realized. Despite this modification, eq. 3.25 shows the importance of the boundary choice of ω for linking the behavioral model to the mathematical concept of probability.

3.7.4 Appendix D: Evolution of Social Pressure

Fig. 3.8a – 3.8d show the evolution of the average social pressure within the network, ω_T. This consists of the social pressure received by all agents, i.e., the social pressure experienced by defectors and the potential social pressure that compliers would receive if they decided to abandon their current strategy. Alternatively, we calculate the average social pressure that only defectors would receive and denote it by ω_D. The graphs show that ω_D always decreases over time, suggesting that neighborhoods are formed where the share of defectors increases.

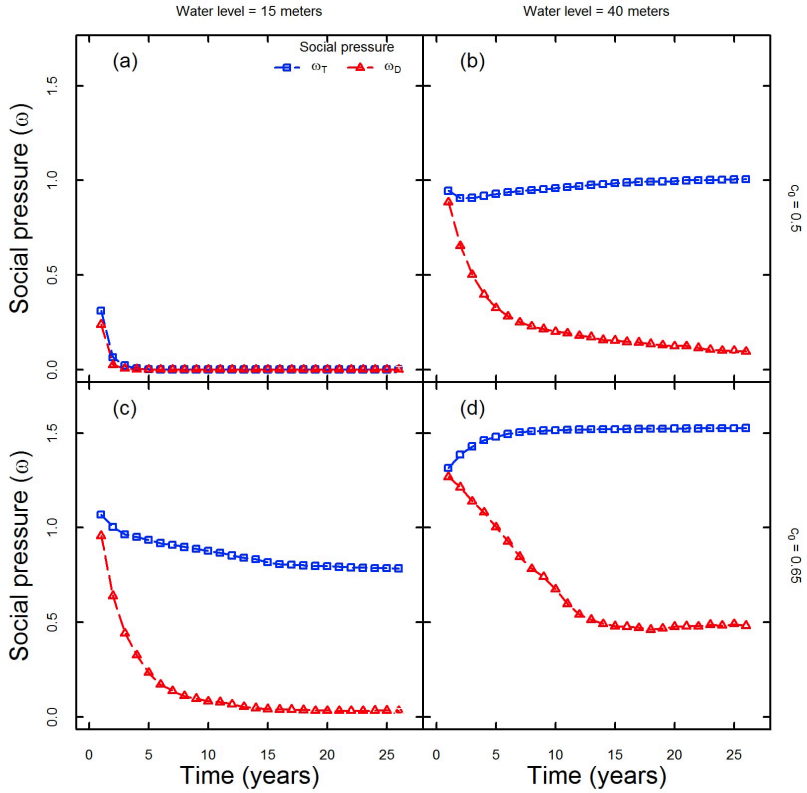

Fig. 3.8 Evolution of social pressure ω

Fig. 3.8a: $c_i = 0.5, s80) = 15$, Fig. 3.8b: $c_i = 0.5, s(0) = 40$, Fig. 3.8c: $c_i = 0.65, s(0) = 15$ and Fig. 3.8d: $c_i = 0.65, s(0) = 40$.

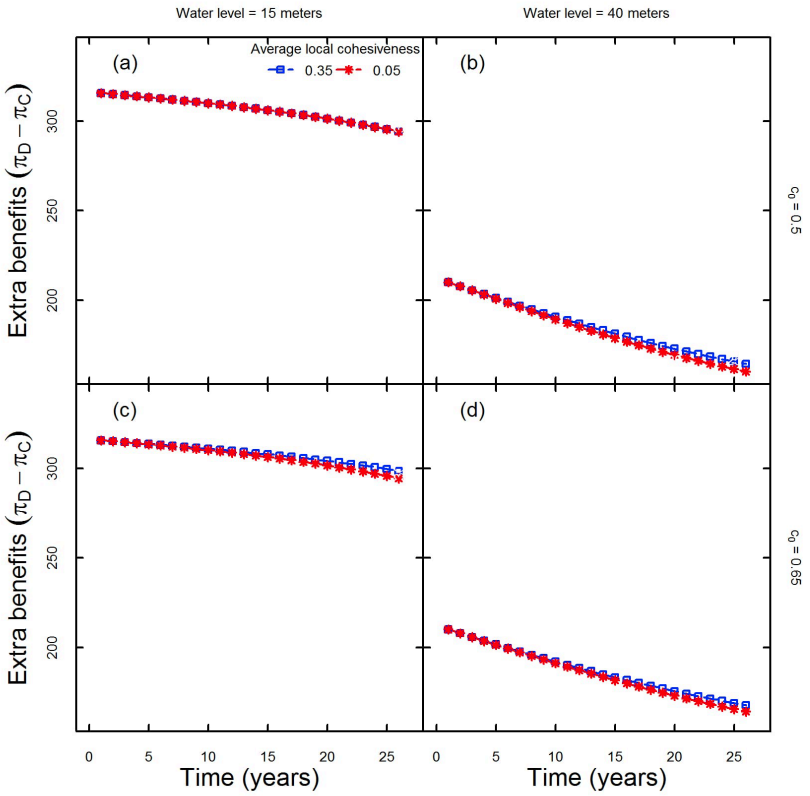

Fig. 3.9 Evolution of defector's extra benefits

Evolution of the defector's extra benefits for different degrees of average local cohesiveness with $\tau = 0.05, 0.15, 0.25 and 0.35$. Fig. 3.9a: $c_i = 0.5, s80) = 15$, Fig. 3.9b: $c_i = 0.5, s(0) = 40$, Fig. 3.9c: $c_i = 0.65, s(0) = 15$ and Fig. 3.9d: $c_i = 0.65, s(0) = 40$.

Chapter 4

Tragedy of the Commons: Traditional Policy Instruments versus Network Policy

Summary

This chapter revisits the problem of the tragedy of the commons. We analyze the role of social networks and social pressure as driving forces for the establishment and maintenance of cooperation in resource use under variable social and environmental conditions. The social-ecological system is coupled and co-evolve in time. We show the extent to which social pressure contributes to overcoming the tragedy of the commons. We find large regions where traditional policy instruments (taxes or subsidies) and network-orientated polices (the higher the local cohesiveness of compliers the higher the social pressure is) can be applied indistinctly, and analyze to what extent such regions depend on the network structure, the state of the natural resource, and the share of compliers.

Keywords: Natural resource management; cooperation; social network; social pressure; mean-field theory

4.1 Introduction

A feature of all societies is that they contain numerous natural resources (i.e., forests, pastures or fishing grounds) that can be exploited by a large amount of agents. The management of such natural resources is a challenging situation because each agent has free access to exploit the natural resource but the use by one agent reduces resource availability for others. If exploitation is unrestricted, agents are tempted to use the resource above sustainable levels and eventually individual decisions cumulate to a tragic overexploitation (Hardin [1968]). The prediction that agents tend to look out for themselves first inspired a generation of environmental regulations imposed on agents by external authorities. However, many authors (Holling [1978]; Jentoft [2000]; McCarthy [2000]; Muse [1990]; Olsson et al. [2004]; Wondolleck et al. [2002]) observed that top-down management is subject to failure in some instances, offering at the same time new perspectives and paradigms for natural resource management. From the 1990s onwards, (Ostrom [1990]; Ostrom et al. [1999]) focused on self-governance. The main characteristics of self-governance are that agents share property rights and management is controlled by the joint agents. By examining successful cases of self-governance in practice, Ostrom and her group observed that cooperation is an efficient strategy to successfully manage natural resources held in common. However, cooperation seems to contradict traditional economic predictions because cooperators increase the profit of other agents at a cost of themselves. According to traditional predictions, in absence of supporting mechanisms, cooperation should decrease and vanish. Thus, the correct identification of such suppoting mechanisms for cooperation is a significant challenge in environmental economics. Over the past decades, many mechanisms have been proposed for the emergence and evolution of cooperation in absence of regulatory institutions: repeated interaction and direct reciprocity (Axelrod and Hamilton [1981]; Trivers [1971]), punishment (Gaechter and Fehr [1997]), voluntary participation (Hauert et al. [2002]), spatially structured populations (Nowak and May [1992]), and indirect reciprocity (Alexander [1987]; Liu et al. [2017]; Nowak and Sigmund [1998]). These mechanisms are capable of supporting cooperation in evolutionary games. Traditionally, evolutionary games are Prisoner's Dilemma games that assume limited rationality, pairwise interaction and well-mixed populations. While the above mechanisms and games help us to identify some driving factors for cooperation (i.e., group size, share of cooperators), we argue that there exist other important drivers for cooperation on natural resource management that need to be analyzed in depth: the level of cohesiveness between cooperators, the state of the natural resource, and the underlying structure of social interactions within the community.

In view of these considerations, we propose a new framework that combines distinctive aspects of three strands of the literature: an evolutionary game based on the solutions to the differential games employed within a social network that accounts for the complexity of the interaction between agents. In the present study we aim to analyze a simple model that departs from traditional evolutionary games by placing emphasis on two driving forces: the asymmetric topology of social interactions, and the social pressure in the direction of norm compliance. In their studies, (Ostrom [1990]) also observed that, in absence of external regulation, management is meditated by social norms of behavior. Cooperators may exert social pressure on agents of the community that do not follow the social norm, however, in some situations social pressure is not enough to maintain cooperation. Alternatively, or in combination with social pressure, the community may decide to employ traditional policy instruments to promote cooperation within the community.

In our model, we analyze cooperation as the outcome of an evolutionary process with successful strategies spreading in the community as a result of a process of imitation. Thus, the higher the social pressure the higher the probability is that agents decide to follow the norm. If social pressure is costly, the positive effects of sanctioning decrease and consequently temptation of non-compliance increases. Agents following the social norms are called compliers. Compliers have long-term perspective because they limit their resource use to the socially optimal amount. Agents who extract above the sustainable level are called defectors. Defectors have short-term perspective because they act in accordance with what they want now, with absolutely no consideration of how actions might affect them in the future. Both types of agents interact in different networks: complete, scale-free, and random networks. While not realistic, complete and random networks allow us to define the upper and lower limits of social pressure respectively. We begin by defining a discrete model in which each agent interacts with her neighborhood and updates her strategy according to a probability that is proportional to utility differences. However, equilibrium is analytically intractable by the potential for multiple equilibria given the asymmetry and complexity of the network and the distribution of compliers.

To analyze the regimes of stationary state of the evolutionary dynamics, we employ an approximation technique from statistical physics known as a mean-field approximation (Weiss [1907]), which has proven useful for study network dynamics in several contexts (Lamberson [2009b]; López-Pintado [2008]; Newman et al. [2000]; Pastor-Satorras and Vespignani [2001]). We prove that this approximation leads us to a continuous model based on the 2-strategy replicator dynamics. Unlike traditional

replicator equation, our model allows for different network topologies. We prove that predictions based on complete networks are often optimistic specially when compared to more realistic networks, i.e., scale-free networks.

According to our replicator equation, we identify stable states and derive conditions for policy options to guarantee cooperation. We then proceed to analyze how equilibrium levels of cooperation depend on the parameters of social pressure, specifically the cohesiveness of compliers, the level of the stock, and the share of compliers.

The study proceeds as follows. In section 4.2, we introduce the different elements of the economic model based on an integrated social-ecological system. In section 4.3, we define a concept for equilibrium and analyze possible equilibria. Then, in section 4.4, we identify policy corridors for the concrete determination of policy options. The study closes with some concluding remarks (section 4.5).

4.2 The economic model

The economic model is based on three different components: the social network that defines the interaction between agents, the resource demand strategies and the agent's chosen strategy. In the following, we present the three components.

4.2.1 A social network as a graph

Our interest is in the interaction between different members of a social network that can be described by a simple graph $N = (A, L)$ which consists of a finite set $A = 1, ..., n, n > 2$ of agents and a set L of links that are the unordered pairs of elements from A. The elements in set L consist of the values of the indicatrix link function $l : A \times A \to \{0, 1\}$:

$$l(i,j) \equiv l_{ij} = \begin{cases} 1; (i,j) \in L \\ 0; (i,j) \in L \end{cases}$$

For any pair of agents, i and j, the expression $l_{ij} = 1$ indicates that the two agents are neighbors, otherwise $l_{ij} = 0$, i.e., they know and relate to each other. By definition, simple graphs are undirected so that $l_{ij} = 1 \Leftrightarrow l_{ji} = 1$[1]. If every agent is connected to all other agents, N forms a complete network. For each agent i, $\mathcal{N}(i)$ denotes their neighborhood, i.e., the set of all neighbors. The degree $k_N(i) = k_i = \sum_j l_{ij}$ of an

[1]Moreover, agents are not linked to themselves (self-loops), i.e., $l_{ii} = 0$, and there is no more than one link between agent i and j (uniqueness of the link).

agent i is the number of links at i, i.e., the number of neighbors i has. Denote by $P(K = k) = p_k$ the degree distribution of N, that is the probability that an agent i in N chosen uniformly at random has exactly k neighbors.

In this work we will analyze the influence different network topologies have on social pressure and finally on cooperation. In particular, we will focus on some representative types of networks (Appendix B): complete networks, random networks and scale-free networks. In complete networks, agents are fully connected such that $k_i = n - 1$ for all agents in the community. Social pressure in complete networks is expected to be effective because compliers know each other and thus they can share on average more information and experiences. However, in large communities agents are only connected with a subset of the population and then social networks are not complete. If the links of all the agents were formed assuming the same probability p, we would obtain a random network whose degree distribution approximately follows a Poisson distribution. In random networks, agents have similar (small) degree with low number of transitive relations. Unlike complete networks, compliers in random networks tend to share little amount of information and consequently social pressure is much less effective. However, empirical studies (Jeong et al. [2000]; Liljeros et al. [2001]) have shown that the degree distribution of large social networks does not follow a Poisson distribution and therefore recent research (Barábasi and Albert [1999]; Clauset et al. [2009]) has focused on scale-free topology. These networks are characterized by a degree distribution that follows the power-law $p_k = k^{-\gamma}$ with $2 < \gamma < 3$ (Nguyen and Tran [2012]). Scale-free networks have more weight in the tails than do random networks where there are few central agents of high degree and many other agents of small degree and thus offer a better match with the social networks observed (Jackson [2008]). Finally, and very importantly, compared to random networks, scale-free networks allow for some organizing principles to be considered (Réka and Barabási [2002]). As shown in Appendix B scale-free networks present a wide variety of network topologies, ranging between random and complete networks. The wide range of topologies in scale-free networks allow us to design network-orientated policies that may help to promote cooperation when the community either lacks the legal power to enforce the social norm or it is too costly to rely on any kind of formal contract.

Our interest in both random and complete networks is because they can serve as a basis for understanding the limits of social pressure. While complete networks will help us to define the upper limits for social pressure, random networks will help us to define the lower limits for social pressure in a community of agents.

4.2.2 Resource demand strategies

Each member of the social network has access to a common property resource. However, extraction based on the maximization of each member's private net benefits would, in the long-run, lead either to the depletion of the resource or to very low annual private net benefits. To overcome the tragedy of the commons, the members of the social network have reached a common understanding of the characteristics of a sustainable extraction path. Let us interpret this common understanding as a social norm. Adherence to the social norm is voluntary and every member of the social network may choose to follow the sustainable extraction path or not. Let us label the behavior of the agents that follow the sustainable extraction path as *compliers* and the behavior of all other agents as $defectors$.

Each member or agent either employs the extracted resource as the input to produce a single good or commercializes it on the market. Let $w_i(t)$ denote the amount of the resource extracted at calendar time t by agent i. The available amount of the resource is denoted by $s(t)$ with $s(0) = s_0$. We assume that all members adjust all other inputs to the extracted amount of the resource such that their net benefits are maximized. Adherence to the social norm by agent i will support sustainable extraction, whereas non-adherence will lead to a non-sustainable extraction path. Non-coordinated individual behavior would result in a sustainable extraction path if all members were to consider stock dependent costs when determining the privately optimal extraction path. These costs will be fully considered if all the agents have a private planning horizon of an infinite length. Consequently, we define compliers, denoted by C, as far-sighted agents with an infinite planning horizon of $T \to \infty$ years, whereas defectors, denoted by D, are short-sighted and their planning horizon is $T \to 0$ year. We assume that the underlying reason for this short-sightedness is related to socioeconomic factors (e.g. age, personal commitment to the community, risk aversion etc.). Each agent determines the privately optimal extraction path (resource demand function) based on the solution of the following decision problems. The resource demand function at time t is given by:

$$w_i^K(t, T, s(\xi)) = arg \max_{w_i^K(\xi)} \int_t^T e^{-r\xi} \pi^K(w_i^K(\xi), s(\xi)) d\xi, \;\; K = C, D \tag{4.1}$$

where r denotes the private inter-temporal discount rate and π the private net benefits of the agent. We assume that compliers and defectors differ only in respect to the length of their planning horizon, but not to their private discount rate. For the case of

compliers eq. 4.1 is also subject to

$$\dot{s}(\xi) = g(s(\xi)) - \sum_{i}^{cn} w_i^C(\xi) - \sum_{cn+1}^{n} w_i^D(\xi), \;\; s(\xi) = s_t \tag{4.2}$$

where a dot over a variable denotes the operator $\frac{d}{dt}$, c the share of compliers within the population of all agents and $g(s(t))$ is the reproduction or growth function of the resource. We assume that the compliers' expectation of the defectors' future extraction at time t, $\bar{w}_i^D$, is based on their current level of extraction, i.e., $\bar{w}_i^D = w_i^D(t)$. The resource demand function (eq. 4.1) is the solution to an open-loop strategy. Based on the circumstance that agents can frequently observe the level of stock remaining, we propose that they are allowed to modify their extraction profile after $T - t$. In other words, the agents determine a new open-loop extraction profile based on the amount of the natural resource they observe. This profile is maintained until the next revision period when new information about the level of the remaining stock is obtained. Since compliers take account of the stock dependent costs in terms of inter-temporal or user costs, denoted by $\eta(t)$, their marginal extraction costs are higher than those of the defectors. Thus, it holds for a given stock $s(t)$ that defectors extract at least as much as compliers and their net benefits are never less than those of the compliers, i.e.,

$$w_i^D(t, T, s(t)) \geq w_i^C(t, T, s(t))$$

and

$$\pi^D(w_i^D(t), s(t)) \geq \pi^C(w_i^C(t), s(t))$$

4.2.3 Strategy choice - an evolutionary game-theoretic approach

Given our focus on the interaction between agents, we analyze how an arbitrary initial distribution of compliers and defectors evolves over time and how this changing distribution affects the evolution of the resource. At every moment of time, agents can change their strategy, i.e., from complier to defector, or vice versa. Strategy choice is based on the evolutionary game-theoretic approach (Osés-Eraso and Viladrich-Grau [2007]; Sethi and Somanathan [1996]). We assume that this decision is influenced by the following factors:

- the difference between the net benefits of a defector and a complier (i.e., the defector's extra benefits) and

- the interaction with other agents (network effects)

In the case of the first point, we assume that the larger the difference is between the maximal net benefits of complying with the strategy, given by $\pi^C(w_i^C(\cdot), s(t))$ and not complying with the strategy, given $\pi^D(w_i^D(\cdot), s(t))$, the greater the chance at moment a complier will become a defector and a defector will not become a complier. The difference between $\pi^D - \pi^C$ is not only important for the agent's strategy, but also presents the magnitude of the loss defectors inflict on those members of the network who are adhering to the social norm. In the absence of an institution that is technically and legally in a position to punish defectors, compliers may retaliate for the defectors' abstraction of the common property resource through social shunning (ostracism) (Ali and Miller [2016]).

In terms of social pressure, we assume that all agents are perfectly informed about the strategy choice their neighbors have made (complete monitoring) and that there is no time delay between detecting non-compliance and retaliation[2].

Social pressure and social punishment

If an agent defects, they will be exposed to social pressure from the compliers[3]. However, making use of the social network suggests that social pressure on defector i depends on the number of compliers and defectors within their local neighborhood $\mathcal{N}(i)$. Let us define the set of compliers within the neighborhood $\mathcal{N}(i)$ by $\mathcal{N}_C(i)$. Thus, the share of compliers in the neighborhood of agent i, c_i, can be defined by $c_i = \frac{|\mathcal{N}_C(i)|}{|\mathcal{N}(i)|}$. This relationship is considered an important factor in determining social pressure because it measures the direct influence the neighborhood has on defector i (Haag and Lagunoff [2006]; Jackson et al. [2012]). The higher the number of compliers of neighborhood $\mathcal{N}(i)$ is, the greater the social pressure on agent i. However, not only is the share of compliers, c_i, important in determining social pressure, but so too is the relationship between the agents who form part of the set $\mathcal{N}_C(i)$. In the case that none of these agents is linked to another agent in this set, one can assume that the social pressure on defector i will not be as high as when each and every agent in set $\mathcal{N}_C(i)$ is linked. In the first case, local cohesiveness between the agents in set $\mathcal{N}_C(i)$ would be zero, whereas in the latter it would be one. Let us denote the cohesiveness among the compliers in the neighborhood by $\tau_{c_i} \in [0, 1]$ (see Appendix E). This measures

[2]Social pressure is the application of the principle of reciprocity as the response to non-compliance of the social norm by defectors.

[3]Instead of the male and female possessive pronoun we use plural form to facilitate the reading.

the degree of connectivity between the compliers in set $\mathcal{N}_C(i)$. (Haag and Lagunoff [2006]) and (Jackson et al. [2012]) employed a different metric, independent of the agents' strategy choice, for connectivity. However, we used a more stringent measure of connectivity since the cohesiveness of compliers is important to analyze the tragedy of the commons. We denote the connectivity of all agents (compliers and defectors) in the neighborhood of agent i by $\tau_i \in [0, 1]$ (also known as transitivity). This measures how close the neighborhood of agent i is to a complete network. Thus, if, $\tau_i = 1$, all neighbors of agent i are connected to each other. Alternatively, the measurement of cohesiveness for nodes or agents can also be measured on a network level. On this scale, we define average transitivity or average local cohesiveness, as the average value of local cohesiveness, i.e., $\bar{\tau} = \frac{1}{n}\sum_i^n \tau_i$. Finally, we assume, if the resource is abundant, the set of compliers $\mathcal{N}_C(i)$ will exert less social pressure on defector i than if it were scarce.

Once the three key elements of social pressure have been introduced, we can then write the social pressure function as $\omega(s(t), c_i(t), \tau_{c_i}(t)) \geq 0$. As explained above, an increase in the stock reduces social pressure (i.e., $\frac{\partial \omega}{\partial t} < 0$), an increase in number of compliers in the neighborhood of defector i increases social pressure (i.e., $\frac{\partial \omega}{\partial c_i} > 0$), and an increase in the strength of social ties between compliers in the neighborhood of defector i raises social pressure (i.e., $\frac{\partial \omega}{\partial \tau_{c_i}} > 0$).

We model social pressure, ω, as a logistic function that is given by $\omega(s, c, \tau_c) = \frac{Ł}{1+s_{max}e^{-sd(c,\tau_c)}}$. The social pressure function is limited above by the parameter Ł such that $0 \leq \omega \leq Ł$, and is displaced along the horizontal axis by the value of the function $d(c, \tau_c)$. Parameter s_{max} refers to maximum stock level, and parameter s refers to the remaining stock at current time $s \in [0, s_{max}]$.

The function d relates to the willingness of compliers to exercise social pressure. We propose to specify the function by $d(c, \tau_c) = c - (c_0 - \tau_c)$ where $c_0 - \tau_c$ fixes the location of the inflection point of the function ω. It is important to remark here that c_0, c, τ_c are always bounded $0 \leq c_0 \leq 1$, $0 \leq c \leq 1$, and $0 \leq \tau_c \leq 1$. Thus the willingness to exercise social pressure increases with the share of compliers and the degree of local cohesiveness of compliers. An increase in the value of s decreases the slope of the function ω. Since the strength of social pressure exerted highly depends on the specification of the function ω we propose a flexible specification that is controlled by the choice of the parameters s_{max}, c_0. Moreover, in order to consider irregular networks we substitute the share of compliers in the network, c, for the share of compliers in the neighborhood of agent i, c_i and the degree of cohesiveness τ_c by local cohesiveness τ_{c_i}. Hence, the modified logistic function depends on the characteristics of the neighborhood

with respect to its share of compliers, the cohesiveness between compliers and the amount of the remaining stock. It is given by the general expression

$$\omega_i(s, c_i, \tau_{c_i}) = \frac{Ł}{1 + s_{max} e^{-s(c_i - (c_0 - \tau_{c_i}))}} \tag{4.3}$$

We assume that social punishment is directly related to the difference between the net benefits of the defector and the complier $\pi^D - \pi^C$. Since these extra benefits present the loss defectors inflict on compliers, any social punishment can be viewed as redemption for the privation suffered by the compilers. However, social punishment is not independent of social interaction among the agents and, therefore, we assume that the loss defectors inflict on the compliers is attenuated or aggravated by the strength of social pressure $\omega_i(s, c_i, \tau_{c_i})$. More precisely, the social pressure produced and the extra benefits the defector gains as a result of incompliance, define the social punishment imposed and is written as:

$$\omega_i(\cdot)(\pi^D(\cdot) - \pi^C(\cdot)) \tag{4.4}$$

Agent utility and strategy choice

We assume that the utility of agent i adhering to the social norm at moment t is given by:

$$U^C(t) = \pi^C(\cdot), \tag{4.5}$$

however, defector's extra benefits represent an incentive that works as a driving force for compliers against norm violators. Hence, compliers decide to sanction defectors whenever they detect norm violation. The utility of the same agent i not adhering to the social norm at moment t is given by:

$$U^D(t) = \pi^D(\cdot) - \Big[\omega_i(s(t), c_i(t), \tau_{c_i}(t)(\pi^D(\cdot) - \pi^C(\cdot)))\Big] + \theta_i(c)(\pi^D(\cdot) - \pi^C(\cdot)). \tag{4.6}$$

Eq. 4.5 indicates that the utility of a complier is equal to their private net benefits[4]. Eq. 4.6 shows that the utility of a defector consists of the net benefits from resource exploitation minus social punishment. Unlike the complier's utility, the defector's utility depends on the position the agent holds within the social network and the characteristics/topology of the social network within their neighborhood. Apart from

[4]Although this formulation implies that agents are risk neutral, we opted for this specification to simplify the model and to concentrate on the interaction between agents in a social network.

the utility obtained from extraction agents may obtain utility from additional benefits or extra costs as a result of implemented policies. These benefits or costs affect defectors, compliers or both, and as such they may change with the share of compliers and may alter the magnitude of the defector's extra benefits. Hence, they influence the agent's strategy choice and are denoted by $\theta_i(c)(\pi^D(\cdot) - \pi^C(\cdot))$. Examples of $\theta_i(c)(\pi^D(\cdot) - \pi^C(\cdot))$ are given by the distribution of the costs of sanctioning among compliers or by a globally fixed subsidy or fine that has to be shared by compliers or defectors respectively.

In the discrete model, adherence to the social norm will evolve as follows. At each time step, every agent decides whether to maintain their current strategy or not. For this purpose, every agent i compares the utility associated with their current strategy $U(t)$ with that of the alternative strategy $U'(t)$. The utility of a complier is independent of their position in the network or the characteristics/topology of the social network within their neighborhood. However, the decision to maintain or to change their current strategy depends on these very elements as they influence the alternative strategy's utility. The agent will probably adopt an alternative strategy if it proves more beneficial, $U'(t) > U(t)$, whereas if $U'(t) \leq U(t)$, the agent will maintain their current strategy. In mathematical terms, the probability of a change in the current strategy adopted by agent i for a given level of stock, is considered proportional to the difference in the utilities.

Let the probability that agent i changes from complier to defector be denoted by $p_i^C(t)$ given by:

$$p_i^C(t) = \left\{ \begin{array}{c} \frac{U^C(t)-U^D(t)}{max\{U^D(t)-U^C(t)\}}, \text{if } \; U^C(t) - U^D(t) < 0 \\ \\ 0 \qquad\qquad , \text{if } \; U^C(t) - U^D(t) \geq 0 \end{array} \right\}, \tag{4.7}$$

and let the probability that agent i changes from defector to complier be denoted by $p_i^D(t)$ given by:

$$p_i^D(t) = \left\{ \begin{array}{c} \frac{U^D(t)-U^C(t)}{max\{U^D(t)-U^C(t)\}}, \text{if } \; U^D(t) - U^C(t) < 0 \\ \\ 0 \qquad\qquad , \text{if } \; U^D(t) - U^C(t) \geq 0 \end{array} \right\}, \tag{4.8}$$

The denominator of eq. 4.7 and 4.8 refers to the maximal difference between the utility of the different strategies for a given level of stock at time t. This means that $U^D(t) - U^C(t)$ is maximal when $U^D(t)$ and $U^C(t)$ are also maximal. This situation

occurs in absence of policy and social pressure. In other words, $U^D = \pi^D$ and $U^C = \pi^C$. Based on eq. 4.5 - 4.8 we observe that the probability that agent i changes from complier to defector is

$$p_i^C(t) = \frac{\pi^C(t) - (\pi^D - \omega_i(\pi^D(t) - \pi^C(t)) + \theta_i(c)(\pi^D(t) - \pi^C(t)))}{\pi^D(t) - \pi^C(t)} = \omega_i(\cdot) - 1 - \theta_i(c). \tag{4.9}$$

When parameter $\theta_i(c) > 0$, it represents policies that favor defectors. These policies reduce the positive effects of social pressure and increase the temptation to defect. On the other hand, if $\theta_i(c) < 0$, the parameter represents policies in the form of subsidies designed to promote cooperation. In this case, subsidies have to be of opposite sign than policies that favor defectors, which means $\theta_i(c) < 0$.

We can easily observe in eq. 4.9 that for social pressure to be effective the following condition $\theta_i(c) <$ Ł needs to be true. We assume there is no time delay from defection to detection and thus compliers immediately sanction defectors once they have observed norm violation. Regarding the magnitude of the sanction, we bound ω_i above by Ł $= 2$, this means social pressure is bounded $0 \leq \omega_i \leq 2$ and individual costs of sanctioning should be lower than Ł such that $\theta_i(c) < 2$.

As $\omega_i \in [0, 2]$ and $\theta_i(c) < 2$ the decision to maintain the current strategy or to adopt the alternative one is limited by $-1 \leq p_i^C \leq 1$. Depending on ω_i and $\theta_i(c)$, compliers will decide to maintain their strategy with probability $p_i^C \in [0, 1]$ (if $U^C \geq U^D$) or to adopt the alternative one with probability $p_i^C \in (0, -1]$ (if $U^C < U^D$). Note that the sign of p only indicates the direction of the decision. On the other hand, the value of p indicates the magnitude of the decision. Analogously, probability $p_i^D(t)$ is symmetrical to $p_i^C(t)$ but with opposite sign such that $p_i^D(t) = 1 + \theta_i(c) - \omega_i$. Again, defectors will decide to maintain their strategy with probability $p_i^D \in [0, 1]$ (if $U^D \geq U^C$) or to adopt the alternative one with probability $p_i^D \in (0, -1]$ (if $U^D < U^C$). All agents simultaneously decide which strategy to choose based on the current distribution of compliers and defectors within the social network, with the probability being p_i^C or p_i^D. We assume that agents do not act strategically, i.e., they do not consider the possible strategy choices of their neighbors when deciding on their own. Given the large size of the social network and the resulting huge set of possible constellations each player needs to consider to make a strategic choice, it would seem to be more realistic to base individual strategy-choice on non-strategic behavior as in (Gale and Kariv [2003]).

4.3 Equilibrium concept

For the dynamics of a resource and a non-structured population, (Sethi and Somanathan [1996]) and (Osés-Eraso and Viladrich-Grau [2007]) identified equilibrium conditions. In the absence of a natural resource (Santos and Pacheco [2005]; Santos et al. [2006, 2012]) used Monte Carlo techniques to identify a window of parameter values for an equilibrium of the dynamics of a population embedded in an asymmetric social network. Given the complexity and irregularity of asymmetric networks the previous literature employed frequently the concept of pairwise stability. It allows abstracting from the complexity and irregularity of the network, since it is based on the relationship between two agents but neither on their position within the network nor topological characteristics of the network. However, in the presence of a stock variable this concept is not sufficient for an equilibrium since any change in the stock abrogates the previous existing pairwise equilibrium. Extending the concept of pairwise stability by an equilibrium condition for the stock variable offers a straightforward extension but still does not consider information about the agents' position within the network or topological characteristics of the network. Below define a general equilibrium concept that takes account of the agents' position within the network and topological characteristics of the network. The latter two aspects form part of the social pressure function ω that is a constituting element of the probabilities for a change in agent's i strategy choice.

Definition 1: (Equilibria conditions):

Any steady state equilibrium concept requires the following three equilibria, a) equilibria with respect to the dynamics of the resource, b) changes in the choice of strategy adopted by the agents and c) the demand the agents make of the resource must be incentive-compatible with the equilibria with respect to the dynamics of the resource.

Equilibria a) demands that $\dot{s}(t) = 0$ which, in turn, requires that

$$g(s(t)) = \sum_{i}^{c} w_i^C(t) + \sum_{c+1}^{n} w_i^D(t) \tag{4.10}$$

Additional to eq. 4.10, none of the agents change their strategy, or the share of compliers c is constant must also hold[5]. Hence, an equilibrium b) in expected values is

[5]The share of compliers can be kept constant if none of the agent changes, i.e., $p_i^C = 0, p_j^D = 0, \forall i, \forall j, i \neq j, i \in I : \{1, ..., cn\}, j \in J : \{cn+1, ..., n\}$. Moreover, there may be a dynamic equilibrium if $p_i^C \neq 0, p_j^D \neq 0, p_k^C = 0, p_l^D = 0, \forall i, \forall j, \forall k, \forall l, i \in I, k \in I, i \neq k, j \in J, l \in J, j \neq l$ and the share of

achieved if:

$$\sum_{i}^{cn} p_i^C - \sum_{cn+1}^{n} p_j^D = 0. \tag{4.11}$$

Finally, equilibrium c) holds if there is a $w_i^C(t)$ and $w_i^D(t)$ that satisfies eq. 4.1, and 4.10. In other words, the amount of extracted resource required satisfies the balance between reproduction and extraction (eq. 4.10) also has to be optimal from an economic point of view for compliers and defectors, i.e., none of the agents changes their strategy. Hence, an equilibrium is defined by eq. 4.1, 4.10 and 4.11.

Corollary:

If the conditions a) and c) of Definition 1 hold and $c_i = c$ and $\omega_i = \omega = 1 + \theta_i(c)$ a steady state equilibria is achieved.

Proof: Eq. 4.5 and 4.6 show for $\omega_i = 1 + \theta_i(c)$ that $U_i^C = U_i^D + \theta_i(c)$ which implies that $p_i^C = p_i^D = 0$, i.e., the agents maintain their current strategies that support the equilibrium level of the stock. Hence, condition b) of Definition 1 is also fulfilled. □

The conditions that $c_i = c$ and $\omega_i = \omega$ hold, are given by all types of networks that are complete. Likewise, it is given by networks that consist of smaller and independent parts that are itself complete. Similarly, these two conditions practically hold for regular lattices with periodic boundary conditions. While these specifications allow characterizing the equilibrium the considered types of networks are quite specific and exclude other networks such as scale-free networks or random networks.

4.3.1 Mean-field analysis

For incomplete or non-regular networks, the great number of agents and the large degree of freedom to satisfy conditions 4.10 and 4.11 makes it hardly impossible to obtain more operational equilibrium conditions that allow determining the equilibrium analytically. Nevertheless, the modern theory of mean-field allows obtaining operational equilibrium conditions that are based on the average values of the topological characteristics of the network. The theory of mean-field takes its departure from particle physics where

compliers of all agents is constant. This implies that strategy changes from compliers to defectors, or vice versa, cancel each other out for agents i and j, meanwhile agents k and l maintain their current strategy. None of these two equilibria are necessarily steady state equilibria.

it designates a highly effective methodology for handling a wide variety of situations in which there are too many particles to permit the dynamics or equilibrium to be described by modeling all the inter-particle interactions. Instead, the particle interaction is described by the contribution of each particle to the creation of a mean-field, and the effect of the mean field on each particle – for example the description of the phase changes of water to gas by the temperature. A large proportion of types of inter-particle interactions, though not all, lend themselves to this methodology: the inter-particle interactions must be sufficiently weak or regular in order for a statistical phenomenon to emerge (Guéant et al. [2011]). Similarly, mean-field theory is applied in economics where particles are replaced by agents who mutually interact in socioeconomic and/or strategic situations (Duernecker and Vega-Redondo [2017]; Galeotti and Rogers [2013]; Guéant et al. [2011]; Jovanovic and Rosenthal [1988]). Like in physics mean-field approximation of the social interactions of individual agents is legitimate (Guéant et al. [2011]) if the network is sufficiently large, regular and individual agents are alike (anonymity of individual agents).

Social equilibrium

Based on the concept of mean-field approximation our interest is in replacing c_i by c and τ_{c_i} by τ_c, i.e., the network is described by the average share of compliers and the average local cohesiveness. We start out with the equilibrium condition for the evolution of the agents (Definition 1, condition b). They are defined in eq 4.11 and the evolution of the share of compliers is governed by the eq. 4.7 and 4.8. In particular, our interest is in the evolution of compliers within the community. In eq 4.9 we have defined the decision rule for compliers in where the difference $(\omega_i - 1 - \theta_i(c))$ determines the direction and magnitude of the decision at each time step. We have argued that costs of sanctioning or subsidies $\theta_i(c) \gtreqless 0$ are shared by compliers. If $\theta_i(c)$ is uniform across compliers we have $\theta_i(c) = \bar{\theta}(c)$ for all agents that decide to conform the norm. Regarding social pressure, ω, in Appendix C we have shown that $c_i \approx c, \forall i \in n$ in irregular networks when compliers are distributed randomly through the community. Moreover, we proved in Appendix C that the average local cohesiveness in any network can be approximated by the following expression $\bar{\tau}_c \approx \bar{\tau} c^2$ (eq. 4.35).

According to these three approximations, we are replacing the interaction of an agent with her neighbors by an interaction with the average behavior in the community. This is the mean-field approximation in where every agent in the community is influenced by remaining others with equal strength. In this case the new decision criteria is governed

by

$$\bar{p} = \bar{\omega} - 1 - \bar{\theta}(c), \tag{4.12}$$

where

$$\bar{\omega} = \frac{Ł}{1 + s_{max} e^{-s(c-(c_0-\bar{\tau}_c))}}. \tag{4.13}$$

For simplicity, we will use ω instead of $\bar{\omega}$ to refer to the average social pressure in the network. We departed from a discrete model where agents revise their strategy at each time step according to a probability that is proportional to the payoff difference. However, social pressure in a network is rendered analytically intractable by the potential for multiple equilibria depending on the specifics of the network of connections and the distribution of compliers and payoffs. For the sake of simplicity, we employ a mean-field analysis to approximate the evolutionary dynamics. Formally, this leads to a continuous model that can be simplified by the 2-strategy replicator equation. The equation is represented as follows

$$\dot{c} \approx c(1-c)(U^C - U^D) \approx c(1-c)\left(\frac{\pi^C - (\pi^D - \omega(\pi^D - \pi^C) + \bar{\theta}(c)(\pi^D - \pi^C))}{\pi^D - \pi^C}\right). \tag{4.14}$$

That can be reduced to

$$\dot{c} = (\omega - 1 - \bar{\theta}(c))c(1-c), \tag{4.15}$$

The term $(\omega - 1 - \bar{\theta}(c))$ is equivalent to the growth rate of compliers. To concentrate of the qualitative characteristics of the growth rate we assume that $\bar{\theta}(c)$ is given by γc with $\gamma \lesseqgtr 0$[6]. Unlike traditional replicator dynamics, our social networks do not necessarily represent well-mixed populations, thus, networks are not always complete. As shown in Appendix C, mean-field approximation works better on regular networks (even on random networks) than on scale-free networks. However, this approximation is valuable because it helps us to identify the 3 stationary points in the system:

$$\dot{c} = (\omega - 1 - \gamma c)c(1-c) = 0 \rightarrow \begin{cases} \underline{c} = 0 \\ \omega(\hat{c}, s, \bar{\tau}\hat{c}^2) = 1 + \gamma\hat{c} \\ \bar{c} = 1 \end{cases} \tag{4.16}$$

[6]The admissible value of γ has to be bounded above by 2 in order to guarantee that the growth rate is always inferior to 3. Higher values of the growth rate may lead to chaotic behavior (May [1976]) of the logistic growth function.

In the intermediate stationary point we denote by $\hat{c}$ the critical mass of compliers needed to obtain $\dot{c} = 0$. Notice that $\underline{c} < \hat{c} < \bar{c}$.

Proposition 1

There exist at most three stationary points. A lower point $\underline{c} = 0$, an intermediate point $c = \hat{c} < 1$, and an upper point $c = \bar{c} \leq 1$. The upper point can be an intermediate or boundary value of the domain of c.

Proof: If $(\omega - 1 - \gamma c) < 0$ for $c < \hat{c}$, the growth rate of compliers is always negative and the only stationary point is given by $c = \underline{c} = 0$. If $(\omega - 1 - \gamma c) > 0$ the growth rate of compliers is always positive such that the population reaches its upper point $c = \hat{c} \leq 1$. In the case that the growth rate changes signs as $c < \bar{c}$ increases we obtain that an intermediate stationary point is reached. It is given by $(\omega - 1 - \gamma c) = 0$, for $c = \hat{c}$. □

Social equilibria in absence of policy instruments

The consideration of different values of the policy instruments and social pressure allows identifying a more precise location of these three stationary points. These results are summarized in Tables 4.1 and 4.2 and are illustrated in Fig. 4.1 and 4.2. The blue and red lines in Fig. 4.1a) – 4.1d) depict the evolution of the social pressure ω as a function of the share of compliers given a remaining stock of 45m, 35m, 20m, and 0m respectively. The blue line presents the evolution of social pressure when local cohesiveness is maximal and the red line when it is minimal. The discontinuous black line indicates the location where social pressure is equal to the benefits or costs of policy instruments plus one.

If policy instruments are absent, $\gamma = 0$, a stationary point to be interior requires that the growth rate $(\omega - 1)$ is equal to 0. This interior point is denoted by $c = \hat{c}$ (case A:1 of Table 4.1, intermediate point). If the share of compliers is below $\hat{c}$ the growth rate $(\omega - 1) < 0$ and consequently all agents will become defectors, i.e., $\underline{c} = 0$. However, if the share of compliers is above all agents will become compliers since social pressure is greater than 1, $(\omega - 1) > 0$, then $\bar{c} = 1$. These three stationary points $(\underline{c} = 0, \hat{c}, \bar{c} = 1)$ are presented in Fig.4.1a) – 4.1d). The precise value of $\hat{c}$ depends on the strength of local cohesiveness which in turn influences the strength of social pressure. If local cohesiveness is maximal (blue line, $\bar{\tau}_c^{max}$) $\hat{c}$ varies between 0.41 and

0.74 for the considered values of the stock. If local cohesiveness is minimal (red line, $\bar{\tau}_c^{min}$) $\hat{c}$ varies between 0.58 and 0.76 for the cases 1b) - 1c). In the case of 1a) does not exist. In this case the social pressure is always lower than 1, the only stationary point is given where all agents are defectors, i.e., $c = \underline{c} = 0$ (case A:2 of Table 4.1, lower point). Fig. 4.1a) – 4.1d) illustrates two facets of the growth rate of compliers: the less stock remains and the higher is the strength of local cohesiveness the lower is the required share of compliers that conduce to the social optimum (full cooperation). Likewise, Fig. 4.1a) – 4.1d) show that the fewer stock remains the less important is the strength of local cohesiveness. This conclusion can be derived from the distance between the blue and red line. It decreases with the remaining stock. In other words, the importance of the strength of local cohesiveness for social pressure is in part replaced by the scarcity of the stock.

Table 4.1 Stationary points in absence of policy instruments.

Cases	Subcases	Growth rate at a stationary point	Stationary points
A: $\gamma = 0$	(1)	$\omega - 1 = 0$	$\underline{c} = 0$, $\hat{c} = arg(\omega = 1)$, $\bar{c} = 1$
A: $\gamma = 0$	(2)	$\omega - 1 < 0$	$\underline{c} = 0$

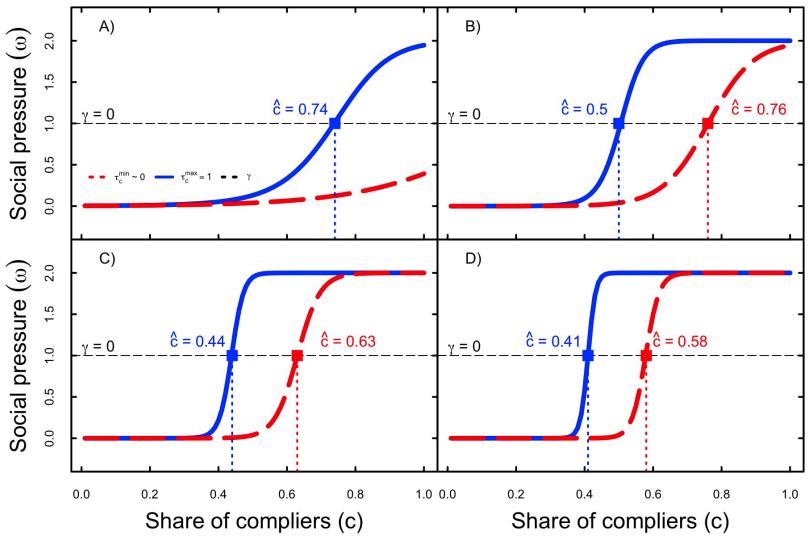

Fig. 4.1 Evolution of social pressure as a funtion of the share of compliers.

This figure shows the evolution of social pressure as a function of the share of compliers in absence of policy instruments, $\gamma = 0$: 1a) $s = 45$, 1b) $s = 35$, 1c) $s = 20$, and 1d) $s = 0$.

Social equilibria when policy instruments are present

Similarly to Table 4.1 and Fig. 4.1a) – 4.1d) one can analyze the stationary point of the evolution of compliers when policy instruments are present, i.e., $\gamma \neq 0$. A stationary point requires that the growth rate $(\omega - 1 - \gamma c)$ is equal to 0. The different cases for stationary points are classified in Table 4.2 and are illustrated in the Fig. 4.2a) – 4.2d). The discontinuous black lines in these figures indicate benefits/costs of the policy instruments plus one. In case that the policy instrument disfavors compliers, or in other words it favors defectors ($\gamma > 0$ case B:1 and B:2, Table 4.1) the share of compliers associated with a mixed equilibrium increases. Moreover, if the effect of the policy is sufficiently large (case B:2,Table 4.1) shows that the all-compliers stationary point at $\bar{c} = 1$ stops to exist and the upper point moves to the left and is converted into a second intermediate stationary point, $\bar{c} \leq 1$, situated between the all-compliers and the first intermediate stationary point. If the policy intervention favors the defectors even stronger the only stationary point is given were all agents are defectors, $\underline{c} = 0$ (case B:3, Table 4.1). Moreover, the latter point is also a stationary point for the cases B:1 and B:2 since the sum of the defector's overall benefits are always superior to social punishment at this point. Fig. 4.2a) illustrates for the case of $\gamma = 1$ that the only stationary points are given by $\underline{c} = 0$ and $\bar{c} = 1$. The intermediate stationary point does not exist. For $\gamma > 1$ only the all-defector equilibrium exists because the defector's overall benefits are always superior to the social punishment. Fig. 4.2a) – 4.2d) show for $\gamma \geq 1$ that as the remaining stock decreases an intermediate stationary points emerges and the upper stationary point is either given by $\bar{c} < 1$, or $\bar{c} = 1$. If the policy instrument leads to extra costs for defectors ($\gamma < 1$) a lower, upper and intermediate stationary point exist. Fig. 4.2a) – 4.2d) also show that the minimum share of compliers necessary for driving the population of compliers to the upper stationary point increases with a decrease in the remaining stock. If the local cohesiveness is maximal ($\bar{\tau}_c^{max} = 1$) the social pressure function is given by the blue line and if it is minimal ($\bar{\tau}_c^{min} = 0$) it is given by the red line. Like in Fig. 4.1, the higher is the strength of local cohesiveness the lower is the necessary share of compliers for driving the population of compliers to its upper stationary points. However, the difference between the blue ($\bar{\tau}_c^{max} = 1$) and red line ($\bar{\tau}_c^{min} = 0$) decreases with a decrease in the remaining stock.

Table 4.2 Stationary points when policy instruments are present.

Cases	Subcases	Growth rate at a stationary point	Stationary points
B: $0 < \gamma < 2$	(1) $0 < \gamma < 1$	$(\omega - 1 - \gamma c) = 0$	$\underline{c} = 0$, $arg(\omega = 1) \leq \hat{c} \leq arg(\omega = 1 + \gamma c)$, $\bar{c} = 1$
B: $0 < \gamma < 2$	(2) $1 < \gamma \leq argmax_{\frac{\partial}{\partial c}} \left(\frac{\omega - 1}{c}\right)$	$(\omega - 1 - \gamma c) = 0$	$\underline{c} = 0$, $arg(\omega = 1 + \gamma c) \leq \hat{c} < \bar{c} \leq 1$
B: $0 < \gamma < 2$	(3) $argmax_{\frac{\partial}{\partial c}} \left(\frac{\omega - 1}{c}\right) < \gamma < 2$	$(\omega - 1 - \gamma c) > 0$	$\underline{c} = 0$
C: $\gamma < 0$	(1)	$(\omega - 1 - \gamma c) = 0$	$\underline{c} = 0$, $0 < \hat{c} < arg(\omega = 1)$, $\bar{c} = 1$

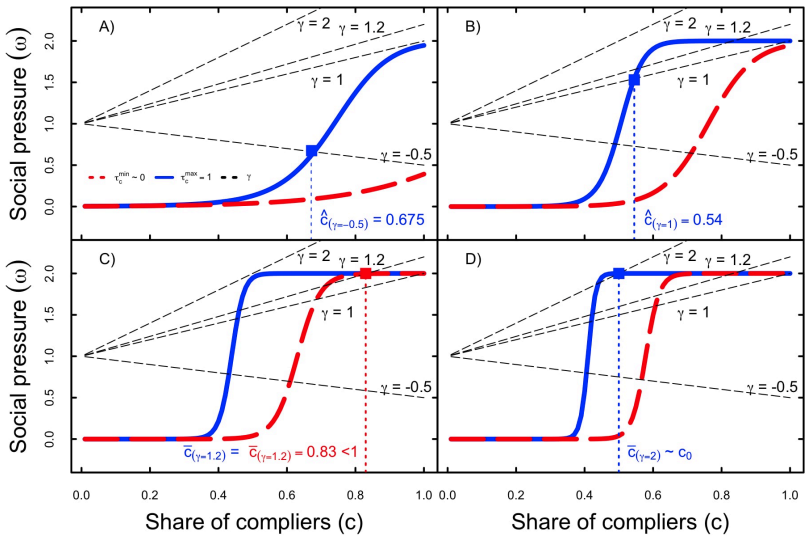

Fig. 4.2 Evolution of social pressure as a funtion of the share of compliers.

This figure shows the evolution of social pressure as a function of the share of compliers in the presence of policy instruments, $\gamma > 0$: 2a) $s = 45$, 2b) $s = 35$, 2c) $s = 20$, and 2d) $s = 0$.

Proposition 2

The lower and upper stationary points $\underline{c} = 0$ and $\bar{c} \leq 1$ are stable while the intermediate stationary point $\hat{c}$ is unstable.

Proof: A slight increase of the share of compliers above $\underline{c} = 0$ cannot be sustained because social pressure ω is much lower than 1, $\omega << 1$, see Fig. 4.1. Consequently, the share of compliers decreases up to the stationary point $\underline{c} = 0$. Similarly, a decrease of the share of compliers below $\bar{c} \leq 1$ cannot be sustained because social pressure ω is close to its maximum $\omega \approx$ Ł and then $(\omega - 1 - \gamma c) > 0$ so that the share of compliers increases again up to $\bar{c} \leq 1$. In the case of $\bar{c} \leq 1$ an increase of the share of compliers cannot be sustained since the defector's extra benefits are superior to social

punishment, $(\omega - 1 - \gamma c) < 0$, and consequently c decreases again to $c = \bar{c} \leq 1$. The intermediate stationary point is however different because it presents a crossroad. If the share of compliers falls below $c = \hat{c}$ the defector's extra benefits are superior to social punishment and thus, the share of compliers continues to decrease up to $\underline{c} = 0$. If the share of compliers rises above $c = \hat{c}$ the defector's extra benefits are inferior to social punishment and thus, the share of compliers continues to increase up to $\bar{c} \leq 1$. □

As an example for a policy that favors defectors one can think of a regulation that imposes the cost of social punishment (e.g. monitoring or penalization costs) on compliers. It increases the defectors' extra benefits so that $\gamma > 0$. In this case the slope of the line that presents the defector's benefits plus one, increases and consequently the intermediate stationary point $\hat{c}$ increases, or it may even be eliminated if the costs of social punishment are sufficiently high. In other words, the effect of this regulation is that the share of compliers necessary to induce cooperativeness increases. At the maximum it has to increase up to the point of $\bar{c} \leq 1$. If $\bar{c} \leq 1$, the stable upper stationary point can be achieved by a share of compliers below one. In this case the introduction of a policy instruments may lead to a stable stationary point that is supported by a mix of compliers and defectors. Thus, a policy that favors defectors (punish compliers) may lead to a stable cooperative stationary point with a lower share of compliers than the corresponding stable cooperative stationary point in the absence of the policy. This somehow counterintuitive result could be policy relevant if in the absence of policy instruments, for one reason or another, an all-complier stationary point cannot be achieved. In this case a policy instrument allows replacing the non-achievable stable all-complier stationary point by a stable intermediate stationary point.

In contrast, if the policy intervention disfavors defectors, i.e. it favors compliers ($\gamma < 0$), the intermediate stationary point $\hat{c}$ moves to the left (case C:1, Table 4.2) in comparison with the case of $\gamma = 0$. An example of such a policy would be the concession of a subsidy where a fixed amount of a good is distributed among all compliers. The lower and upper stationary points $\underline{c} = 0$ and $\bar{c} = 1$ are unaffected. Thus, a policy where the defector's extra benefits decrease leads to a lower intermediate stationary point and as such the share of compliers necessary for inducing cooperativeness decreases.

After analyzing condition b) of Definition 1 we turn our attention to the conditions a) and c) of Definition 1. We employ some simple specification of the employed functions that allow us to reduce the three equilibria conditions to one equation with one variable. Obviously, a more complex specification of the employed functions would

provide a more realistic formulation but not necessarily more insights. In particular the simpler formulation allows illustrating the equilibrium concept and relating the topological characteristics of the network with the stability of the different identified equilibria. Independent from the realism of the specification the employed equilibrium concept is valid for any specification of the employed function.

Social-ecological equilibrium

As we have seen in Definition 1, the overall equilibrium of the social-ecological system not only depend on social dynamics but also on the state of the natural resource. Next, we treat both systems (social and natural) as coupled and coevolving, and provide arguments to define the global equilibrium.

Let us assume that the number of agents $n = 1000$ and their resource demand functions according to the eq. 4.1 are given by

$$w_i^c = \alpha_0 + \alpha_1 s, \quad w_i^D = \beta_0 + \beta_1 s, \tag{4.17}$$

where $\beta_0 > \alpha_0$ and $\alpha_1 > \beta_1$ such that $w_i^D > w_i^C$ always holds. Moreover, we assume that the growth function $gr(s)$ is constant and independent from the stock. Let this exogenous regeneration or recharge rate per agent be denoted by R. With respect to this rate one can think of groundwater recharge in m^3 per ha and the variable stock s indicates the height of the groundwater measured from the bottom of the well. Other interpretations are possible; however, for the sake of concreteness we formulate our analysis along this example. For illustrative purposes we present the two resource demand functions in Fig. 4.3.

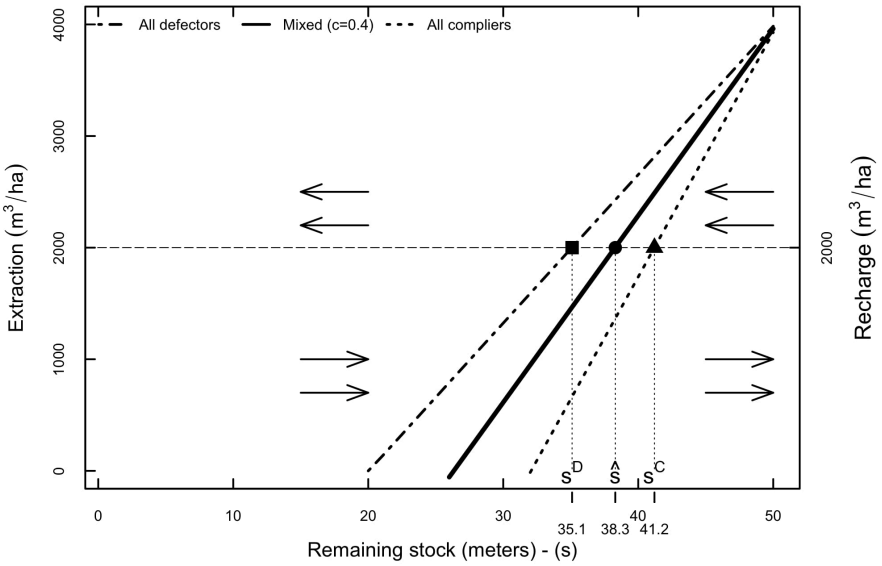

Fig. 4.3 Demand functions and recharge.

This figure presents the demand functions for defectors ($w^D(s)$) and compliers ($w^C(s)$), and the regeneration rate R for the values $\alpha_0 = -7022$, $\alpha_1 = 219$, $\beta_0 = -2666$, $\beta_1 = 133$, $R = 2000m^3/ha$.

The resource demand per ha if all agents were defectors $w^D(s)$ is depicted by the dotted dashed line and the one if all agents were compliers $w^C(s)$ by the dashed line. Given the regeneration rate per agent $R = 2000m^3/ha$ Fig. 4.3 shows that the stock $s^D = 35.1m$ supports an all defector extraction equilibrium, i.e., where extraction is equal to regeneration. Equivalently, the stock $s^C = 41.2m$ supports an all-complier extraction equilibrium. Thus, any possible extraction equilibrium $\hat{s}$ is located between $s^D = 35.1m$ and $s^C = 41.2m$. If the stock is greater than $\hat{s}$ the optimal resource demand is higher than the regeneration rate and thus, the stock decreases. If the stock is smaller than the optimal resource demand is smaller than the regeneration rate and thus, the stock increases. We indicate a positive or negative sign of the growth rate of the stock by an arrow to the right or to the left respectively. According to the eq. 4.2 and 4.10 the biophysical equilibrium condition requires that

$$R = cn(\alpha_0 - \alpha_1 s(t)) + (1-c)n(\beta_0 - \beta_1 s(t)). \tag{4.18}$$

Solving eq. 4.18 for s allows to formulate the stock as a function of the regeneration rate, the size of the community, and the share of compliers in the network at time t.

Let us denote the solution of this biophysical equilibrium by s^B. It is given by

$$s^B(R, n, c(t)) = \frac{K}{M}, \tag{4.19}$$

where $K = R - (c(t)n\alpha_0 + (1 - c(t))n\beta_0)$ and $M = c(t)n\alpha_1 + (1 - c(t))n\beta_1$. Eq. 4.19 satisfies condition a) and c) of Definition 1. The condition b) of Definition 1 requires that agents have no incentives to change their strategies, i.e., $\omega = 1 + \gamma c$, which translates to the necessary equilibrium condition

$$\omega = \frac{Ł}{1 + s_{max}e^{-s(c-(c_0-\bar{\tau}_c))}} = 1 + \gamma c. \tag{4.20}$$

Utilizing eq. 4.20 provides the stock s^N as a function of the share of compliers. It is given by

$$s^N(c) = \frac{ln\left(\left(\frac{Ł}{1+\gamma c} - 1\right)\frac{1}{s_{max}}\right)}{c_0 - \bar{\tau}_c - c}. \tag{4.21}$$

Fig. 4.4 illustrates the argument and value of the function $s^N(c)$ as defined in eq. 4.21, if social pressure is equal to 1 and $\gamma = 0$. The continuous line depicts the iso-social pressure function given a strength of average local cohesiveness of $\bar{\tau}_c = 0.5$. If the initial values of c and s are to the right of this line the share of compliers increases since social punishment is superior to the defector's extra benefits. We indicate the sign of the dynamics of the share of compliers by arrows to the right. If the initial values of c and s are to the left of this line the share of compliers decreases since social punishment is inferior to the defector's extra benefits. The sign of the dynamics of the share of compliers is indicated in this case by arrows to the left. Moreover, Fig. 4.4 also indicates the function if the strength of local cohesiveness is maximal, $\bar{\tau}_c^{max} = 1$, (dashed line) and if it is minimal, $\bar{\tau}_c^{min} = 0$, (dotted line). Thus, the grey area between these two lines indicate all possible locations of the iso-social pressure function that always presents a separating line with respect to the sign of the changes of the share on compliers.

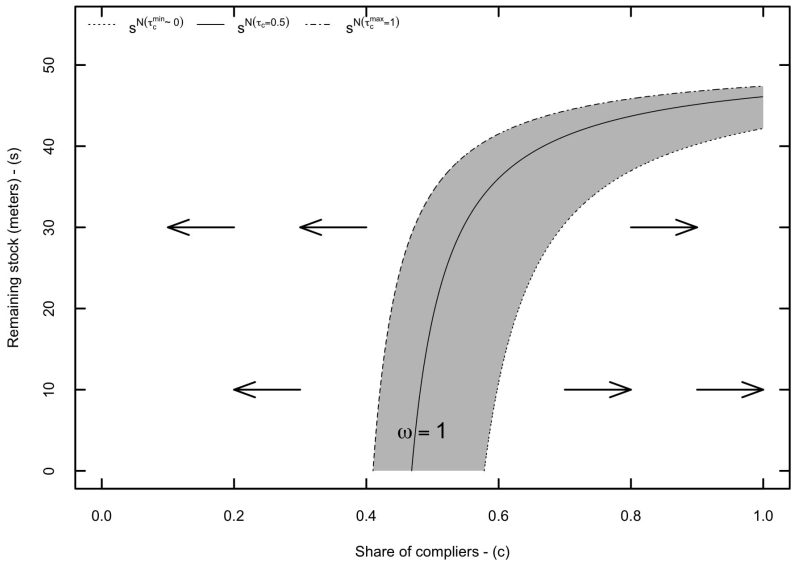

Fig. 4.4 The iso-social pressure function.

This figure shows $\omega = 1$ for different networks (from random to complete networks). As different networks have different degrees of strength of cohesiveness $\bar{\tau}_c$, the grey area represents the range of variation with respect to c, s and $\bar{\tau}_c$.

With respect to the equilibrium Definition 1 conditions a) –c) are satisfied if it holds that

$$s^B(R, n, c(t)) = s^N(c). \tag{4.22}$$

4.4 Policy corridors

According to the mean-field analysis and the overall equilibrium described in eq. 4.22, we want to identify policy corridors for the concrete determination of policy options. Concretely, we want to answer the question about when network-orientated and economic-orientated policies may be best applied. In any case, policies must take into account the share of compliers in the community, their levels of association and the state of the natural resource.

A graphical presentation of the eq. 4.19 and 4.21 where policy instruments are absent($\gamma = 0$) is shown in Fig. 4.5.

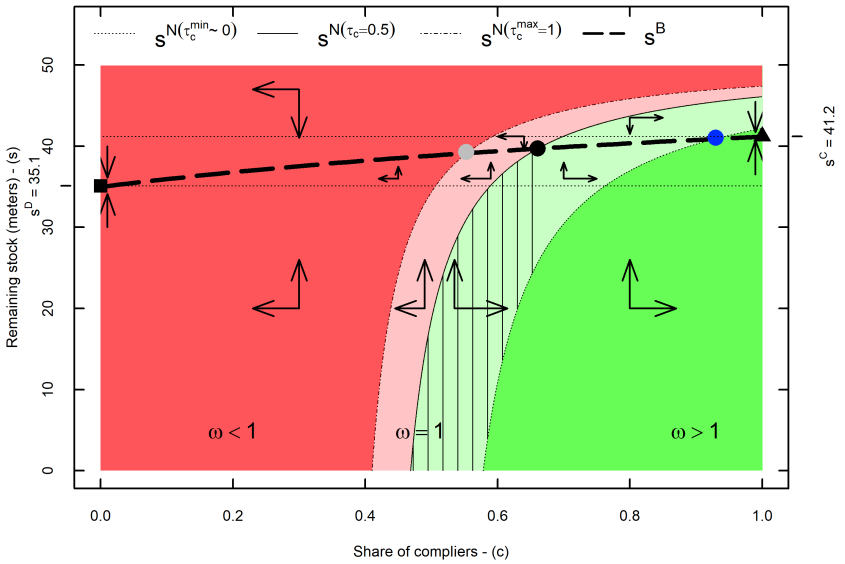

Fig. 4.5 Policy corridors for the concrete determination of policy options.

Presentation of $s^B(R, n, c(t))$ and $s^N(c)$ for the values $\alpha_0 = -7022$, $\alpha_1 = 219$, $\beta_0 = -2666$, $\omega = 1$, $\beta_1 = 133$, $R = 2000m^3/ha$. In this figure, the three possible equilibria are represented by a bold triangle (all-complier equilibrium), colored circles (mixed equilibria when $\bar{\tau}_c = \{0$ (blue), 0.5 (bold), 1 (gray)$\}$), and a bold square (all-defector equilibrium). The green area represents the basin of attraction for the all-complier equilibrium. The red area represents the basin of attraction for the all-defector equilibrium.

The bold discontinuous line in Fig. 4.5 presents the function $s^B(R, n, c(t))$ as given in eq. 4.19. The non-bold continuous line presents the function $s^N(c)$ given in eq. 4.21 for $\bar{\tau}_c = 0.5$. The intersection of the two functions (eq. 4.22) indicates an equilibrium that fulfils the conditions stated in Definition 1. Since $c = \hat{c}$ we observe a mixed equilibrium denoted by a bold circle $E_{\gamma=0}^{\bar{\tau}_c=0.5} = (\hat{c}, s) = (0.66, 39.7)$. Fig. 4.5 also indicates the mixed equilibria for the maximal and minimal strength of local cohesiveness, given by $\bar{\tau}_c^{max} = 1$ and $\bar{\tau}_c^{min} \approx 0$ respectively. Accordingly, we obtain the equilibria $E_{\gamma=0}^{\bar{\tau}_c=1} = (0.55, 39.25)$, denoted by a gray circle; and $E_{\gamma=0}^{\bar{\tau}_c=0} = (0.93, 41.0)$, denoted by a blue circle. In the former case the iso-social pressure function moves to the left and in the latter case it moves to the right. The resulting functions are indicated by a dashed and a dotted line respectively. Combining the signs of the growth rates of the stock illustrated in Fig. 4.3, with the signs of the growth rate of the share of compliers illustrated in Fig. 4.4 allows visualizing the directions of the growth of the "stock-share of compliers" system. Fig. 4.5 shows that the basin of attraction for

the all-defector equilibrium, denoted by a bold square ($\underline{c} = 0, s = s^D = 35.1$), is given by the red area; and the basin of attraction for the all-complier equilibrium, denoted by a bold triangle ($\bar{c} = 1, s = s^C = 41.2$), is given by the green area. Initial values located within the red area indicate that the tragedy of the commons cannot be avoided whereas initial values located in the green would allow overcoming the tragedy of the commons and achieving the socially optimal outcome. Likewise, Fig. 4.5 shows that there exists an area marked with vertical lines where the sign of the growth rate of the system is not sufficient for determining the dynamics of the system. For this area the precise values of the growth rates are required for the determination of the dynamics of the system. For the specified functions of our study we show that the growth rate of the share of compliers dominates the growth rates of the stock (for more details, see appendix A) such that the marked area also leads to the all-complier equilibrium. In other words it belongs as well to the green area. Finally, the graphical analysis also confirms that the intermediate stationary point $\hat{c}$ is not stable (Proposition 1).

The size of the green area varies with the strength of local cohesiveness. It is maximal if the strength of local cohesiveness is maximal and thus, an initial share of compliers slightly above the dashed line is already sufficient for driving the system to full cooperativeness. However, if the strength of local cohesiveness is minimal likewise is the size of the green area. In this case, however, the initial share of compliers has to be slightly superior to the value of the dotted line. The area between the dotted and dotted dashed lines (transparent corridor) indicates the possible location of the iso-social pressure function if the value of $\bar{\tau}_c$ is not given by its boundary values. For any value of the strength of cohesiveness the iso-social pressure function traces out a single line located within the transparent corridor. This line presents in arbitrary small terms the lower limit of the green area and the upper limit of the red area.

The analysis of Fig. 4.5 suggests different options for policy interventions. Since initial values of c and s located in the green area are sufficient for achieving full cooperation we refer to the green area as the "no-policy corridor". The transparent corridor is very important not only as it bounds the range of possible equilibria as a function of the strength of local cohesiveness but also because it indicates the maximal outcome of network policies. The objective of these policies is to improve cohesiveness between agents. At the maximum they are able to achieve the strength of cohesiveness of one and thus, at the maximum they are able to reduce the minimum share of complier for cooperativeness that is exemplified by the dashed line. For this reason we refer to the transparent area as the "network policy" corridor. Here, one can think of the foundation of a compliers association or the organization of seminar, workshops

for compliers. All these initiatives have the objective to improve the cohesiveness between compliers which in turn leads to higher social pressure on defectors. Initial values located in the red area lead to social pressure lower than one and thus, the system will end up in the all-defector equilibrium. Thus, direct policy interventions, for instance in form of economic incentives, are required if one aims to overcome the tragedy of the commons. For this reason we refer to the red area as the "policy instrument" corridor. If the initial values of c and s are located in "policy instrument" corridor the use of policy instruments is indispensable. These instruments may be complemented or replaced by network policies based on some cost-benefit analysis for the different options. The "policy instrument" corridor also includes as a special case the traditional economic analysis (tragedy of the commons) where networks and social pressure were not considered. In the absence of social networks the degree of each agent would be zero and consequently all agents would act independently from each other. Consequently, the absence of local cohesiveness and the unimportance of the remaining stock do not activate any social pressure ($\omega \approx 0$). Thus, the "no-policy" and the "network policy" corridor would disappear and we are left with the policy instrument corridor which leads to the all-defector equilibrium in the absence of policies.

Observation 1: *The strength of cohesiveness, the size of the stock and the social pressure function allow tracing out "no-policy", "network policy" and "policy instruments" corridors.*

Fig. 4.6 shows for the maximal degree of cohesiveness, $\bar{\tau}_c^{max} = 1$, that the equilibrium is given by the point $E_{\gamma=0}^{\bar{\tau}_c^{max}}$. The maximal value of local cohesiveness is always achieved if the considered network is complete, i.e., if the degree of the agents is always equal to the number of agents minus 1. Hence in the case of a complete network social pressure is highest and the transparent corridor in Fig. 4.5 can be narrowed down to a line so that we can determine the exact value of the equilibrium. This brings up the question whether information about the type of network allows limiting the strength of social pressure that narrows down the transparent corridor in general or whether this only holds for complete networks. The answer to this question is illustrated in Fig. 4.6. It shows that there is a relationship between the type of network and size of the transparent corridor. Thus, the type of network is not only important for determining possible locations of equilibrium but also indicates the size of the "network policy" corridor, i.e. the perimeter of the possible outcome of network policies.

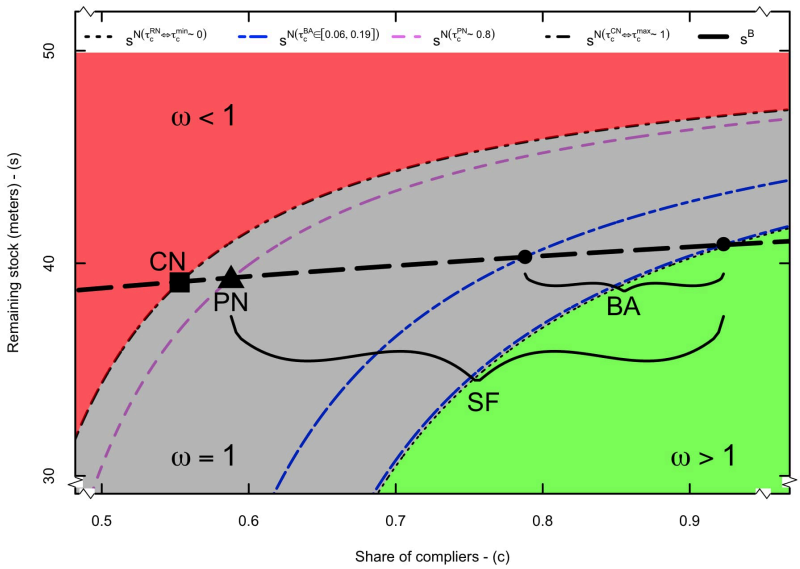

Fig. 4.6 Influence of the type of the network on the size of the "network policy".

This figure is connected with Fig. 4.5. If we zoom in the Fig. 4.5, we can observe how network structures affect social pressure. Again, results are obtained for the values $\alpha_0 = -7022$, $\alpha_1 = 219$, $\beta_0 = -2666$, $\beta_1 = 133$, $R = 2000m^3/ha$. Different types of networks, CN (Complete Networks), PN (Pseudofractal Networks), and BA (Barabasi-Albert Networks) are used to represent the size of the "network policy" corridor. Scale-free networks (SF) may range from BA to PN networks.

In Appendix B we determined the minimum and maximum values of average local cohesiveness for two types of scale-free networks: the deterministic Pseudofractal Networks (PF) and Barabási-Albert Networks (BA). Both types are representative for social networks (Jackson [2008]). While the BA network is a non- extreme scale-free network, the PF network can be considered as the scale-free network of which strength of cohesiveness come closest to the one of a complete network. For example, PF network represents well the strength of cohesiveness in scientific networks. According to the calculation in Appendix B and the specification of the values of this study, the strength of cohesiveness of BA networks may range from 0.06 to 0.19 while the strength of cohesiveness of PF networks is a single value and is equal to 0.8. It is 0.2 below the maximal value of a complete network (CN). Based on these values Fig. 4.6 shows that the "network policy" corridor for scale-free networks may range from $(0, 0.8]$. The concrete size of the "network policy" corridor depends on the specific type of the scale-free network. The smaller "network policy" corridor, the larger is

the "policy instruments" corridor. Thus, for small "network policy" corridors the community or regulator has to rely more on policy instruments like taxes, subsidies or direct regulations in order to induce cooperativeness. Whereas for larger "network policy" corridors the community or regulator can chose between all policy options.

Apart from the mentioned policy options the community or the regulator may consider policies that improve the regeneration rate or extend or limit the number of agents. According to eq. 4.19 we find for an increase in the regeneration rate R that the curve s^B moves upward ($\frac{\partial s^B}{\partial R} > 0$) and possible equilibria points are characterized by a higher stock and a higher share of compliers. Consequently the minimal share of compliers that is necessary for leading the system to full cooperation increases. The intuition for this result is that a higher regeneration rate would lead to an increase in the remaining stock and thus, to a decrease in social pressure. In order to offset this decrease the share of compliers needs to rise. On the contrary, if the size of the community n increases we find that the curve s^B shifts downwards $\frac{\partial s^B}{\partial n} < 0$ such that possible equilibria points are characterized by a lower stock and a lower share of compliers necessary for inducing cooperativeness.

Fig. 4.5 categorized corridors that identified the available policy options. Yet, the "policy instrument" corridor in Fig. 4.5 is only helpful for discarding the options "no policy" and "network polices" if the initial values of c and s lie within the "policy instrument" corridor. For the concrete determination of the effect of policy instruments one has to take into account that the presence (costs of social punishment) or introduction of policy instruments like taxes or subsidies alter the compliers' and defectors' utility. Thus, the growth rate of compliers is now given by $(\omega - 1 - \gamma c)$ where γ is not any longer equal to 0. Fig. 4.7 illustrates the consequences of the presence or introduction of a policy that favors defectors. As before Fig. 4.7 is based on the functions s^B, eq. 4.19 and s^N, eq. 4.21 and as an example we have chosen $\gamma = 1.2$.

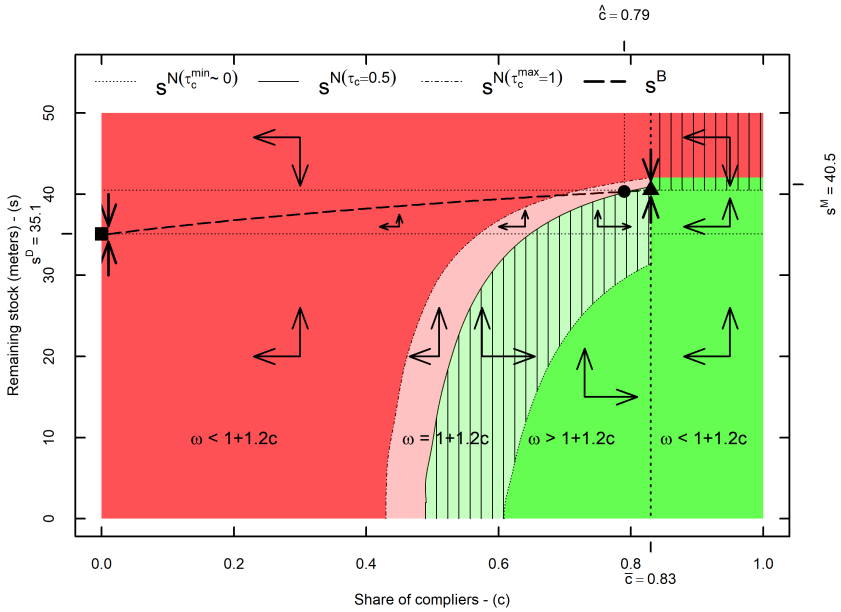

Fig. 4.7 Consequences of the presence or introduction of policy instruments that favors defectors' utility.

Presentation of $s^B(R, n, c(t))$ and $s^N(c)$ for the values $\alpha_0 = -7022$, $\alpha_1 = 219$, $\beta_0 = -2666$, $\omega = 1$, $\gamma = 1.2$, $\beta_1 = 133$, $R = 2000m^3/ha$. In this figure, the three possible equilibria are represented by a bold triangle (all-complier equilibrium), bold circle (mixed equilibrium when $\bar{\tau}_c = 0.5$), and bold square (all-defector equilibrium). The green area represents the basin of attraction for the all-complier equilibrium. The red area represents the basin of attraction for the all-defector equilibrium.

Fig. 4.7 shows for $\gamma > 0$ and a strength of social cohesiveness of $\bar{\tau}_c = 0.5$ in comparison with Fig. 4.5 that the curve s^N moves to the right and the new mixed equilibrium and the upper limit equilibrium are given by $E^{\bar{\tau}_c=0.5}_{\gamma=1.2} = (\hat{c}, s) = (0.79, 40.3)$, denoted by a bold circle; and $E^{\bar{\tau}_c=0.5}_{\gamma=1.2} = (\bar{c}, s) = (0.83, 40.5)$, denoted by a bold triangle, respectively. For the opposite case where $\gamma < 0$ (e.g. additional benefits for compliers) we observe that the curve s^N moves to the left and the new equilibria moves south-west $E^{\bar{\tau}_c=0.5}_{\gamma=-0.2} = (\hat{c}, s) = (0.71, 40)$ (not shown in Fig. 4.7). Thus, less compliers and a lower level of the remaining stock are necessary for this new equilibrium. Comparing the mixed equilibrium shown in Fig. 4.5 $E^{\bar{\tau}_c=0.5}_{\gamma=0} = (\hat{c}, s) = (0.66, 39.7)$ with the mixed equilibrium in Fig. 4.7 $E^{\bar{\tau}_c=0.5}_{\gamma=1.2} = (\hat{c}, s) = (0.79, 40.3)$ shows that the introduction of a policy instrument where $\gamma > 0$ (e.g. cost of social punishment) leads to an increase in the share of compliers and the remaining stock. Since $\gamma > 0$ the defectors extra benefits increases and more compliers and a higher stock are necessary for the mixed equilibrium.

Consequently, the initial share of compliers necessary for achieving cooperativeness also increases.

Furthermore, the dashed line and the dotted line indicate the values of the function s^N for the case of the maximal and minimal strength of cohesiveness respectively. The area between these two lines shows as before the "network policy" corridor. It is reported again in more transparent colors and shows the limits of the effects of network policies. A comparison with Fig. 4.5 shows for $\gamma > 0$ that the "network policy" corridor has moved to the right and increased in width. This finding suggests for our study the following observation.

Observation 2: *The introduction or presence of policy instruments not only affects the location of the "no policy", "network policy" and "policy instruments" corridors but also their size. For the specification of the functions of this study the perimeter of the applicability of network policies has increased.*

Observation 2 suggests that the evaluation of the policy options should be realized simultaneously since the stipulation and effectiveness of the policy options are interdependent. Moreover, Fig. 4.7 shows that the upper stationary point $\bar{c}$ is less than one, $\bar{c} = 0.83$. Thus, there exists besides the mixed equilibrium $\hat{c}$ another mixed equilibrium $\bar{c}$ but an all-complier equilibrium does not exist. Analyzing graphically the sign of the growth rates of the share of compliers and the stock shows that the mixed equilibrium $\hat{c}$ is unstable while the upper limit equilibrium $\bar{c}$ is stable. Like in Fig. 4.5 the green area indicates the basis of attraction for the stable equilibrium and the red area the basin of attraction of the all-defector equilibrium. The area marked by vertical lines is made up of initial values of c and s where the sign of the growth rates is not sufficient for determining the basin of attraction. Only with information about the concrete values of the growth rate of c and s one can determine the trajectory of these variables. A numerical evaluation for the specified functions of this study shows that the green area marked by vertical lines belongs to the basin of attraction of the stable mixed equilibrium and the red area marked by vertical lines to the basin of attraction of the all defector equilibrium. Finally, Fig. 4.7 also suggests the following observation.

Observation 3: *The introduction or presence of policy instruments may favor the emergence of an upper limit stable equilibrium that is mixed and located within the "network policy" corridor.*

Observation 2 suggests that the presence or introduction of policies may lead to a relocation and amplification of the network policy corridor. Within this context Observation 3 states that network policies may obtain a more prominent role since they might be able induce the stable equilibrium directly without relying on the dynamics of the system once the green area is reached.

4.5 Concluding remarks

In this study, we analyze the evolution of cooperation within a community of agents exploiting a natural resource. The community defines a social norm based on the socially-optimal management of the natural resource. Two types of agents, compliers (long-term behavior) and defectors (short-term behavior) interact according to the underlying structure of the social network. Adherence to the social norm is voluntary and agents may change their strategy at next time steps. Both types of agents update their strategy based on utility differences. Concretely, the probability of changing current strategy to the alternative one is proportional to utility differences. Compliers can reduce the utility of defectors using social pressure, and social pressure varies depending on the share of compliers in the neighborhood of agents, the state of the resource, and the level of local cohesiveness between compliers. However, the utility obtained from extraction may be reduced/increased from additional benefits or extra costs as a result of economic-orientated policies. These policies affect defectors or compliers, and as such they may change with the share of compliers and may alter utility differences. If policy intervention favors defectors, the positive effects of social pressure are reduced and thus temptation to defect increases. If policy intervention disfavors defectors, defector's extra gains are reduced and thus the probability to comply with the norm increases.

This formulation aims to analyze what exactly are the social and natural conditions required to promote cooperation within the community. If all equilibrium conditions hold, an overall equilibrium (with respect to the dynamics of the resource, the social network and the resource demand) may emerge. However, social pressure in a social network is rendered analytically intractable by the potential for multiple equilibria given the asymmetry and complexity of the network and the distribution of compliers through the network. Following the theory of mean-field, we employ a mean-field analysis to approximate system dynamics. Intuitively, this approximation can be thought of every agent interacting with the average behavior in the community. This approximation method ignores much of the complexity of the decision-making process.

Nevertheless, even with this simplified representation we can observe how distinct network topologies affect cooperation differently. Applying mean-field, we can study the regimes of stationary state of the evolutionary dynamics in a simpler way. Given our specifications for strategy choice, we identify 3 stationary points in the system: all-defector equilibrium (stable), all-complier equilibrium (stable), and mixed equilibrium (stable or unstable). The stationary points and their stability allow us to identify policy corridors for the concrete determination of policy options.

The results show that the strength of cohesiveness, the state of the natural resource and the social pressure allow tracing out 3 corridors for policy options: "no-policy", "network policy" and "policy instruments". Social pressure is undertaken by the compliers themselves without presence of external authorities. When the share of compliers is sufficiently high within the community, social pressure leads to full cooperation. We define the area where social pressure is completely effective as "no-policy" corridor. In some situations social pressure cannot maintain adherence to the social norm. When the share of compliers is very low and/or the stock is fully available for agents the temptation to defect is very high. In those situations social pressure will go almost unnoticed and economic-orientated policies will be indispensable. We define the area where taxes or subsidies are indispensable as "policy instruments" corridor. However, there exists an intermediate area in where the influence of network structure is key for the determination of cooperation. Under this area, the wide variety of network topologies allows us to define network-orientated policies. Examples of network-orientated policies are all those initiatives designed to increase the local cohesiveness of compliers. By increasing local cohesiveness of compliers we increase the sanctioning ability of the cooperating community. For a complete understanding of the "network policy" corridor we use representative types of networks: complete, scale-free and random networks. While not realistic, complete and random networks allow us to define the upper and lower limits for social pressure respectively. On the other hand, scale-free networks are more suitable for representing the observed patterns of social interaction in real-world networks. Thus, the "network policy" corridor is bounded above by the sanctioning ability of compliers in complete networks, and is bounded below by the sanctioning ability of compliers in random networks. Hence, complete and random networks represent two ends of a continuum along with one can find realistic social networks, i.e., scale-free networks with increasing levels of link correlations.

The results show large regions where both "policy instruments" and "network policy" corridors coexist, this means different policies can be applied indistinctly or in combination. However, network policies may be more effective than traditional analysis

when agents perceive taxes/subsidies as disproportionate or meaningless (Bicchieri and Muldoon [2014]).

The results also show that the presence or introduction of policy instruments lead to a relocation of the policy corridors. We observe that the perimeter of the applicability of network-orientated policies increases with the introduction of policy instruments. When policy instruments are present, network-orientated policies obtain a more prominent role since they induce mixed equilibrium to be stable. Moreover, the stationary point in the mixed equilibrium is located within the "network policy" corridor.

This study allows for policy options favoring the sustainable management of the natural resource to be identified and targeted, where the system ultimately converges depend on the initial conditions of the system and the path followed.

4.6 Appendices

4.6.1 Appendix A: Equilibrium Points and Basin of Attraction

The social pressure function ω is sigmoidal and symmetric in c. An equilibrium point is characterized by the fact that social pressure is identical to the defector's extra benefits. This condition is expressed mathematically by

$$\omega = \frac{Ł}{1 + s_{max} e^{-s(c-(c_0-\bar{\tau}_c))}} = 1 + \gamma c. \tag{4.23}$$

By subtracting $-1-\gamma c$ on both sides of eq. 4.23 we obtain the new function $\omega - 1 - \gamma c$ that we identified as the growth rate of the share of compliers in eq. 4.16. If it is positive it indicates that social pressure is superior to the defector's extra benefits and thus, defectors will become compliers. If it is negative compliers will turn into defectors. Taking the first and second derivative of the growth rate we obtain that

$$\frac{\partial(\omega - 1 - \gamma c)}{\partial c} = \frac{Ł s_{max} s e^{-s(c-(c_0-\bar{\tau}_c))}}{\left(1 + s_{max} e^{-s(c-(c_0-\bar{\tau}_c))}\right)^2} - \gamma. \tag{4.24}$$

$$\frac{\partial(\omega - 1 - \gamma c)}{\partial s} = \frac{Ł s_{max} \left(c - (c_0 - \bar{\tau}_c)\right) s e^{-s(c-(c_0-\bar{\tau}_c))}}{\left(1 + s_{max} e^{-s(c-(c_0-\bar{\tau}_c))}\right)^2} - \gamma. \tag{4.25}$$

$$\frac{\partial(\omega - 1 - \gamma c)}{\partial^2 c} = \frac{Ł s_{max} s e^{-s(c-(c_0-\bar{\tau}_c))} \left(e^{s(c-(c_0-\bar{\tau}_c))} - s_{max}\right)}{\left(s_{max} e^{-s(c-(c_0-\bar{\tau}_c))}\right)^3}. \tag{4.26}$$

For the case where $\gamma = 0$ we observe from eq. 4.24 that $\frac{\partial(\omega-1-\gamma c)}{\partial c} > 0$. Moreover, we can solve eq. 4.23 directly and obtain the fixed point $c = ln(s_{max})\frac{1}{s}c_0 - \bar{\tau}_c$. Employing this solution in eq. 4.26 shows that $\frac{\partial(\omega-1-\gamma c)}{\partial^2 c} = 0$. To obtain this result it is sufficient to evaluate the factor $e^{s(c-(c_0-\bar{\tau}_c))} - s_{max}$ in the nominator. Hence, the solution $c = ln(s_{max})\frac{1}{s}c_0 - \bar{\tau}_c$ indicates an inflection point and corresponds to Proposition 1 to $c = \hat{c}$. If $\gamma \neq 0$ eq. 4.23 cannot be solved analytically and one has to resort to numerical techniques that we used also for the determination of the equilibria and iso-social pressure lines in the Fig. 4.1 - Fig. 4.7.

For the evaluation of the area marked with vertical lines in Fig. 4.5 and Fig. 4.7 the basin of attraction could not be determined unambiguously since the signs of the growth rates of the share of compliers and the stock were not sufficient. To determine

the magnitude of the changes of the growth rates we evaluate the sign of their difference, denoted by δ. Thus, δ is given by $\frac{\partial(\omega-1-\gamma c)}{\partial c} - \frac{\partial(\omega-1-\gamma c)}{\partial s}$. If δ is positive we observe that the growth rate of the share of compliers dominates the growth rate of the stock. On the contrary if it is negative we see that the growth rate of the stock dominates the growth rate of the share of compliers. For the specified functions of this study we obtain that $\frac{\partial(\omega-1-\gamma c)}{\partial c} > \frac{\partial(\omega-1-\gamma c)}{\partial s}$. Note that the sign of δ is positive if it holds that $c > c_0 - \bar{\tau}_c - 1$. Since this condition always holds, it shows that a small perturbation along the function s^N leads to an increase in compliers and therefore, the area marked by vertical lines in Fig. 4.5 and Fig. 4.7 is a basin of attraction for the all-complier equilibrium. Yet, there is also an area marked by vertical lines beyond the upper equilibrium, $\bar{c} = 0.83$. Since the function s^N does not exist beyond the point $\bar{c} = 0.83$ we cannot interfere the magnitude of the growth rates of the share of complier and of the stock. Numerical evaluation however, suggest that in part it belongs the basin of attraction of the stable mixed equilibrium, and in part to the basin of attraction of the all-defector equilibrium as indicated by the green and red area.

4.6.2 Appendix B: Average cohesiveness in different types of social networks

In this study, we focus on 4 types of networks that are representative of the wide variety of network structures that one can find in social networks. As before, we define the social network as the pair of sets $N = (A, L)$, where A refers to the set of agents and L refers to the set of links. Local cohesiveness, τ_i, is defined in Appendix E, and average local cohesiveness, $\bar{\tau}$, is defined in section 4.2.3 as a topological property of any network that measures how close is on average the neighborhood of agent i to be a complete network. Average cohesiveness is bounded between 0 and 1, $0 \leq \bar{\tau} \leq 1$.

1. Complete Networks

A complete network (CN) is a network with $|A| = n$ agents and a link between every two agents, such that $|L| = \ell = \frac{n(n-1)}{2}$ links. In complete networks, all agents are interconnected and then the number of links grows quadratically with the number of agents n. However, since links seem to be costly in social networks we observe that the larger the community, the lower the probability is to find complete network structure. As all agents are interconnected, the average cohesiveness is maximal, $\bar{\tau} = 1$.

2. Barabasi-Albert Networks

For large networks, large n, empirical observations (Barábasi and Albert [1999]; Faloutros et al. [1999]; Muchnik et al. [2013]; Newman [2003a]) have shown the high asymmetry in the distribution of links, which means that a few highly connected agents (also called hubs) coexist with a large number of agents with small degree. In large social networks, the degree sequence $\{k_1, k_2, ..., k_n\}$ can be approximated by the power law distribution $p_k = k^{-\gamma}$, with $2 < \gamma < 3$. Networks with power law distributions are called scale-free networks (SF) because power laws have the same functional form at all scales.

Since Price (Price [1976]) and Barabasi-Albert (Barábasi and Albert [1999]) models were published, it is commonly accepted that the power law pattern of social networks emerges as a result of a dynamic process in where networks grow monotonically and agents are involved in some sort of competition for links. Competition means that individual preferences for interaction seem to be biased and not all agents are equally

connected. The definition of social network as competitive system is motivated by the existence of hubs in social networks.

To date, the Barabasi-Albert network (BA) is probably the best known model to generate power law networks. In this model, the network develops following two driving mechanisms: network growth and preferential attachment. Network growth means that, at each time step, a new agent is added to the network and creates m links that connects her to previously added agents. Preferential attachment is a probabilistic mechanism in where the probability of a new link to end up in an agent is proportional to her degree, k_i, such that $p_i = m\frac{k_i}{\sum_j k_j}$.

To complete the characterization of the BA model, it has been proven that the number of links in the network is $\ell = mn$, where $|A| = n$ is the number of agents, and the average degree $\bar{k}$ is $\bar{k} = 2m$. Moreover, it is easy to prove that the average cohesiveness is independent to the degree of agents and decreases with the size of the network, $\bar{\tau} = \frac{m-1}{8}\frac{(log\ n)^2}{n}$.

Note that, at increasing m above a certain threshold the power law pattern becomes increasingly weaker. This threshold bounds the maximal number of links to be added at a constant rate by newcomers, $\hat{m}$, and can be estimated using the natural cut-off of power law networks. Denote by $F(k) = Pr(K \geq k)$ the cumulative distribution function (CDF) of a power law distributed variable, where again k represents the degree of agents. Then k_{min} and k_{max} represent the minimum and maximum degree in the social network respectively. For instance, in the continuous case

$$F(k) = \int_k^\infty p(k)dk = \left(\frac{k}{k_{min}}\right)^{-\gamma+1} \tag{4.27}$$

and the integral of $p(k)$ over two different degrees

$$F(k) = \int_{k_1}^{k_2} p(k)dk \tag{4.28}$$

provides the probability that a randomly chosen agent has degree between k_1 and k_2. To calculate k_{max} we assume that in a network of n agents we expect at most one agent whose degree exceeds k_{max}, then

$$F(k) = \int_{k_{max}}^\infty p(k)dk = \left(\frac{k_{max}}{k_{min}}\right)^{-\gamma+1} = \frac{1}{n} \tag{4.29}$$

this yields

$$k_{max} = k_{min}n^{\frac{1}{\gamma-1}} \tag{4.30}$$

and by inverting eq. 4.30 in the limits, $2 \leq \gamma \leq 3$, we obtain

$$\begin{cases} \frac{k_{max}}{n} = k_{min} & \text{if} \quad \gamma = 2 \\ \\ \frac{k_{max}}{\sqrt{n}} = k_{min} & \text{if} \quad \gamma = 3 \end{cases} \tag{4.31}$$

Neither self-loops nor multiple links are allowed in our network so that $k_{max} < n$. Let $k_{max} = n-1$ represent the extreme case in where all agents are connected to the largest hub (except herself). Let us assume that in a heterogeneous population there always exist an agent with ability to attract links very low. This agent with very low ability to attract links will have exactly m links once the network has been constructed, thus, $k_{min} = m$ in the network. Introducing $k_{max} = n-1$ and $k_{min} = m$ in eq. 4.31, we can prove that the number of links to be added at a constant rate by newcomers before the power law becomes weaker falls into the range $1 \leq m \leq \sqrt{n}$. In other words, if we want $2 < \gamma = \frac{ln(n)}{ln\left(\frac{k_{max}}{k_{min}}\right)} + 1 < 3$, we need $1 \leq k_{min} = m < \sqrt{n}$. Notice that $1 < k_{max} < n$.

If k_{max} nears the network size, $k_{max} \to n$, the CDF of the degree sequence does not follow the power law distribution, however, it serves to define the upper limits of m, this is $\hat{m}$. Using this information, we can define the limits of the average cohesiveness in the BA model: $0 \leq \bar{\tau} \leq \frac{(log\ n)^2}{8\sqrt{n}}$.

3. Pseudo-fractal Networks

As we have seen, the BA model is a useful tool to generate scale-free networks with certain degree of cohesiveness; however, this model cannot reproduce well the structure observed in some social networks, i.e., scientific networks (Foster et al. [2011]). These networks are scale-free but present a high level of cohesiveness.

To reproduce such network structure we use a deterministic model proposed by (Dorogovtsev and Mendes [2002]). In their model, they use pseudo-fractal networks (PN) to generate scale-free networks with strong link correlations. The pseudo-fractal network is considered a deterministic network because of its growing assumptions (Fig. 4.8). In this model, network properties depends exclusively on t, i.e., at each time step the number of agents grows according to $n = \frac{3(3^t+1)}{2}$, the number of links according to $\ell = 3^{t+1}$, and the average degree of agents results in $\bar{k} = 2\frac{\ell}{n} = \frac{4}{(1+3^{-t})}$.

However, our interest in this model is because of the distribution of local cohesiveness, that follows another power law distribution that depends on individual degree, such that $\tau_i = \frac{2}{k_i}$. The resulting average cohesiveness $\bar{\tau}$ in the network approximates a

constant value $\bar{\tau} = \frac{4}{5}$. Compared to BA networks this value is very high, for this reason we consider this model an effective manner to simulate the upper limit of average cohesiveness in scale-free networks.

Notice that (Klemm and Eguíluz [2002]) proposed an alternative model to reproduce scale-free networks with higher average cohesiveness, $\bar{\tau} = \frac{5}{6}$, however, pseudo-fractal networks are easier to model.

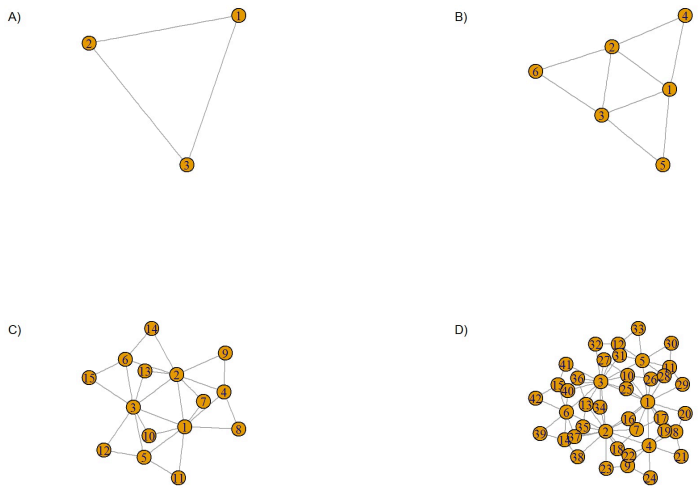

Fig. 4.8 The pseudofractal network.

Starting from a single link connecting two agents ($t = 1$), at each time step, every link in the network generates a new agent and the new agent connects to both of the end agents of the link. In the figure, we show the structure of the pseudo-fractal network at time $t = \{2, 3, 4, 5\}$ in where A) $t = 2$, B) $t = 3$, C) $t = 4$ and D) $t = 5$.

4. Random Networks

In random networks, and contrary to BA model, choices for interaction are independent of current network structure. This means all agents have similar probabilities to be selected by others and, thus, agents have comparable degree. While is very unlikely that social networks form like this, Random Networks (RN) can help us to understand interesting properties of social networks such as cohesiveness.

The Erdos-Renyi model (Erdős and Rényi [1960]) is the most popular model for generating random networks. In the simplest possible model, we start with all isolated agents, $|A| = n$, and add links between pairs of agents one at a time randomly. Hence,

for each of the ℓ possible links, $\ell = \frac{n(n-1)}{2}$, we flip a coin (biased) that comes up "success" (link connect two agents) with probability p. The random network can be defined as $N = (n, p)$. In order to compare average cohesiveness between power law and random networks, we use the same parameter m. For example, if we use $p = \frac{2m}{n}$, we obtain that average agent degree $\bar{k} = p(n-1) \approx 2m$ and density $d = \bar{k}n = 2mn$ are the same in both cases (power law and random networks). However, average cohesiveness in random networks is $\bar{\tau} = \frac{2m}{n}$. As we want to compare networks, m is bounded as before, $1 \leq m \leq \sqrt{n}$, and then the average cohesiveness for random networks falls into the range $\frac{2}{n} \leq \bar{\tau} \leq \frac{2}{\sqrt{n}}$. In most cases (when $n > 55$ and $m > 2$) we observe that scale-free networks are more cohesive than random networks. Note that random networks are characterized by homogeneous degree between agents,$k_{min} \approx k_{max}$, and homogeneous cohesiveness distribution, $\tau_{min} \approx \tau_{max}$.

5. Summary

To sum up, we represent an ordering sequence of average cohesiveness for the 4 types of networks:

$$\bar{\tau} : \{\bar{\tau}_{RN} < \bar{\tau}_{BA} < \bar{\tau}_{PN} < \bar{\tau}_{CN}\}, \tag{4.32}$$

where

$$\bar{\tau}_{RN} \in \left[\frac{2}{n}, \frac{2}{\sqrt{n}}\right), \quad \bar{\tau}_{BA} \in \left[0, \frac{(log\ n)^2}{8\sqrt{n}}\right), \quad \bar{\tau}_{PN} = \frac{4}{5}, \quad \bar{\tau}_{CN} = 1. \tag{4.33}$$

4.6.3 Appendix C: The mean-field approximation. Average local cohesiveness of compliers in any type of network

To calculate the average local cohesiveness of compliers in any network, $\bar{\tau}_c$,we need to find the probability p_i that a link connects two compliers in the neighborhood of any agent i. The size of i's neighborhood is measured by her degree, $|\mathcal{N}(i)| = k_i$. To find p_i we can imagine a box with k_i marbles. According to the share of compliers in $\mathcal{N}(i)$, $0 \leq c_i \leq 1$, we know that the box contains $|\mathcal{N}_c(i)| = c_i k_i$ marbles that are compliers (green marbles) and the rest are defectors (red marbles). Note that $\mathcal{N}_c(i)$ represents the subset of compliers in $\mathcal{N}(i)$, $\mathcal{N}_c(i) \subset \mathcal{N}(i)$, and then $|\mathcal{N}_c(i)| \leq |\mathcal{N}(i)|$. We want to find the probability of drawing two consecutive green marbles, which is:

$$p_i = \frac{\frac{(c_i k_i)!}{2!(c_i k_i - 2)!}}{\frac{k_i!}{2!(k_i-2)!}} = \frac{(c_i k_i)!(k_i - 2)!}{k_i!(c_i k_i - 2)!} = \frac{(c_i k_i)(c_i k_i - 1)}{k_i(k_i - 1)}, \tag{4.34}$$

and can be approximated by $p_i \approx c_i^2$. Let S represent the number of times that a link connects two compliers (success) in a given $\mathcal{N}(i)$. We argue that the variable follows the binomial distribution $X \sim Binomial(m, p)$ and $S = \mathbb{E}[X] = m_i p_i$, in where m_i represents the number of attempts in $\mathcal{N}(i)$. Note that m_i is bounded by the maximal number of links M_i in $\mathcal{N}(i)$, then $m_i \leq M_i = \frac{k_i(k_i-1)}{2}$. If we want to normalize S, $S \in [0, 1]$, we obtain that $S = \frac{m_i p_i}{M_i}$. When $m_i = M_i$, the $\mathcal{N}(i)$ is complete and $S \approx c_i^2$. It is important to remark that the ratio $\frac{m_i}{M_i}$ is nothing but cohesiveness of i, $\tau_i = \frac{m_i}{M_i}$.

As we are measuring the number of connections among compliers in a given neighborhood, S also represents the average local cohesiveness of compliers in $\mathcal{N}(i)$, such that $S = \bar{\tau}_{c_i} \approx \tau_i c_i^2$.

In any network, if compliers are distributed randomly (Fig. 4.10) through the network we obtain that $c_i \approx c, \forall i \in n$, where c represents the share of compliers in the whole network. In complete networks $c_i = c$ holds. Thus, the probability that one link connects two compliers is similar in all neighborhoods, such that $p \approx c^2$. At network level, the expected number of successes $S = \bar{\tau}_c$ is calculated as the average number of attempts, $\bar{\tau}$, multiplied by the probability of one success, p, such that

$$S = \bar{\tau}_c \approx \bar{\tau} c^2. \tag{4.35}$$

As we are reducing a multi-agent problem to a mean-agent problem, $c_i \approx c$ and $\bar{\tau}_c \approx \bar{\tau} c^2$ bring the notion of mean-field approximation.

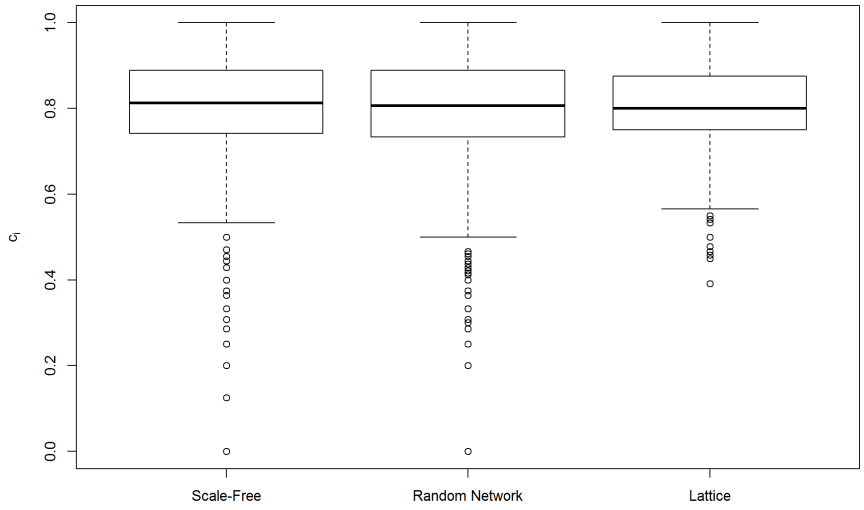

Fig. 4.9 Variability of the share of compliers in the neighborhoods of agents for different types of networks.

Once complete network structure is broken, the share of compliers c_i in the neighborhood of agents is not constant. This figure shows the values of c_i for every agent i in the network. Results are shown as boxplots after 1000 simulations. The results suggest that variability is higher in scale-free than random networks or lattices. This means the mean-field approximation will work better on lattices (and random networks) than on scale-free networks. However, boxplots show that most neighborhoods have comparable values of c_i. In particular, in scale-free networks $\bar{c} = \frac{1}{n}\sum_{i=1}^{n} c_i = 0.8 \pm 0.13$, and $c = 0.8$.

4.6.4 Appendix D: The mean-field approximation. Critical mass of compliers in mixed equilibrium when policy instruments are absent

In absence of policy eq. 4.15 can be reduced to the following expression:

$$\dot{c} = (\omega - 1)c(1 - c), \tag{4.36}$$

and eq. 4.16 gives us the new 3 equilibria points in the system and their stability:

$$\dot{c} = (\omega - 1)\bar{c}(1 - \bar{c}) \rightarrow \begin{cases} c = 0, & \text{stable} \\ \omega = 1, & \text{unstable} \\ c = 1, & \text{stable} \end{cases} \tag{4.37}$$

We want to compute the critical mass of compliers $\hat{c}$ needed to obtain $\bar{\omega} = 1$ for any type of network (from complete to random networks). Applying mean-field, the average social pressure in the equilibrium is

$$\omega = \frac{Ł}{1 + s_{max}e^{-s(c-(c_0-\bar{\tau}_c))}} = 1. \tag{4.38}$$

Reordering eq. 4.38, we have that

$$\frac{-ln\left(\frac{Ł-1}{s_{max}}\right)}{s} = c - c_0 + \bar{\tau}_c. \tag{4.39}$$

Parameter c_0 is constant, and we now know that $\bar{\tau}_c = \bar{\tau}c^2$ (Apprendix C); we use z as $z = \frac{-ln\left(\frac{Ł-1}{s_{max}}\right)}{s} + c_0$. Hence, eq. 4.39 can be expressed in its reduced form

$$z = c + \bar{\tau}c^2. \tag{4.40}$$

And this expression can be solved as follows

$$\hat{c} = \frac{-1 + \sqrt{1 + 4\bar{\tau}z}}{2\bar{\tau}}. \tag{4.41}$$

Note that we discard one of the possible solutions of eq. 4.40 because the share of compliers is always a positive number, then $0 \leq \hat{c} \leq 1$. We obtain this way the critical mass of compliers when $\omega = 1$ for any possible network configuration. The average cohesiveness, $0 \leq \bar{\tau} \leq 1$, is a well-known metric in the literature of networks and is easy to compute.

As a reference, we remark that $\bar{\tau} \approx 0$ in random networks and $\bar{\tau} = 1$ in complete networks. Scale-free networks are in between $0 \leq \bar{\tau} \leq \frac{4}{5}$. Thus, we can observe how the critical mass of compliers in the mixed equilibrium $\hat{c}$ decreases as a consequence of increasing the average cohesiveness of networks $\bar{\tau}$.

4.6.5 Appendix E: Local cohesiveness of compliers

In a network $N = (A, L)$ where A is the set of agents and L is the set of links, the transitivity or local cohesiveness coefficient τ_i measures how close the neighborhood $\mathcal{N}(i)$ of agent i is to a complete network. If agent i has k_i neighbors, there can be, at most, $\binom{k_i}{2} = \frac{k_i(k_i-1)}{2}$ links connecting agent i's neighbors. If we define a transitive relation in the neighborhood of i as $\forall i \in A$, $\forall u, v \in \mathcal{N}(i) : (uRi \wedge iRu) \Rightarrow uRv$, where $\mathcal{N}(i) = \{a_u : l_{iu} \in L \vee l_{ui} \in L\}$, the local cohesiveness can be quantified as

$$\tau_i = \frac{2\left|\{l_{uv} : a_u, a_v \in \mathcal{N}(i), l_{uv} \in L)\}\right|}{k_i(k_i - 1)}. \tag{4.42}$$

Local cohesiveness lies within the range $\tau_i \in [0, 1]$. Likewise, the local cohesiveness of compliers coefficient τ_{c_i} measures how close the set of compliers in agent i's neighborhood, $\mathcal{N}_C(i)$, is to a complete network. Its definition is given by

$$\tau_{c_i} = \frac{2\left|\{l_{uv} : a_u, a_v \in \mathcal{N}_C(i), l_{uv} \in L)\}\right|}{k_i(k_i - 1)}. \tag{4.43}$$

The upper value of local cohesiveness $\tau_{c_i}^{max}$ can be approximated by

$$\tau_{c_i}^{max} = \frac{c_i k_i(c_i k_i - 1)}{k_i(k_i - 1)} = \frac{c_i(c_i k_i - 1)}{(k_i - 1)} \approx \frac{c_i^2 k_i}{k_i} \approx c_i^2. \tag{4.44}$$

Note that $\tau_{c_i}^{max}$ is calculated when $\tau_i = 1$. Since for this measurement only the share of compliers in the neighborhood is needed, k_i does not need to be considered. In the other cases, when $\tau_i < 1$, we can estimate τ_{c_i} by $\tau_{c_i} \approx \tau_i c_i^2$ (see Appendix C).

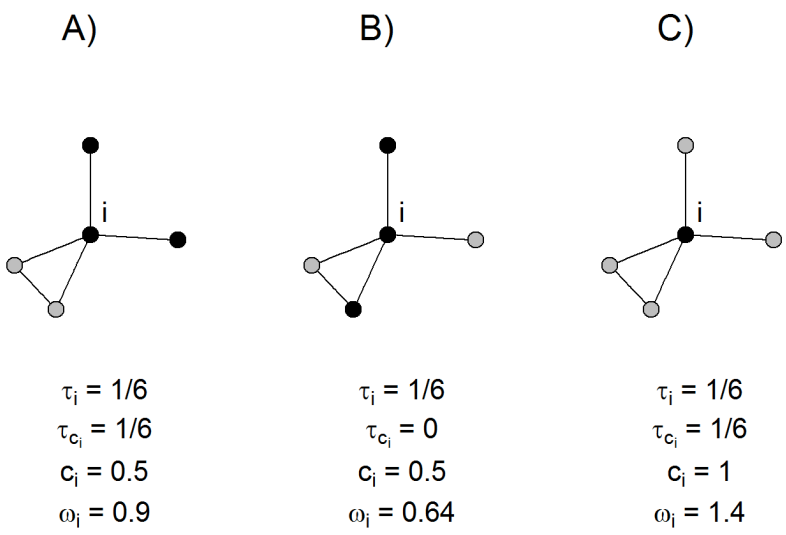

Fig. 4.10 Local cohesiveness of compliers and its influence in social pressure.

This figure represents three different scenarios (A,B,C) in agent i's neighborhood at a given stock (s), share of compliers (c_i) and local cohesiveness (τ_i). Local cohesiveness is, in all three cases, $\tau_i = \frac{1}{6}$ and the stock is $s = 30$ meters. Black dots represent agents who are defectors and gray dots represent agents who are compliers. In scenarios A and B, the share of compliers is equal, two defectors and two compliers, so $c_i = 0.5$, and differences in social pressure ω_i depend on the level of local cohesiveness of compliers τ_{c_i}. In scenario A the two compliers are connected so $\tau_{c_i} = \tau_i$, whereas in scenario B $\tau_{c_i} = 0$ because one defector and one complier are linked. The link between agents with different strategies do not contribute to increase local cohesiveness of compliers and, finally, social pressure. Thus, ω_i in scenario A ($\omega_i = 0.9$) is greater than in scenario B ($\omega_i = 0.64$). Scenario C represents the maximal social pressure ($\omega_i = 1.4$) for agent i at given stock and local cohesiveness levels because all i's neighbors are compliers, $c_i = 1$.

Chapter 5

Conclusions and future research

5.1 Main findings

Traditionally economists have studied the interaction between agents in a centralized and anonymous way where prices are the principal vehicle to coordinate individual actions. Agents are considered as being rational individuals, whose decisions are not influenced by the type and patterns of interaction with other individuals. While this approach seems legitimate for studying many social and economic phenomena it falls short of explaining the importance of personal contacts or the emergence of cooperativeness. In these situations, individual behavior cannot be considered independent of the choices made by other individuals, but rather influenced by the patterns of connections between individuals. This suggests that the structure of social interactions may be viewed as an instance of an informal institution that supplements regulatory institutions in the presence of imperfect or asymmetric information, or that provides a basis for social cohesiveness and incentives of complying with social norms. Based on these considerations social networks are gaining attention in natural resource management discussions. However, several gaps still exist in the literature. First, while existing studies have identified a number of network properties that are seemingly important for the sustainable management of natural resources, the way in which they are linked has been analyzed separately. This may be because traditional network generative models are limited in terms of realism. Hence, the joint effect of these properties on cooperation remains largely unknown. Secondly, the concrete role of stock dynamics in adherence to a social norm has not been thoroughly analyzed, yet stock dynamics is a fundamental element of management. Finally, although there is documented evidence that social pressure plays an important role in promoting cooperation, the monetary value of this intangible good has, as yet, not been studied.

Thus, this thesis aims to contribute to the existing literature by attempting to fill in the above mentioned gaps. This is done by modeling the evolution of a social norm in realistic social networks, and its co-evolution with a stock dynamic. Coupling social and resource dynamics allows us to determine the stability of cooperation within a community of agents who share property rights and have free access to the natural resource. The cooperating community places social pressure on defectors, which ultimately results in economic losses.

The main findings are specified below following the research questions described at the beginning of the thesis:

1. *To develop a new network generative model to simulate more realistic social networks.*

In Chapter 2 we investigate the influence the microscopic properties of networks (the fitness of agents) have on network formation. We propose that fitness is a combination of the multiple socioeconomic attributes of the agents that can be expressed as a single numerical value. According to competitive theories, agents compete for links and fitness represents the ability of agents to attract links. If the underlying fitness distribution within the population follows any heavy-tailed distribution, we have proved that social networks are scale-free. The proposed model allows us to generate an ordered sequence of realistic networks. Concretely, all generated networks are power law with increasing levels of link correlations (assortativity, modularity, transitivity). In contrast to traditional models, we argue that the degree of agents is the consequence of network dynamics rather than its driving force. The advantages of fitness-based network generative models are twofold. First, fitness allows multi-scaling networks to be generated. By increasing the asymmetry of the heavy-tailed fitness distribution, we decrease the scale of the power law degree distribution. As a consequence of asymmetry, the level of competition for links decreases in the population and therefore some agents tend to accumulate a greater number of links. However, modelers face a tradeoff between multi-scaling and computational performance. We have proved that the higher the level of competition is, the faster the algorithm is. Second, fitness also can shed light on homophilous behavior, or the tendency of agents to connect with similar agents. We introduce a new argument, link stability, to simulate the evolution of homophily in social networks. We argue that connections between agents are costly and costs are supposed to be lower between agents with similar fitness. Thus, connections between agents with similar fitness are more stable and should last longer. According to a cost-link minimization condition, we observe how the evolution of homophily within

the population increases the levels of link correlations in the social network.

2. *To propose a new theoretical framework that treats the integrated social-ecological system as the key unit for analyzing collective action.*

In Chapters 3 and 4 we investigate the role that network structure and stock dynamics play in the evolution of cooperation within a community of agents exploiting a natural resource. We use a social pressure function to capture both network and stock effects. Previous studies (Chung et al. [2014]; Tavoni et al. [2012]) have analyzed similar models of coupled social and resource dynamics, however, results are based on either complete or simpler social networks (i.e., local cohesiveness of compliers is not taken into account).

Contrary to what these previous studies observe, our results in Chapter 3 suggest there is always a certain (small) number of agents that receive no or very little social pressure. In other words, these agents always become defectors. To understand this result better, we use Fig. 2.4 and Fig 2.6 in Chapter 2. In Fig. 2.4 we observe hierarchical clustering in social networks, where the neighborhoods of the hubs are less cohesive than the rest of the neighborhoods. In Fig. 2.6 we observe that assortativity values are largely controlled by connections between hubs. This means hubs receive very little pressure and they are interconnected. In the literature on social networks, the interconnectivity of hubs is often described as the "rich-club phenomenon". Because of this rich-club phenomenon, if all hubs defect to the norm, they can survive even when the rest of agents within the community are compliers. The observation that hubs can survive is analogous to a finding in the non-cooperative game literature where (Bramoullé [2007]) observed that agents have an incentive to anti-coordinate if they are embedded in a bipartite network. Additionally, anticoordination is also observed in isolated agents or groups. Agents or groups that are poorly connected to the rest of the social network tend to receive very little social pressure and, consequently, they can survive even in high levels of cooperation.

In Chapter 4, we show that predictions based on well-mixed population assumptions are optimistic. Social networks are not complete networks and therefore the critical mass of compliers in the mixed equilibrium is always higher than that expected in complete networks. However, scale-free networks allow for a wide range of possible topologies. By varying these topologies, we can approach complete cohesiveness, but even in the best case (pseudo-fractal networks) we are still 20% below complete cohesiveness.

3. *To identify and rank the driving factors behind disposition to comply with a social norm.*

Many authors have highlighted the importance the share of compliers (Osés-Eraso and Viladrich-Grau [2007]; Sethi and Somanathan [1996]; Tavoni et al. [2012]) has for the socially efficient management of a resource. However, the share of compliers is independent of the size and the structure of the social network. In Chapter 3 we show that the share of compliers alone is an inaccurate indicator of cooperativeness and to be interpreted needs to be accompanied by other characteristics of social pressure such as the local cohesiveness of the compliers or the state of the natural resource.

We also show that density (the number of total links in the network) does not necessarily favor compliance with the social norm. There is a large anumber of redundant links that do not contribute to higher social pressure. The reason is that the level of local cohesiveness of compliers in a given neighborhood depends on the share of compliers in this neighborhood. We can calculate the lower and upper limits of local cohesiveness of compliers for any neighborhood and thus the maximal number of links needed to increase social pressure. Notice that only links connecting two compliers are efficient, in other words, contribute to higher social pressure. The fact that links are redundant sheds new light on the findings in the previous literature (Coleman [1988]; Karlan et al. [2009]), where an increase in density favors compliance to the social norm. We show that an increase in links only favors such compliance up to the point where density is equal to the upper limit of the local cohesiveness of compliers. Beyond this limit density does not contribute to higher social pressure. The conclusion is that density of a social network is an imprecise indicator for cooperativeness because it considers not only the links that help to increase social pressure but also redundant links.

In terms of the the size (the number of total agents in the network), in Chapter 4 (Appendix B) we have shown that, in the absence of homophily, the average local cohesiveness decreases with the size of the social network. Thus, given the same share of compliers in small and large networks, we obtain that small networks tend to comply to the norm more than the larger networks do. Our results support the widespread hypothesis (Ostrom et al. [1999]) that a small community can exercise more social pressure than a large community can.

In Chapters 3 and 4, we model social pressure as a sigmoidal function where compliers adapt the pressure they exert to defectors according to the remaining stock.

When the natural resource is fully available for agents social pressure is practically unnoticed, even with high levels of cooperativeness within the community. In this situation, agents are likely to defect.

According to our analysis, we propose to study both network and stock effects holistically and not separately. As we have seen, single properties of networks, taken separately, are imprecise indicators for predicting cooperativeness.

4. *To determine resource management strategies to encourage cooperation (community approach) and policies to improve the conservation of natural resources (policy approach).*

In Chapter 3, we determine the magnitude of error of a traditional "first-best" tax compared to a tax that takes into account social interactions and social pressure. Our results suggest that when shortsighted behavior is the origin of the tragedy of the commons problem, it is also the starting point for a solution in the form of a one-time payment. Two types of agents, defectors and compliers, interact within the social network. Defectors maximize their short-term benefits. On the other hand, agents complying with a social norm that prescribes conformity to an agreed extraction level are able to place social pressure on the defectors. Social pressure eventually produces economic losses to defectors. The difference between the defector's extra benefits and the economic losses from social pressure determines the amount required for the one-time payment. As agents update their strategies according to utility differences, once defectors have changed their strategy, the increased number of compliers hampers them from reverting.

In Chapter 4, we have identified policy corridors for the real determination of policy options. We find large regions where traditional policy instruments and network-orientated policies can be applied indistinctly or in combination. A significant characteristic of common property resources is that the community lacks the legal power to enforce social norms; however, social pressure is the driving force for cooperation. In the case that social pressure cannot maintain adherence to the social norm, the community may decide to employ regulatory instruments, i.e., taxes or subsidies. Our results show that when the share of compliers is sufficiently high within the community, social pressure leads to full cooperation. On the contrary, when the share of compliers is very low or the stock is fully available for agents, agents are likely to defect. Nevertheless, we find a large intermediate region where the joint effects of network structure, stock dynamics and the share of compliers are of fundamental importance for predicting

cooperativeness. In the intermediate region both types of policies coexist. Where the social-ecological system ultimately converges depends on the policy decisions adopted.

5. *To valuate in monetary terms social pressure under variable social and environmental conditions.*

In Chapters 3 and 4, we provide a monetary valuation of an intangible good: social pressure. An extended analysis is provided in Chapter 3 using the case of the western La Mancha Aquifer in Spain. We refer to the economic losses compliers inflict on the defectors as social punishment. Social punishment allows us to determine to what extent network effects and stock dynamics contribute to overcoming the tragedy of the commons. For the sake of simplicity and to stress that defector's utility is directly affected by social pressure, we assume that social punishment is linearly related to the difference between the net benefits of the defector and the complier. Since the extra benefits present the loss defectors inflict on compliers, any social punishment can be viewed as redemption for the privation suffered by the compliers. However, social punishment is not independent of social interaction among the agents and, therefore, we assume that the loss defectors inflict on the compliers is attenuated or aggravated by the strength of social pressure. Concretely, the social pressure produced and the extra benefits the defector gains as a result of incompliance define the social punishment imposed.

We analyze the marginal economic value of social punishment. Results show that an increase in the share of compliers or local cohesiveness of compliers will unambiguously increase the economic value of social punishment, whereas an increment in stock will lead to an increase or decrease in the economic value of social punishment.

This result is counterintuitive given that social pressure increases with a decrease in the remaining stock. However, the lower the stock is, the higher the extraction costs for both strategies are. Thus, the difference between the extraction profiles and the corresponding net benefits decreases. Hence, if stock-dependent extraction costs are not dominant for the overall net benefits, social pusnihment decreases with an increase in stock. Otherwise, if stock-dependent extraction costs are dominant, social punishment will increase with an increase in the stock.

5.2 Implications of the research

Our research has established that network-orientated policies may help to overcome the tragedy of the commons. A local common is a single but abundant local natural resource exploited by a large community of economic agents. To moderate or avoid depletion, the agents in the community need to reach a common understanding of the characteristics a sustainable extraction path will have. If there is a social norm prescribing conformity to an agreed extraction path, the social norm allows the resource use behavior to be defined. Concretely, social pressure is an informal mechanism to establish and maintain cooperative behavior required to exploit the natural resource in question. At the community level, the strength of the local cohesiveness of the compliers, the size of the community, the state of the natural resource, and the share of compliers allow the size of the region where network-orientated policies can be best applied to be mapped out.

We have shown large regions where traditional policies and network-orientated policies can be applied indistinctly or in combination. However, network-orientated policies may be more efficient that traditional policies when agents perceive taxes or subsidies as disproportionate or meaningless (Bicchieri and Muldoon [2014]). Traditional policies are focused on direct intervention in the form of initiatives that reduce or increase the net benefits of a given resource behavior. However, network-orientated policies are based on indirect intervention in the form of initiatives that increase social pressure, i.e., seminars or workshops.

Our results suggest that the presence or introduction of policy instruments lead to a relocation of policy corridors. We observe that the region where network-orientated policies are applicable increases with the introduction of policy instruments. In this situation, network-orientated policies play an important role in policy design since (i) they induce mixed equilibrium to be stable, and (ii) the stationary point in the mixed equilibrium is located within the region of applicability of the network-orientated policies.

Finally, how best to design network-orientated policies to promote cooperation within a community remains an interesting topic for future research. We can derive from our results that (i) agents who have a large quantity of links (hubs) receive less social pressure than the rest of agents in the social network, (ii) agents who have a small quantity of links (low-degree agents) contribute more to the average local cohesiveness of social networks, (iii) links connecting agents with similar socioeconomic attributes seems to be more stable and should last longer, and (iv) links between agents

complying with the social norm are efficient (increase social pressure), whereas other links are redundant (do not increase social pressure).

5.3 Limitations of this research and directions for future research

The results of this research have enabled us to discern general implications about the role social networks play in natural resource management. Nevertheless, we acknowledge that there are some limitations in the research and suggest how these could be addressed in the future:

1.*Social pressure functions.*

In this work, we have studied the effectiveness social pressure has on natural resource overuse by promoting sustainable extraction paths. In line with previous research (Chung et al. [2014]; Lindbeck [1997]; Tavoni et al. [2012]), we have modeled social pressure as sigmoidal functions. In Chapter 3, we use the Gompertz function, which is an asymmetric sigmoidal function with two growth rates, while in Chapter 4, we use the logistic function; which is a symmetric sigmoidal function with a tunable inflection point. In both cases, we have assumed that social pressure is a non-negative, bounded function that increases along with the number of agents complying with the social norm. Different parameters allow us to capture the tangible effects network structure and stock dynamics have on the disposition to comply with the norm. However, these functions have not yet been calibrated in laboratory experiments. Thus, our results are theoretical results and they must be contrasted with laboratory experiments and/or field research. As we have seen, these functions are complex to deal with. Given the specifications of our models, the regimes of the stationary state of the evolutionary dynamics are difficult to determine analytically. Nevertheless, other techniques allow equilibrium conditions to be reached. In Chapter 3 we use numerical analysis, whereas in Chapter 4 we use mean-field analysis. To validate our assumptions about social pressure, experimental research would be helpful, i.e., the estimation of the parameters of the social pressure function.

2.*Structural elements of the social network.*

In looking towards future research in the area of social networks and natural re-

source management there is much to be done. In Chapter 2, we focus on the limitations of traditional network generative models, suggesting that social networks may have features that cannot be captured by traditional approaches of network formation. In Newman's words (Newman [2003b]), "We have as yet no theoretical framework to tell us if we are looking in the right place. A true understanding of which properties of networks are the important ones to focus on will almost certainly require to state first what questions we are interested in answering about a particular network".

To our knowledge, the metric "local cohesiveness of compliers" has not been considered before in the related literature. We argue that this property is an important factor in the willingness to comply with a social norm, and therefore it can be used to design network-orientated policies, i.e, initiatives designed to create new links among compliers. However, economics of networks has, as yet, not drawn any clear conclusion about link stability, especially if new links are created externally through network-orientated policies. A correct understanding of link formation and link stability in real-world networks is a challenge for further research.

3. *Trust networks and cooperative games.*

Based on their extensive field-work, (Ostrom [1990]; Ostrom et al. [1999]) developed a list of eight design principles for natural resource management to function well. Many of them, (e.g., communication, monitoring and social sanctions), depend on the underlying structure of social interactions. In recent years (Berkes et al. [2003]; Jentoft [2000]; McCarthy [2000]; Olsson et al. [2004]; Wondolleck et al. [2002]) the list has been extended. For example, (Olsson et al. [2004]) argues that resilience of social-ecological systems is facilitated by trust among agents.

One of the most important features in a social network is the ability of agents to share opinions, information or experiences. However, the success of such attempts relies on the level of trust that agents have with each other. In a social network, the level of trust can be measured by the nature and quantity of interactions among its agents. The "nature of interactions" refers to individual confidence (homophily) between pairs of linked agents, while the "quantity of interactions" refers to direct and indirect interaction through the network. Direct interaction defines the collective confidence associated with the group, and can be measured by density or local cohesiveness. Indirect interaction, on the other hand, can modify collective confidence, i.e., community membership (measured by modularity) or a chain of referrals (measured by betweeness centrality). Trust networks are often represented as directed networks.

Interestingly, trust has been identified as an important factor that influences cooperation in social dilemmas (Yamagishi [1988]), in other words, trust acts like a lubricant for social pressure (Parks et al. [2013]). Further research could combine our framework with trust networks. Again, fitness of agents can be used to define the properties of trust networks such as social influence and reputation.

Furthermore, cooperative games played on networks is an interesting line for future research. Network properties (modularity, local cohesiveness) and multi-layer networks may help to define alliances (coalitions) between groups of agents.

4.*Governance of global commons: triggering scaling up.*

The management of local natural resources takes place within a national jurisdiction of a particular state designed to serve the needs of the communities. The physical and technical properties of local commons produce very high institutional costs. These costs mainly consist of high exclusion costs, which mean that complete privatisation of rights is economically inefficient and consequently, in situations of this kind, common property rights are more efficient than individual rights. However, other natural resources are beyond the limits of a single national jurisdiction. For example, forests and rivers shared by two or more states. Furthermore, the atmosphere cannot be privatized nor it can be expropriated by any state.

In economics, supranational and international natural resources are considered global commons (table 5.1). Large-scale natural resources are subject to an open access regime and protecting them is extremely costly. In these cases, solutions to problems like climate change rely on voluntary cooperation between the various classes of appropriators.

Table 5.1 Differences between local and global commons.

Characteristics	Local commons	Global commons
Geographic scale	Regional	International
Number of resource users	Thousands, Tens to thousands	Millions to billions
Salience: users' awareness of degradation	Resource use is conscious purpose	Actions causing degradation are of low importance for most users
Property rights	Common property	Open access
Distribution of interests and power	Benefits and costs mainly internal to group of appropriators	Differences of interest and power among classes of appropriators
Cultural and institutional homogeneity	Homogeneous	Heterogenous
Feasibility of learning	Good	Limited
Regenerating of degrading resource	Renewable over less than a human generation	Regeneration over more than a human generation
Ease of understanding resource dynamics	Reasible without extensive scientific training	Scientifically complex with limited predictive ability
Stability of resource dynamics	Stable, though variable	Dynamic systems with changing rules
Ability to learn accross places	Possible	Difficult
Examples	Coastal fisheries, forests, aquifers	Atmosphere, polar regions, trans-boundary forests

A promising line of research is to systematically analyze human cooperation from a local to global scale, and determine the differences between those scales. To date,

the literature has focused on local and regional cooperation problems but the findings cannot be directly transferred to the international level (Nyborg et al. [2016]).

Bibliography

Acemoglu, D.; Dahleh, M. A.; Lobel, I., and Ozdaglar, A. Bayesian learning in social networks. *The Review of Economic Studies*, 2011.

Adamic, L. A. and Huberman, B. A. Power-law distribution of the world wide web. *Science*, 287:2115, 2000.

Alexander, R. *The Biology of Moral Systems*. de Gruyter, A., 1987.

Ali, S. N. and Miller, D. A. Ostracism and forgiveness. *American Economic Review*, 106(8):2329–48, August 2016.

Amaral, L.; Scala, A.; Barthelemy, M., and Stanley, H. Classes of small-world networks. *P Natl Acad Sci USA*, 97(21):11149–52, 2000.

Axelrod, R. and Hamilton, W. D. The evolution of cooperation. *Science*, 211(4489): 1390–1396, 1981. ISSN 0036-8075.

Ballester, C.; Calvó-Armengol, A., and Zenou, Y. Who's who in networks. wanted: The key player. *Econometrica*, 74:1403–1417, 2006.

Barábasi, A. L. and Albert, R. Emergence of scaling in random networks. *Science*, 286:509–512, 1999.

Berkes, F.; Colding, J., and Folke, C. *Navigating Social-Ecological Systems: Building Resilience for Complexity and Change*. Cambridge University Press, Cambridge, 2003.

Bianconi, G. and Barabási, A. L. Bose-einstein condensation in complex networks. *Phys. Rev. Lett.*, 86:5632–5635, Jun 2001.

Bianconi, G. and Barabási, A. L. Competition and multiscaling in evolving networks. *EPL (Europhysics Letters)*, 54(4):436, 2001.

Bicchieri, C. and Muldoon, R. Social norms. In Zalta, Edward N., editor, *The Stanford Encyclopedia of Philosophy*. Metaphysics Research Lab, Stanford University, spring 2014 edition, 2014.

Bodin, O. and Crona, B. I. The role of social networks in natural resource governance: What relational patterns make a difference? *Global Environmental Change*, 19(3): 366 – 374, 2009. ISSN 0959-3780.

Bowles, S. *Bowles, S.: Microeconomics: Behavior, Institutions, and Evolution.* 2004.

Bramoullé, Y. Anti-coordination and social interactions. *Games and Economic Behavior*, 58(1):30 – 49, 2007. ISSN 0899-8256.

Bramoullé, Y.; Currarini, S.; Jackson, M. O.; Pin, P., and Rogers, B. W. Homophily and long-run integration in social networks. *Journal of Economic Theory*, 147(5): 1754 – 1786, 2012. ISSN 0022-0531.

Bramoullé, Y.; Kranton, R., and D'Amours, M. Strategic interaction and networks. *American Economic Review*, 104(3):898–930, March 2014.

Bramoullé, Y.; Galeotti, A., and Rogers, B. W. *The Oxford handbook of the economics of networks*. New York : Oxford University Press, Oxford handbooks, 2016a.

Bramoullé, Y.; Galeotti, A., and Rogers, B. W. *The past and the future of neteor analyisis in economics. The Oxford handbook of the economics of networks*. New York : Oxford University Press, Oxford handbooks, 2016b.

Caldarelli, G.; Capocci, A.; De Los Rios, P., and Muñoz, M. A. Scale-free networks from varying vertex intrinsic fitness. *Phys. Rev. Lett.*, 89:258702, Dec 2002.

Catanzaro, M.; Caldarelli, G., and Pietronero, L. Assortative model for social networks. *Phys. Rev. E*, 70:037101, Sep 2004.

Chung, N. N.; Chew, L. Y., and Lai, C. H. Influence of community structure on cooperative dynamics in coupled socio-ecological systems. *Acta Physica Polonica B Proceedings Supplement*, 7, 2014.

Clauset, A.; Shalizi, C. R., and Newman, M. E. Power-law distributions in empirical data. *SIAM review*, 51 (4):661–703, 2009.

Cohen, R. and Havlin, S. Scale-free networks are ultrasmall. *Phys. Rev. Lett.*, 90: 058701, Feb 2003.

Coleman, J. S. Social capital in the creation of human capital. *American Journal of Sociology*, 94:S95–S120, 1988. ISSN 00029602, 15375390.

Currarini, S.; Marchiori, C., and Tavoni, A. Network economics and the environment: Insights and perspectives. *Environmental and Resource Economics*, 65(1):159–189, 2016. ISSN 1573-1502.

Dorogovtsev, S. and Mendes, J. Evolution of networks. *Advances in Physics*, 51: 1079–1187, 2002.

Dorogovtsev, S. N.; Goltsev, A. V., and Mendes, J. F. F. Pseudofractal scale-free web. *Phys. Rev. E*, 65:066122, Jun 2002.

Duernecker, G. and Vega-Redondo, F. Social networks and the process of globalization. *The Review of Economic Studies*, page rdx054, 2017.

Encarna, E. and Albiac, J. Groundwater and ecosystems damages: Questioning the gisser–sánchez effect. *Ecological Economics*, 70(11):2062 – 2069, 2011. ISSN 0921-8009. Special Section - Earth System Governance: Accountability and Legitimacy.

Erdős, P. and Rényi, A. On the evolution of random graphs. In *Publication of the mathematical Institute of the Hungarian Academy of Sciences*, pages 17–61, 1960.

Esteban, E. and Albiac, J. The problem of sustainable groundwater management: the case of la mancha aquifers, spain. *Hydrogeology Journal*, 20(5):851–863, 2012. ISSN 1431-2174.

Faloutros, M.; Faloutros, P., and Faloutros, C. On power-law relationship of the internet topology. *ACC SIGCOM 99, Comp. Comm. Rev.*, 29:251–260, 1999.

Farkas, I.; Derényi, I.; Palla, G., and Vicsek, T. *Equilibrium Statistical Mechanicsof Network Structures*, pages 163–187. Springer Berlin Heidelberg, Berlin, Heidelberg, 2004. ISBN 978-3-540-44485-5.

Feld, S. L. The focused organization of social ties. *American Journal of Sociology*, 86 (5):1015–1035, 1981. ISSN 00029602, 15375390.

Foster, D. V.; Foster, J. G.; Grassberger, P., and Paczuski, M. Clustering drives assortativity and community structure in ensembles of networks. *Phys. Rev. E*, 84: 066117, Dec 2011.

Gaechter, S. and Fehr, E. Altruistic punishment in humans. 01 1997.

Gale, D. and Kariv, S. Bayesian learning in social networks. *Games and Economic Behavior*, 45(2):329–346, 2003. URL https://EconPapers.repec.org/RePEc:eee:gamebe:v:45:y:2003:i:2:p:329-346.

Galeotti, A. and Rogers, B. W. Strategic immunization and group structure. *American Economic Journal: Microeconomics*, 5(2):1–32, 2013. ISSN 19457669, 19457685.

Goyal, S. *Connections: An Introduction to the Economics of Networks*. Princeton University Press, stu - student edition edition, 2007. ISBN 9780691141183.

Greaker, M. and Midttømme, K. Network effects and environmental externalities: Do clean technologies suffer from excess inertia? *Journal of Public Economics*, 143:27 – 38, 2016. ISSN 0047-2727.

Gutiérrez, I. B.; Ortega, C. V., and Flichman, G. Cost-effectiveness of groundwater conservation measures: A multi-level analysis with policy implications. *Agricultural Water Management*, 98(4):639–652, February 2011.

Guéant, O.; Lasry, J. M., and Lions, P. L. *Mean Field Games and Applications*. Paris-Princeton Lectures on Mathematical Finance 2010. Lecture Notes in Mathematics, vol 2003., Springer, Berlin, Heidelberg, 2011.

Haag, M. and Lagunoff, R. Social norms, local interaction, and neighborhood planning*. *International Economic Review*, 47(1):265–296, 2006. ISSN 1468-2354.

Hamm, V. J. Do birds of a feather flock together? the variable bases for african american, asian american, and european american adolescents' selection of similar friends. 36:209–19, 04 2000.

Hanaki, N.; Peterhansl, A.; Dodds, P. S., and Watts, D. J. Cooperation in evolving social networks. *Management Science*, 53(7):1036–1050, 2007.

Hardin, G. The tragedy of the commons. *Science*, 162(3859):1243–1248, 1968. ISSN 0036-8075.

Hauert, C.; De Monte, S.; Hofbauer, J., and Sigmund, K. Volunteering as red queen mechanism for cooperation in public goods games. *Science*, 296(5570):1129–1132, 2002. ISSN 0036-8075.

Holling, C. S. *Adaptive environmental assessment and management / edited by C. S. Holling ; sponsored by the United Nations Environmental Program.* International Institute for Applied Systems Analysis ; Wiley [Laxenburg, Austria] : Chichester ; New York, 1978. ISBN 0471996327.

Holme, P. and Kim, B. J. Growing scale-free networks with tunable clustering. *Phys. Rev. E*, 65:026107, Jan 2002.

Hyvonen, J.; Saramaki, J., and Kaski, K. Efficient data structures for sparse network representation. *Int. J. Comput. Math*, 85:1219–1233, 2008.

Jackson, M. O. *Social and Economic Networks.* Princeton University Press, Princeton, NJ, USA, 2008. ISBN 0691134405, 9780691134406.

Jackson, M. O.; Rodriguez-Barraquer, T., and Tan, X. Social capital and social quilts: Network patterns of favor exchange. *American Economic Review*, 102(5):1857–97, May 2012.

Jackson, M. O.; Rogers, B. W., and Zenou, Y. The economic consequences of social-network structure. *Journal of Economic Literature*, 55(1):49–95, March 2017.

Jentoft, S. Co-managing the coastal zone: Is the task too complex? 43:527–535, 01 2000.

Jeong, H.; Tombor, B.; Albert, R.; Oltvai, N., and Barábasi, A. L. The large-scale organization of metabolic networks. *Nature*, 407:651–654, 2000.

Jin, E. M.; Girvan, M., and Newman, M. E. J. Structure of growing social networks. *Phys. Rev. E*, 64:046132, Sep 2001.

Jovanovic, B. and Rosenthal, R. W. Anonymous sequential games. *Journal of Mathematical Economics*, 17(1):77 – 87, 1988. ISSN 0304-4068.

Karlan, D.; Mobius, M.; Rosenblat, T., and Szeidl, A. Trust and social collateral*. *The Quarterly Journal of Economics*, 124(3):1307–1361, 2009.

Klemm, K. and Eguíluz, V. M. Growing scale-free networks with small-world behavior. *Phys. Rev. E*, 65:057102, May 2002.

Kossinets, G. and Watts, D. J. Origins of homophily in an evolving social network. *American Journal of Sociology*, 115:405–450, 2009.

Krapivsky, P. L. and Redner, S. Organization of growing random networks. *Phys. Rev. E*, 63:066123, May 2001.

Lamberson, PJ. Social learning in social networks. *MIT Sloan Research Paper No. 4763-09*, 2009a.

Lamberson, PJ. Linking network structure and diffusion through stochastic dominance. 09 2009b.

Lancichinetti, A.; Fortunato, S., and Radicchi, F. Benchmark graphs for testing community detection algorithms. *Phys. Rev. E*, 78:046110, Oct 2008.

Leenders, R. T. A. Evolution of friendship and best friendship choices. *The Journal of Mathematical Sociology*, 21(1-2):133–148, 1996.

Liljeros, F.; Edling, C.R.; Amaral, L. A. N.; Stanley, H. E., and Aberg, Y. The web of human sexual contacts. *Nature*, 411:907–908, 2001.

Lindbeck, A. Incentives and social norms in household behavior. Seminar Papers 622, Stockholm University, Institute for International Economic Studies, 1997.

Lipowski, A. and Lipowska, D. Roulette-wheel selection via stochastic acceptance. *Physica A: Statistical Mechanics and its Applications*, 391(6):2193 – 2196, 2012. ISSN 0378-4371.

Liu, A.; Wang, L.; Zhang, Y., and Sun, C. Coevolution of cooperation and complex networks via indirect reciprocity. In Liu, Derong; Xie, Shengli; Li, Yuanqing; Zhao, Dongbin, and El-Alfy, El-Sayed M., editors, *Neural Information Processing*, pages 919–926, Cham, 2017. Springer International Publishing. ISBN 978-3-319-70139-4.

López-Pintado, D. Diffusion in complex social networks. *Games and Economic Behavior*, 62(2):573 – 590, 2008. ISSN 0899-8256.

Martínez-Santos, P.; De Stefano, L.; Llamas, M. R., and Martínez-Alfaro, P. E. Wetland restoration in the mancha occidental aquifer, spain: A critical perspective on water, agricultural, and environmental policies. *Restoration Ecology*, 16(3):511–521, 2008. ISSN 1526-100X.

May, R. Simple mathematical models with very complicated dynamics. 26:457, 07 1976.

McCarthy, N. Linking social and ecological systems: Management practices and social mechanisms for building resilience: Fikret berkes, carl folke, johan colding (eds.), cambridge university press, cambridge, 1998, 459 pp, isbn 0-521-59140-6. *Agricultural Economics*, 24(2):230–233, 2000.

McPherson, M.; Smith-Lovin, L., and Cook, J. M. Birds of a feather: Homophily in social networks. *Annual Review of Sociology*, 27(1):415–444, 2001.

Muchnik, L.; Pei, S.; Parra, L. C.; Reis, S. D.; Andrade, J. S.; Havlin, S., and Makse, H. A. Origins of power-law degree distribution in the heterogeneity of human activity in social networks. *Nature scientific reports*, 3, 2013.

Muse, B. Pinkerton, evelyn, ed. co-operative management of local fisheries: New directions for improved management, community development. vancouver: University of british columbia press, 1989. *American Journal of Agricultural Economics*, 72(4): 1101–1102, 1990.

Newman, M. The structure and functions of complex networks. *SIAM Review*, 45: 167–256, 2003a.

Newman, M.; Moore, C., and Watts, D. Mean-field solution of the small-world network model. 04 2000.

Newman, M. E. J. Assortative mixing in networks. *Phys. Rev. Lett.*, 89(20):208701, 2002.

Newman, M. E. J. Mixing patterns in networks. *Phys. Rev. E*, 67(2):026126, 2003b.

Newman, M. E. J. Modularity and community structure in networks. *Proceedings of the National Academy of Sciences*, 103(23):8577–8582, 2006.

Newman, M. E. J. and Girvan, M. Finding and evaluating community structure in networks. *Physical Review*, E 69(026113), 2004.

Nguyen, K. and Tran, D. A. *Fitness-Based Generative Models for Power-Law Networks*, pages 39–53. Springer US, Boston, MA, 2012. ISBN 978-1-4614-0754-6.

Nowak, M. and Sigmund, K. Evolution of indirect reciprocity by image scoring. 393: 573–7, 07 1998.

Nowak, M. A. and May, R. M. Evolutionary games and spatial chaos. *Nature*, 359:826, 1992.

Nyborg, K.; Anderies, J. M.; Dannenberg, A.; Lindahl, T.; Schill, C.; Schlüter, M.; Adger, W. N.; Arrow, K. J.; Barrett, S.; Carpenter, S.; Chapin, F. S.; Crépin, A. S.; Daily, G.; Ehrlich, P.; Folke, C.; Jager, W.; Kautsky, N.; Levin, S. A.; Madsen, O. J.; Polasky, S.; Scheffer, M.; Walker, B.; Weber, E. U.; Wilen, J.; Xepapadeas, A., and de Zeeuw, A. Social norms as solutions. *Science*, 354(6308):42–43, 2016. ISSN 0036-8075.

Olsson, P.; Folke, C., and Berkes, F. Adaptive comanagement for building resilience in social–ecological systems. *Environmental Management*, 34(1):75–90, Jul 2004. ISSN 1432-1009.

Orman, K.; Labatut, V., and Cherifi, H. *An Empirical Study of the Relation between Community Structure and Transitivity*, pages 99–110. Springer Berlin Heidelberg, Berlin, Heidelberg, 2013. ISBN 978-3-642-30287-9.

Ortega, C. V.; Gutiérrez, I. B.; Swartz, C. H., and Downing, T. E. Balancing groundwater conservation and rural livelihoods under water and climate uncertainties: An integrated hydro-economic modeling framework. *Global Environmental Change*, 21(2):604 – 619, 2011. ISSN 0959-3780. Special Issue on The Politics and Policy of Carbon Capture and Storage.

Ostrom, E. *Governing the commons. The evolution of institutions for collective actions*. Political economy of institutions and decisions, 1990.

Ostrom, E.; Burger, J.; Field, C. B.; Norgaard, R. B., and Policansky, D. Revisiting the commons: Local lessons, global challenges. *Science*, 284(5412):278–282, 1999. ISSN 0036-8075.

Osés-Eraso, N. and Viladrich-Grau, M. On the sustainability of common property resources. *Journal of Environmental Economics and Management*, 53(3):393 – 410, 2007. ISSN 0095-0696.

Parks, C. D.; Joireman, J., and Van Lange, P. A. Cooperation, trust, and antagonism: How public goods are promoted. *Psychological Science in the Public Interest*, 14(3): 119–165, 2013.

Pastor-Satorras, R. and Vespignani, A. Epidemic dynamics and endemic states in complex networks. *Phys. Rev. E*, 63:066117, May 2001.

Perman, R. J.; Ma, Y.; Common, M.; Maddison, D., and McGilvray, J. W. *Natural resource and environmental economics*. 4th edition, 7 2011. ISBN 9780321417534.

Price, D. S. A general theory of bibliometric and other cumulative advantage processes. *Journal of the American Society for Information Science*, 27(5):292–306, 1976. ISSN 1097-4571.

Ravasz, E. and Barabási, A. L. Hierarchical organization in complex networks. *Phys. Rev. E*, 67:026112, Feb 2003.

Ravasz, E.; Somera, A. L.; Mongru, D. A.; Oltvai, Z. N., and Barabási, A. L. Hierarchical organization of modularity in metabolic networks. *Science*, 297(5586):1551–1555, 2002. ISSN 0036-8075.

Redner, S. How popular is your paper? an empirical study of the citation distribution. *Eur. Phys. J. B*, 4(2):131–134, 1998.

Réka, A. and Barabási, A. L. Statistical mechanics of complex networks. *Rev. Mod. Phys.*, 74:47–97, Jan 2002.

Santos, F. C. and Pacheco, J. M. Scale-free networks provide a unifying framework for the emergence of cooperation. *Phys. Rev. Lett.*, 95:098104, Aug 2005.

Santos, F. C.; Pacheco, J. M., and Lenaerts, T. Evolutionary dynamics of social dilemmas in structured heterogeneous populations. *Proceedings of the National Academy of Sciences of the United States of America*, 103(9):3490–3494, 2006.

Santos, F. C.; Pinheiro, F. L.; Lenaerts, T., and Pacheco, J. M. The role of diversity in the evolution of cooperation. *Journal of Theoretical Biology*, 299:88 – 96, 2012. ISSN 0022-5193. Evolution of Cooperation.

Schomers, S. and Matzdorf, B. Payments for ecosystem services: A review and comparison of developing and industrialized countries. *Ecosystem Services*, 6:16 – 30, 2013. ISSN 2212-0416. Payments for Ecosystem Services and Their Institutional Dimensions: Analyzing the Diversity of Existing PES Approaches in Developing and Industrialized Countries.

Sendiña-Nadal, I.; Danziger, M. M.; Wang, Z.; Havlin, S., and Boccaletti, S. Assortativity and leadership emerge from anti-preferential attachment in heterogeneous networks. *Scientific Reports*, 6, 2016.

Servedio, V. D. P.; Caldarelli, G., and Buttà, P. Vertex intrinsic fitness: How to produce arbitrary scale-free networks. *Phys. Rev. E*, 70:056126, Nov 2004.

Sethi, R. and Somanathan, E. The evolution of social norms in common property resource use. *The American Economic Review*, 86(4):766–788, 1996. ISSN 00028282.

Szabó, G.; Alava, M., and Kertész, J. Structural transitions in scale-free networks. *Phys. Rev. E*, 67:056102, May 2003.

Szabó, G. and Fáth, G. Evolutionary games on graphs. *Physics Reports*, 446(4–6):97 – 216, 2007. ISSN 0370-1573.

Tavoni, A.; Schlüter, M., and Levin, S. The survival of the conformist: Social pressure and renewable resource management. *Journal of Theoretical Biology*, 299:152 – 161, 2012. ISSN 0022-5193.

Trivers, R. The evolution of reciprocal altruism. 46:35–57., 03 1971.

Vose, D. *Risk analysis - a Quantitative Guide*. Chichester, John Wiley and Sons, 2012.

Wang, Y. H. On the number of successes in independent trials. *Statistica Sinica*, 3(2): 295–312, 1993. ISSN 10170405, 19968507.

Weiss, P. L'hypothèse du champ moléculaire et la propriété ferromagnétique. *J. Phys. Theor. Appl.*, 6(1):661–690, 1907.

Wenegrat, B.; Castillo-Yee, E., and Abrams, L. Social norm compliance as a signaling system. ii. studies of fitness-related attributions consequent on a group norm violation. *Ethology and Sociobiology*, 17(6):417 – 429, 1996. ISSN 0162-3095.

Wondolleck, J. M.; Yaffee, S. L., and Roush, D. Making collaboration work: Lessons from innovation in natural resource management. 01 2002.

Xu, X.; Zhang, J., and Small, M. Rich-club connectivity dominates assortativity and transitivity of complex networks. *Phys. Rev. E*, 82:046117, Oct 2010.

Xulvi-Brunet, R. and Sokolov, I. M. Reshuffling scale-free networks: From random to assortative. *Phys. Rev. E*, 70:066102, Dec 2004.

Yamagishi, T. The provision of a sanctioning system in the united states and japan. *Social Psychology Quarterly*, 51(3):265–271, 1988. ISSN 01902725.